Mapping of Seismically Induced Landslippage in the Benton Hills and Crowley's Ridge, New Madrid Seismic Zone, Missouri and Arkansas

by

J. David Rogers

and

Briget C. Doyle

Department of Geological Sciences & Engineering
University of Missouri-Rolla

ABSTRACT

Crowley's Ridge is a semi-continuous elevated upland over 380 km long within the upper Mississippi Embayment. Crowley's Ridge was subjected to over 2,000 felt earthquakes during the 1811-1812 New Madrid earthquake sequence, including at least three events with $M_s > 8.0$. Crowley's Ridge was not settled at the time of the earthquakes, but numerous seismically-induced landslides were reported near populated areas along the Chickasaw Bluffs at the eastern edge of the Mississippi Embayment. 220 slides were subsequently mapped in the Chickasaw Bluffs by Jibson and Keefer (1988) between Walls, MS, and Barlow, KY.

Landslides have only occasionally been noted along Crowley's Ridge since the area was settled in the mid-19th Century. Most of these slides have been of relative small scale, caused by human activity. In an effort to identify possible seismically-induced earth movement along Crowley's Ridge related to either the 1811-12 earthquakes or paleoseismic events, this report studied the feasibility of recognizing landslide and lateral spread features using topographic algorithms. The algorithms use drainage and topographic keys to recognize anomalous site characteristics typical of various landslide

forms, including lateral spreads, slumps and retrogressive slump complexes, earthflows, translational block slides, and theater-head erosion complexes. This research shows that the use of topographic algorithms as a reconnaissance method will prove valuable as a screening tool in evaluating earth-movement hazards across large areas. This study focused on five 7.5-minute United States Geological Survey quadrangles on Crowley's Ridge; the Helena, West Helena, Stubbs Island and LaGrange, AR, and Valley Ridge, MO, quadrangles. A total of 921 definite and probable landslides were identified on these five quadrangles, including 525 slumps and retrogressive slump complexes, 159 block slides, 176 earth flows, and 39 lateral spread features. Slide size, type, and morphology indicate that the majority of the slides were likely seismically-induced.

ACKNOWLEDGMENTS

The authors would like to thank the numerous people who assisted in the investigation for and preparation of this report, including: Dave Hoffman, Jim Vaughn, and Jim Palmer of the Missouri Department of Natural Resources Geological Survey and Resource Assessment Division for their assistance in obtaining data and joining the author in the field; Gary Krizanich, Norm Spurgeon, and Shelley Silch of the USGS Mid-Continent Mapping Center for assistance with the GIS program ArcView, obtaining digital map products, and printing the final map plates; the National Resource Conservation Service in Helena, AR, the USDA Service Center and Farm Services Administration in Marianna, AR, and Doug Hansen of the Arkansas Geological Commission for their assistance in obtaining information about the research area; and Mrs. Catherine O. West of Marianna, AR, and Mrs. Frank Clancy, her son Frank Clancy, and their family of Helena, AR, for generously allowing access to their property for geophysical surveys.

The authors would also like to acknowledge the help of Craig Kaibel and Conor Watkins of the UMR Geological Engineering program; and Dr. Estella Atekwana, Anthony Buccellato and Garret Euler of the Department of Geology and Geophysics for assistance with geophysical investigations. This work was funded in part by the United States Geological Survey National Earthquake Hazard Reduction Program (NEHRP) and by the University of Missouri Research Board.

TABLE OF CONTENTS

Page

LIST OF ILLUSTRATIONS

Figure Page

LIST OF TABLES

Table Page

1. INTRODUCTION

1.1. PROBLEM STATEMENT

Between December, 1811, and March, 1812, the largest series of earthquakes ever recorded in United States struck the upper Mississippi Valley, centered near New Madrid, Missouri. The region was subjected to repeated episodes of wide-scale liquefaction, ground subsidence and uplift, as well as landslides and earth movement towards channels. Work carried out by Nuttli (1973) and others suggests that the largest earthquakes in the New Madrid earthquake sequence had surface-wave magnitudes (M_s) between 8.0 and 8.8, and these are the most cited magnitudes used in describing the 1811-12 earthquake sequence. Figure 1.1 shows the locations and magnitudes of the five largest earthquakes of the New Madrid series as identified by Nuttli (1973). However, recent studies utilizing paleoliquefaction suggest that M_s for the New Madrid earthquakes may have been somewhat lower, between 7.0 and 7.9 (Schweig, 2003).

At the present time, little research into the presence of seismically-induced slope movements has been completed within the New Madrid Seismic Zone (NMSZ), exclusive of the Chickasaw Bluffs escarpment on the eastern-most edge of the upper Mississippi Embayment. First-hand accounts of seismically-induced landslippage were recorded in the Chickasaw Bluffs because the only habitations at the time (Caruthersville, Tiptonville and New Madrid) were located nearby, along the Mississippi River (Fuller, 1912). Figure 1.2 is a portion of the map made by Fuller that indicates seismically-induced landslides occurred along the Chickasaw Bluffs escarpment in the eastern NMSZ, but no landslides were mapped west of the Mississippi River, along Crowley's Ridge or the Ozark Escarpment. At the time of the 1811-12 earthquakes the wet bottomlands west of the Mississippi River were uninhabited and surrounded Crowley's Ridge. It would appear that the absence of eyewitnesses in this area precluded the reporting of ground disturbances. The features investigated and reported upon by Fuller almost a century later in the western Embayment were based on his observations, not on eyewitness accounts. In 1811-12 New Madrid, MO was the nearest settlement to Crowley's Ridge, some 27 mi (43.35 km) away, along the Mississippi River.

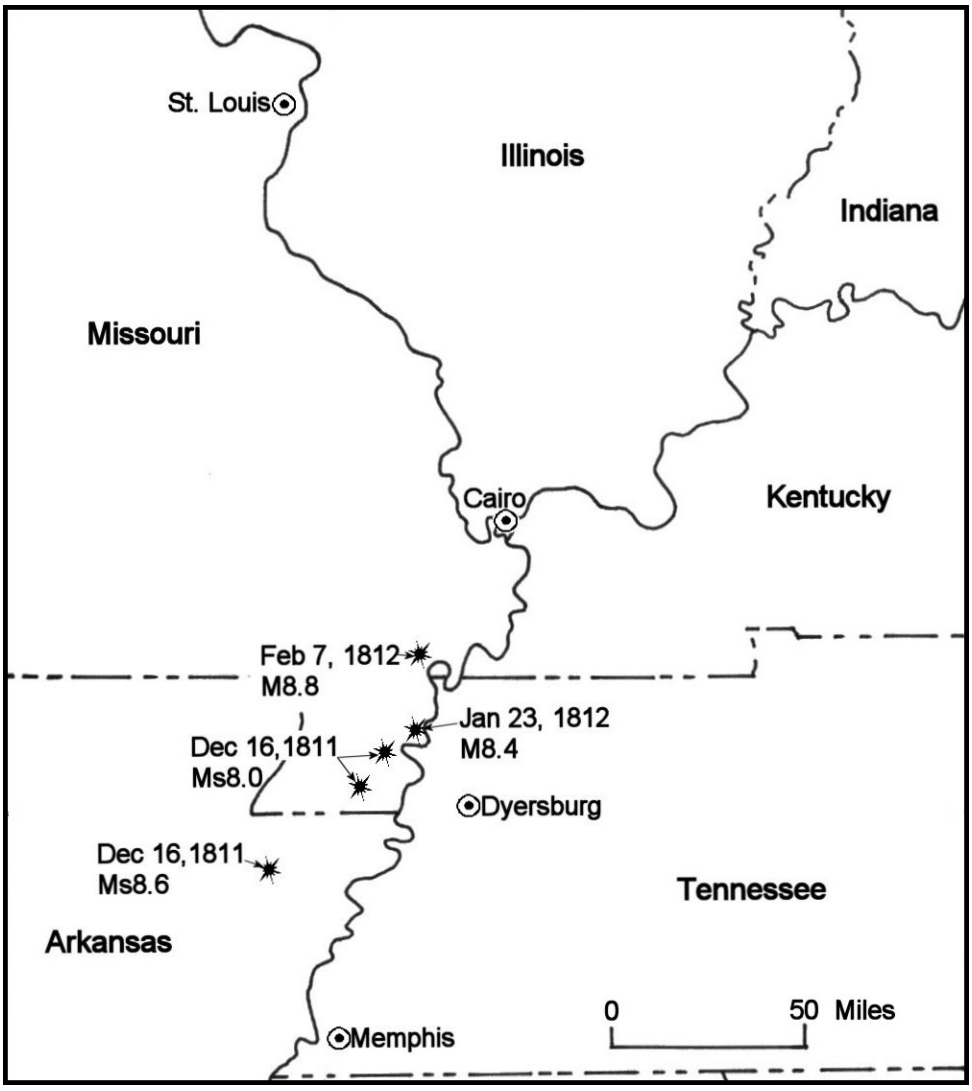

Figure 1.1 Locations, dates, and magnitudes of the five M8.0+ earthquakes of the 1811-1812 New Madrid Earthquake sequence (adapted from Jibson and Keefer, 1988).

Jibson (1985) and Jibson and Keefer (1988, 1994) studied landslides along the Chickasaw Bluffs in Kentucky and Tennessee and identified three main landslides types: old coherent translational block slides; single and multiple rotational slumps; and earthflows. Figure 1.3 shows block diagrams by Jibson and Keefer of the three landslide types they studied along the Chickasaw Bluffs.

Initial studies of potential landsliding in the western NMSZ (Ding, 1991) focused on the landslide types described by Jibson and Keefer (1988, 1994). The study

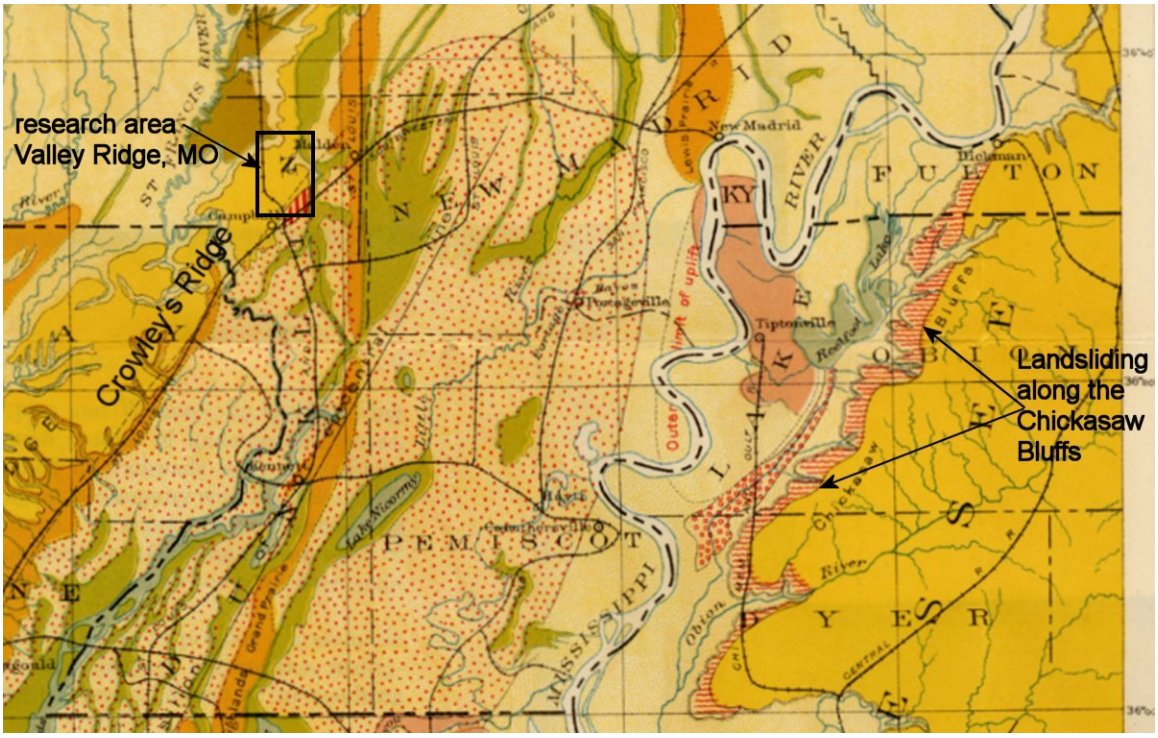

Figure 1.2 A portion of the earthquake effects map made by Myron Fuller (1912) showing areas of mapped landslides along the Chickasaw Bluffs in Kentucky and Tennessee (horizontal red lines). No landslide areas are mapped along Crowley's Ridge to the west, although Fuller did map areas of "numerous sand dikes" near and within the Valley Ridge, MO, 7.5-minute quadrangle.

undertaken for this research focused on the eastern escarpment of Crowley's Ridge in the upper Mississippi Embayment. Lateral spreads and theater-head erosion complexes, in addition to the translational block slides, slumps, and earth flows similar to those described by Jibson and Keefer were found in the course of this study. Field work carried out as a part of this research suggests that extensive landslippage and lateral spreading likely occurred on and adjacent to Crowley's Ridge during the 1811-1812 New Madrid earthquake sequence. The identification the these seismically-induced landslides is a necessary first step in making people aware that such hazards exist in the western NMSZ and could impact the area during future medium- to high-magnitude earthquakes.

According to Hamilton and Johnson (1990) and CUSEC (1999) the region is presently overdue for a M_s 6.8 event. Events of this magnitude occur on average about once every 70 ± 15 years. The last M_s 6.8 event was the 1895 Charleston, Missouri,

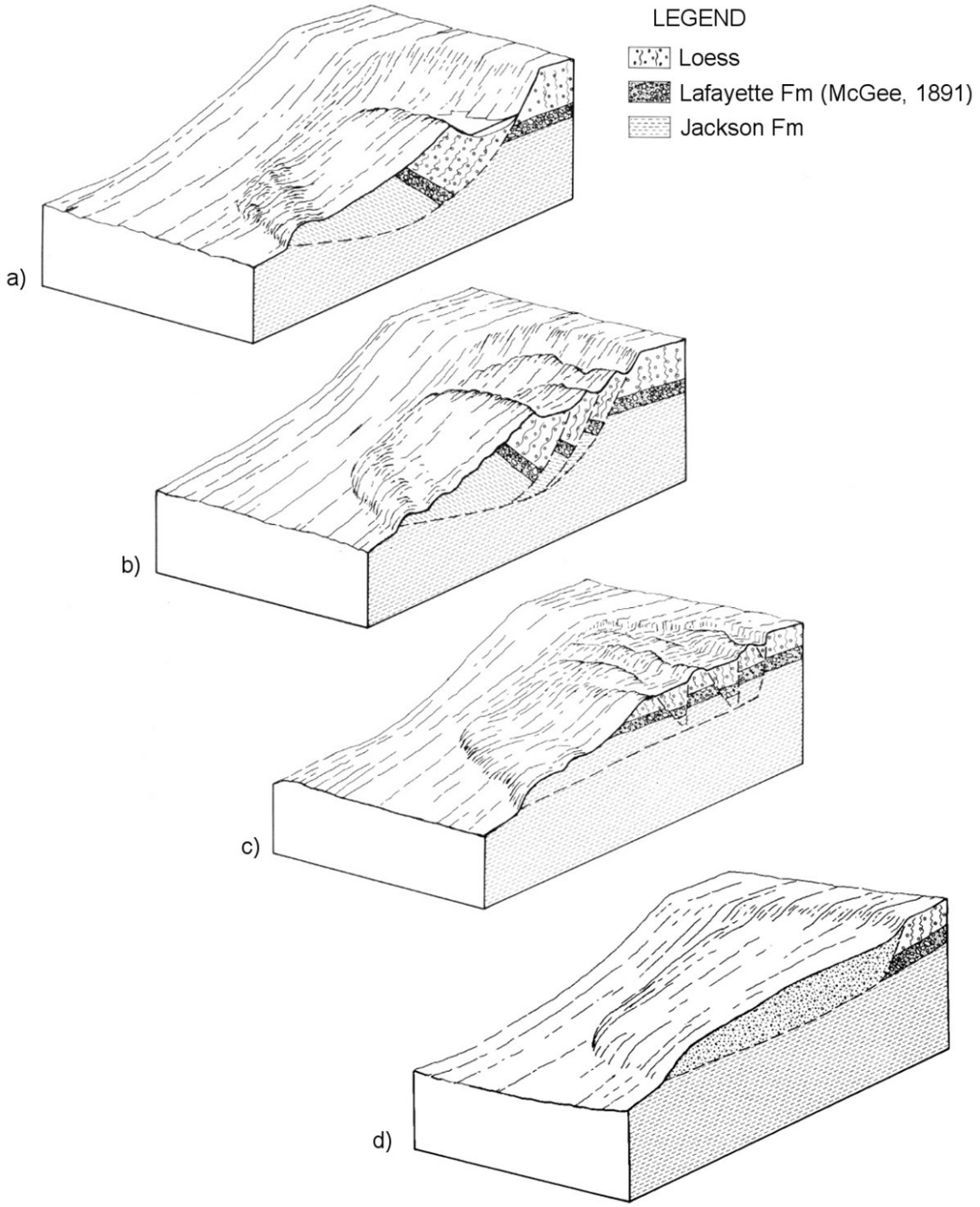

Figure 1.3 Conceptual block diagrams by Jibson and Keefer (1988) of the landslides types they identified along the Chickasaw Bluffs. a) simple rotational slump; b) multiple rotational slump; c) old coherent translational block slide; d) earthflow

earthquake, which affected a large portion of the central United States. Even a Charleston size event could cause ground lurching, liquefaction and landslippage in zones containing saturated low density sands because of wave impedance contrast and low bedrock attenuation (Rogers, Bray, and Rathje, in press).

The final results of this research may be applied in order to:

1. raise awareness about the potential for seismically-induced earth movement in the NMSZ;
2. help identify the source of anomalous geomorphic features along the southeastern escarpment of Crowley's Ridge that may be ascribable to either Holocene faulting, lateral spreading or paleolandslippage;
3. identify areas for future site specific studies that may allow post-failure analyses to determine the level of ground motion that would have been required to initiate movement;
4. identify candidate sites for post-failure analyses to evaluate shaking-induced liquefaction;
5. enable better predictions of seismic slope stability and lateral spreading potential for the region's three Interstate highways, 11 federal highways, dozens of state and county highways and two national railroad links;
6. aid in ongoing assessments of the stability of water storage reservoirs along Crowley's Ridge; and,
7. aid state and federal departments of transportation and state and federal disaster planning and relief agencies in making planning decisions about emergency access corridors, possible seismic retrofitting of existing infrastructure, and disaster planning.

1.2. SCOPE OF WORK

The objective of this study was to compile an inventory of seismically-induced landslides and lateral spreading along portions of Crowley's Ridge and evaluate complex lateral spreads and coherent translational block slides not previously identified in the western New Madrid Seismic Zone. After making a preliminary evaluation of 52 7.5-minute (1:24,000 scale) topographic quadrangles covering Crowley's Ridge, it was

decided to concentrate efforts on landslippage along two portions of Crowley's Ridge: the LaGrange, Stubbs Island, Helena and West Helena quadrangles near Helena, AR, and the Valley Ridge quadrangle just north of Campbell, MO (Figure 1.4). Studies on the eastern side of the NMSZ have identified over 200 landslides along the Chickasaw Bluffs (Jibson, 1985; Jibson and Keefer, 1988) through aerial photography and field identification, but little comparable work has been conducted in the western NMSZ. The mapping methodology to be used in this work focused on the use of aerial photographs and topographic mapping protocols to identify potential landslide features, followed by field investigation of candidate sites in the two study areas.

The topographic mapping protocols use drainage and topographic keys to recognize anomalous site characteristics typical of various landslide forms. Landslides were tentatively identified through the examination of digitized versions of United States Geological Survey (USGS) topographic maps, digital elevation models (DEMs), and aerial photographs using the Geographic Information Systems (GIS) ArcView 8.2 (ArcGIS), Global Mapper, and Terra Base II.

Following initial identification of both definite and probable landslide sites on the LaGrange, Stubbs Island, Helena, West Helena and Valley Ridge quadrangles, detailed mapping and analyses were carried out on the upland areas of these quadrangles to ascertain whether or not the anomalous topographic features were actually seismically-induced landslides (see Section 5).

1.3. LANDSLIDE MAPPING CONCEPTS

Landslide mapping has traditionally been accomplished through the examination of stereopair aerial photographs and aerial and field reconnaissance of the suspect area (Liang and Belcher, 1958). The method used in this research focused on initial identification of suspected landslide areas using the topographic mapping protocol, followed by examination of aerial photos, and then, by field reconnaissance and geophysical profiling. Areas of past landslippage typically exhibit anomalous topography and drainage patterns relative to surrounding areas which are not disturbed by landslippage. Additionally, different types of landslides exhibit different topographic and drainage characteristics (Varnes, 1958; 1978). The anomalies characteristic of

topography and drainage, and the related slide types, are described in more detail in Section 4.

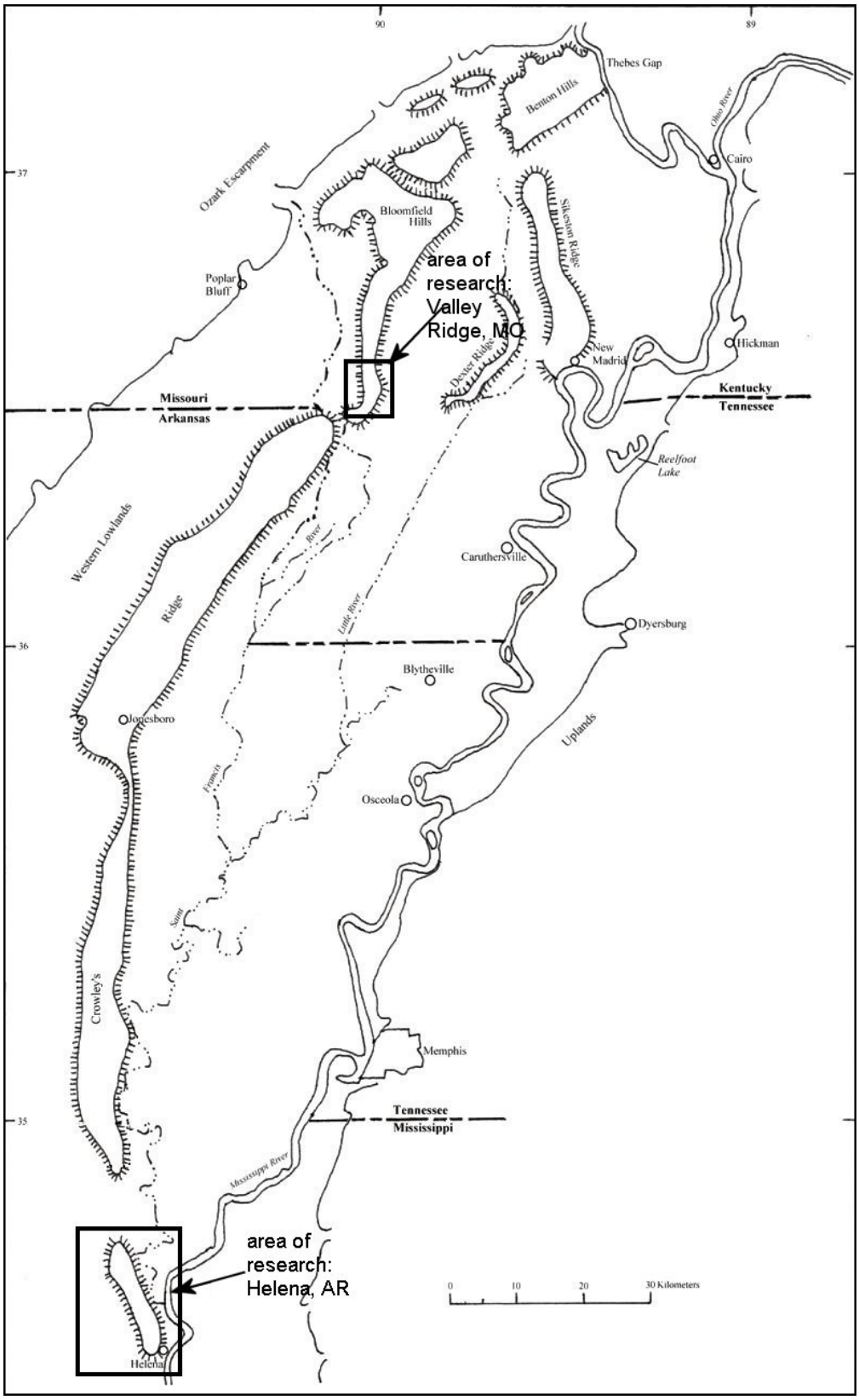

Figure 1.4 Map showing the location of Crowley's Ridge and areas of research focus.

2. LITERATURE REVIEW

2.1. LANDSLIDE MAPPING BY FIELD RECONNAISSANCE

Landslides can occur on almost any slope, provided that conditions exists that are adverse to long-term stability. A slope's sensitivity to de-stabilizing factors varies as a function of the underlying geologic make-up, slope steepness, height, moisture content, vegetative cover and artificial disturbance. Experience with slides worldwide has demonstrated that landslides are common in some locations, but relatively rare in others.

Geomorphologists (Way, 1973; Selby, 1982) classified landforms according to their topographic expression and drainage patterns. Dietrich and Rogers (1987) suggested that hillslope profile could be a key factor in assessing past landslippage. Hillslope profile is largely influenced by hydrologic requirements, including slope, roughness, runoff quantity; and by mass movement processes, such as soil creep, colluvium production and landslides.

In any given area or geologic terrain, geomorphologists and engineering geologists can gain an appreciation of which factors tend to control landslippage by comparing two basic slope forms: those typical of quasi-equilibrium conditions and those of a slope with varying profile, which may not be in equilibrium. In the early 1900's William Morris Davis (1909) formulated the since-accepted premise of a mature slope in equilibrium spawning a concave-straight-convex profile. Slopes form in response to geologic uplift due to regional tectonic forces, or to localized downcutting due to changes in erosive base level. Absent landsliding, slope form in sedimentary strata is largely controlled by hydrologic criteria, such as lithology, height of slope, and tributary watershed area (Bryan, 1940; Leopold, Wollman and Miller, 1964). A series of hillsides in quasi-equilibrium may exhibit differing slopes due to proximity of the controlling base level, such as the position of the trunk stream channel (Rogers, 1980).

If a range of hills are uplifted or a lower base level is imposed upon the region due to lowering sea level, trunk streams occupying valley bottoms can be expected to downcut, thereby steepening side slopes, increasing slope height, and thereby, perturbing equilibrium. The profile of such a slope will generally exhibit a nickpoint **(**Penck, 1927**)**, or sudden change in profile. The slopes exposed along either side of Crowley's Ridge

exhibit nickpoints, usually in the upper portion of the slopes, close to the drainage divides.

In cases of erosive downcutting, such as occurs adjacent to major channels, like the St. Francis and Mississippi Rivers, steeper slope profiles generally emerge at the toe of the affected slope, causing oversteepening. Shallow groundwater flow patterns can be expected to emerge from such undercut slopes in these newly excavated areas. This emergent seepage is able to issue forth from the newly-excavated slope face and initiate raveling and seep undercutting. Emergent seepage pressures play a large role in destabilizing the near-slope area, within 3 m (10 ft) of the ground surface (Cedargren, 1989).

Until this study, traditional methods of landslide mapping have generally focused on direct field investigation and examination of stereopair aerial photography to identify and delineate probable landslides, based on geomorphic expression. Geomorphic assessments of landslide hazard mapping were outlined by Keinholz (1977), whereby landslide features are identified in the field by a geomorphologist or engineering geologist. The ability to discern landslides in the field and rate the potential hazard they may pose is a function of the investigator's individual experience and the local geologic conditions (Soeters and van Westen, 1996). Such field investigations have been the accepted method for the study of landslides over the last half century (Philbrick and Cleaves, 1958; Sowers and Royster, 1978). Turner and McGuffey (1996) presented a protocol method for investigating landslides, which established a series of investigative steps, with considerable focus on field investigation.

2.2. BASIC BACKGROUND INFORMATION

Rogers (1998) presented a list of steps that should be taken undertaken to gather sufficient background information on an area prior to performing evaluations of past landslippage. These included:

1. All existing information of the area of study is assembled. This includes all available topographic maps, ground photos, historical accounts, records of slope instability or geologic hazards identified by others, university research, dissertations, published references, etc;

2. All available information on bedrock geology, structural geology (faults and folds) is standardized with the most accepted stratigraphic nomenclature and overlain on a master map of the study area. In this manner the zones of similar parent material are identified;
3. All first order and greater natural stream courses (both ephemeral and perennial) are plotted and texture of the drainage patterns identified. This pattern is then compared to the bedrock geologic compilation to ascertain where underlying structural control is likely exerted on the stream system;
4. Soil survey maps are also compiled, and relationships between soil types, underlying bedrock, drainage courses, salient geologic structures, and slope are delineated.
5. In many instances it is desirable to construct a few representative stream profiles. Profiles are one of the best indicators of massive system perturbation, by such features as ancient paleolandslides, megalandslides, or depending on the scale of the topographic data, of even geologically recent landslippage.

The above-listed information comprises the "basic data" from which to begin a photogeologic assessment. The zones of basic parent material are identified from the geologic maps. Within these zones subunits may be identified based on soils information. Soils will exude various textures depending on their slope, thickness (sometimes called stoniness), water content at the time of imaging, sun angle/incidence, vegetation, and degree of erosion. Common surface textures are sought out and identified within those discrete areas within which the photointerpreter has first-hand experience, or reliable data upon which to "ground truth" the texture.

2.3. LANDSLIDE MAPPING USING AERIAL PHTOGRAPHS

The use of aerial photography to identify various types of landslides evolved quickly during the Second World War and became the method of choice for investigating landslide prone terrain soon thereafter (Liang, 1952; Liang and Belcher, 1958).

Rib and Liang (1978) and Rogers (1994) suggested similar steps be undertaken in evaluating past landslippage using stereopair aerial photography. The first step in such assessments should be to identify landform units. To do this, the geologist examines visual

pattern elements exposed in stereopair aerial photos and utilizes deductive reasoning to sort out what must underlie the ground surface to account for the patterns observed. This process is enhanced by researching and reviewing all available geologic information regarding the area of interest (as discussed in Subsection 1.2). For instance, information on underlying rock formations, previous interpretations of geologic structure, soil science information, first-hand data on depth of soil cover at discrete, identifiable locations within or immediately adjacent to the study area, hydrologic regimen (rainfall, seasonal intensities, mass permeability, water well information, or petroleum exploration efforts), and an historic sense of past physical processes.

In viewing the aerial photos, the interpreter generally searches for geomorphic and/or topographic anomalies. These include the following steps:

1. A basic overview of the drainage system, searching for reproducible versus anomalous patterns. For instance, if a dendritic drainage network appears to dominate the landscape, the search might focus of first-order channels or swales which are non-dendritic, such as derainged, parallel or parallel converging tracks. Other drainage course anomalies often diagnostic of past landslippage include semi-circular drainage courses around some sort of topographic obstruction; rapids or channel rills in locations devoid of tributary side-entry; meandering, low-gradient channels upstream of steeply-inclined linear rapids; and closed depressions within topographic benches (often formed by landslide headscarp pull-apart grabens).
2. A basic overview of hillslopes, searching for anomalous topographic expression. The most common anomaly is hummocky surface expression, followed by discontinuous arcuate topographic steps, discontinuous topographic benches, anomalously large lobate features extending from small watershed catchments, and sag ponds.
3. Searching for slopes with anomalously lower hillslope profiles, in comparison with adjacent slopes. If one slope is much flatter than the slopes on either side of it, one should ascertain whether there exist underlying control on slope morphology by lithologic or structural geologic changes (Twidale, 1971).
4. Any evidence of anomalous vegetation patterns, such as might be expected from rapid denudation by rockslide, debris flows, avalanches or slower moving landslides.

In assessing landslide-prone terrain, a basic understanding of past weather patterns and the manner, scale, and distribution of slope stability problems can also prove valuable. Within any given environmental extremes (such as a tropical storm) there exists a finite number of old landslides or colluvial-filled ravines that are "ripe" for failure (Terzaghi, 1950), or in engineering terms, exists on the very verge of failure. One great storm may be enough to trigger failure of such slopes, but insufficient, in of itself, to trigger many more. Some people would feel a sense of security if no landslippage had ever been experienced, but in fact, the simple passage of time may be acting to bring a slope closer and closer to the point of failure. For this reason, viewing of aerial photographs imaged soon after such extreme events may prove quite useful, whereas images taken during years of below normal precipitation may not show useful information.

More recently, Soeters and van Westen (1996) and Keaton and DeGraff (1996) both described the use of aerial photography and the importance of photograph scale in landslide interpretation. In aerial photography, difficulties may be encountered with insufficient scale, thick vegetation, or unfavorable sun angle (Rogers and Doyle, in press). Generally, scales of 1:15,000 or larger have the detail necessary for accurate landslide mapping (Keaton and DeGraff, 1996).

2.4. LANDSLIDE MAPPING IN THE NEW MADRID SEISMIC ZONE

Although significant studies have been made of the geology, geophysical characteristics, and seismicity and paleoseismicity of the NMSZ, very few studies have focused on landslippage related to seismic activity, especially in the western portion of the NMSZ. In 1912, Myron Fuller (1912) published the first scientific study of the effects of the 1811-1812 New Madrid earthquake sequence. Fuller used both field investigation and eyewitness accounts to describe the effects of the 1811-1812 earthquakes on the land surface. This report was a general study of the earthquake effects and not specifically focused on landslippage, although Fuller did devote part to description of seismically-induced landslippage, including descriptions of landslides near Hickman, Kentucky and Reelfoot Lake, Tennessee (Fuller, 1912).

The first major studies to focus on landslides in the NMSZ were by Jibson (1985) and Jibson and Keefer (1988, 1994). The studies focused on the Chickasaw Bluffs on the

eastern flank of the northern Mississippi Embayment and in the NMSZ. Jibson and Keefer mapped 221 landslides greater than 50 meters wide along over 300 km of bluffs between Cairo, IL, and Memphis, TN, using aerial photographs and field reconnaisaance. The slides were classified into one of three types: old coherent slides, earth flows, and young rotational slumps. 65% of the slides identified by Jibson and Keefer (1994) were classified as old coherent slides. The category of old coherent slides included both translational block slides and older rotational slumps, because of difficulty distinguishing between the two types due to tree cover and eroded features. Slope stability analysis of representative slides indicated that the slides failed due to strong earthquake shaking and not high groundwater levels or other aseismic conditions (Jibson and Keefer, 1994).

There have been two studies that investigated the occurrence of landsliding in the western NMSZ, both in Arkansas. A Masters thesis by Zheng Ding (1991) studied landslides along Crowley's Ridge in Arkansas and attempted to determine whether the slides were related to the 1811-12 earthquakes. 46 landslides were identified in the central portion of Crowley's Ridge in Arkansas, 31 of which were classified as old coherent landslides, as defined by Jibson (1985) and Jibson and Keefer (1988, 1994). Limit equilibrium slope stability analyses similar to those employed by Jibson and Keefer suggested that the identified landslides were most likely seismically induced. However, no landslides were identified in the northern and extreme southern portions of Crowley's Ridge in Arkansas. A map of the slides identified by Ding is included in her thesis at a scale of approximately 1:124,000, making location of specific landslides difficult to determine.

In 1992, J.D. McFarland of the Arkansas Geological Commission published a study of landslides along Crowley's Ridge in Arkansas. Landslides identified in the study were small in scale, modern in age, and mostly a result of human activity. The landslides identified by McFarland were mainly located along roads, in old quarries, and in recently logged areas as well as in stream cuts and loess "canyons" (McFarland, 1992). No landslides believed to be related to the 1811-1812 earthquake sequence were identified.

3. GEOLOGIC SETTING

3.1. MISSISSIPPI EMBAYMENT

The Mississippi Embayment is a south-plunging syncline of Cretaceous and Tertiary sedimentary deposits that is a reentrant onto the North American craton. According to Shedlock and Johnston (1994), it exhibits many geophysical characteristics of a failed triple junction. The Embayment is surrounded by the Illinois Basin to the north; the Southern Appalachian Plateau and Nashville Dome to the east; and the Ozark and Ouachita Uplifts to the west.

Four Tertiary basin-fill units are found in the Mississippi Embayment. These sediments mainly overlay Ordovician limestones and dolomites. The units also crop out on various parts of Crowley's Ridge. The oldest unit is the Paleocene Midway Group, containing massive fissile shales, clay shales, and clays with sandy clay beds. Overlying the Midway Group are three Eocene units. The Wilcox Group, consisting of interbedded sand, silt, clay, and some lignite deposited in a fluvial –deltaic environment lies just above the Midway. Well data indicates that the Wilcox is approximately 775 feet thick near Helena, AR. The Claiborne Group is a mix of fine sand, silt, sandy clays, and minor lignite deposits that overlies the Wilcox Group. The Claiborne was deposited in deltaic and nearshore environments, and is approximately 690 feet thick in the Helena area. The youngest Eocene unit is the Jackson Group, which is approximately 490 feet thick and consists of sandy clay, silt, and glauconitic, fossiliferous sandy clay, believed to have been deposited in a nearshore marine environment (Guccione, Prior, and Rutledge, 1986; Saucier, 1994).

The Mississippi Embayment narrows to the north and broadens towards the south-southwest, with the axis of the syncline roughly underlying the present-day Mississippi River. Figures 3.1 and 3.2 present cross-sections of the Mississippi Embayment. Figure 3.1 is just north of Helena, AR, where the axis of the Embayment passes under Crowley's Ridge and diverges southwestward, away from the present-day Mississippi River. Figure 3.2 is in the northern part of the embayment, along U.S. Highway 60 near Dexter, MO.

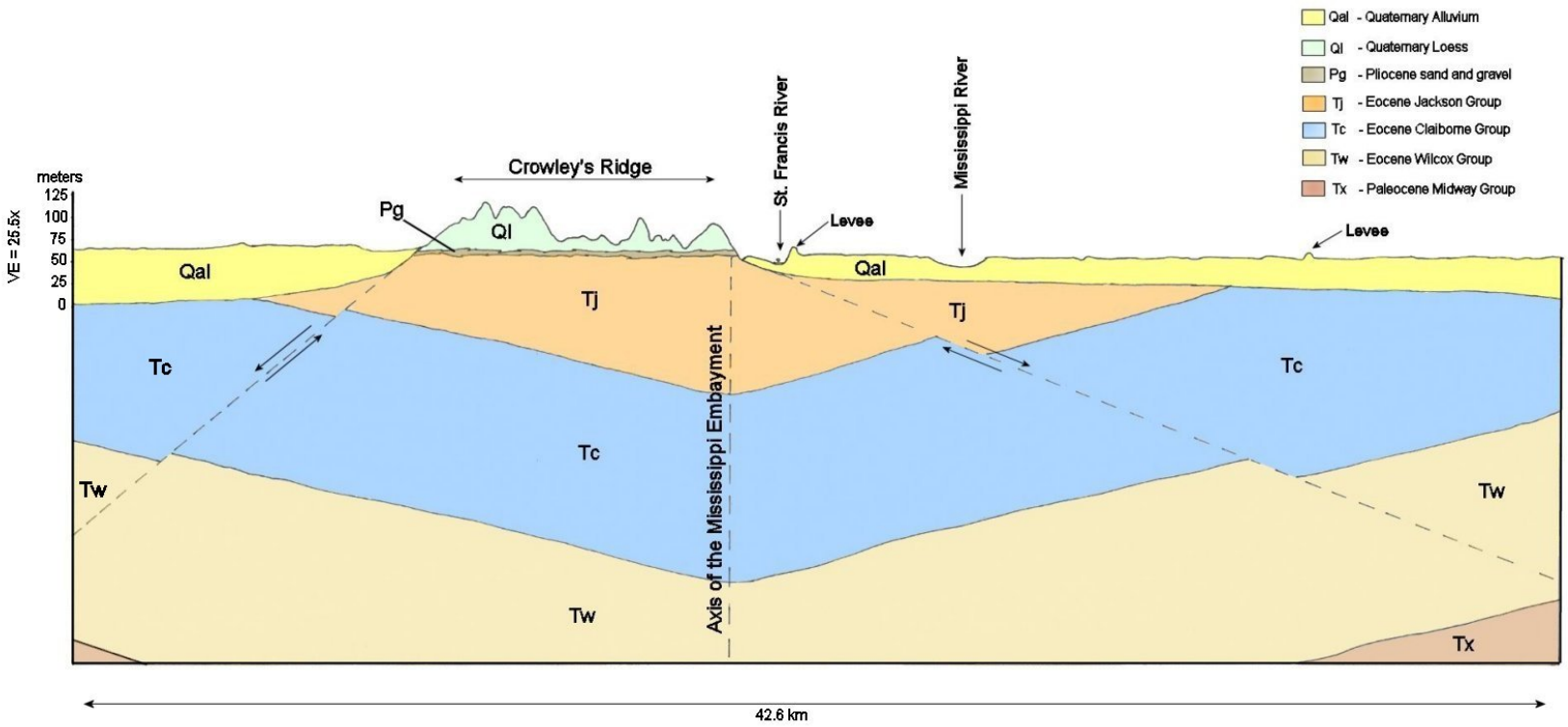

Figure 3.1 Cross-section of the Mississippi Embayment near Helena, AR, showing the axis of the Mississippi Embayment and the faults bounding Crowley's Ridge, based on data in Saucier (1994a, 1994b), Fisk (1944), and Guccione, et al, (1986).

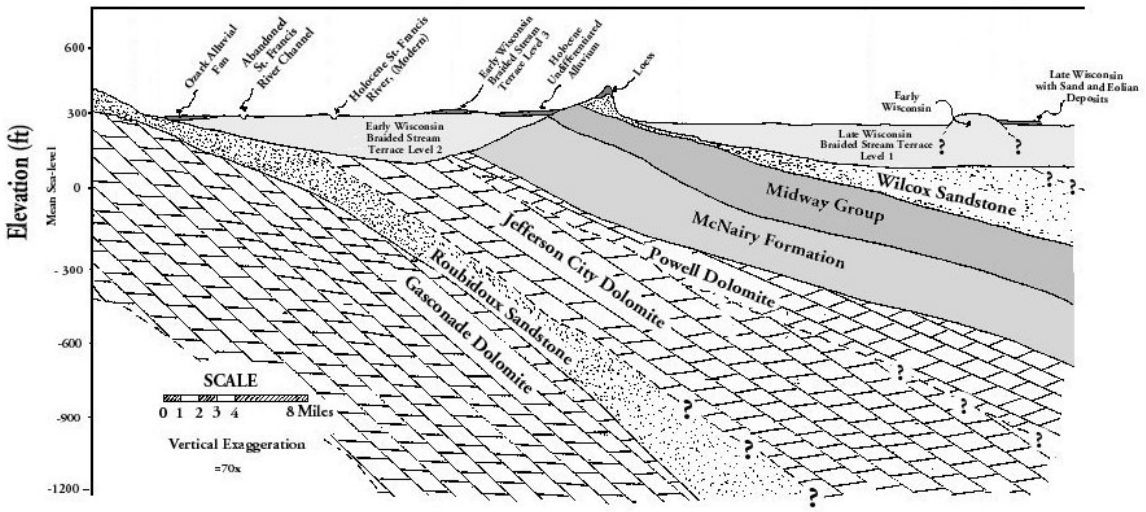

Figure 3.2 Cross-section of the Mississippi Embayment near Valley Ridge, MO, showing structure beneath Crowley's Ridge in the Missouri bootheel (from Santi and Neuner, 2002).

3.2. REELFOOT RIFT AND COMMERCE GEOPHYSICAL LINEAMENT

The most prominent buried structure in the Embayment is the Reelfoot Rift. The structure is a 300 km long, 70 km wide buried Late Precambrian to Cambrian failed rift structure within the Mississippi Embayment (Shedlock and Johnston, 1994; Van Arsdale, 1997). The majority of the earthquakes that occur in the central United States seem to be related to the rift and nearby igneous bodies. The Reelfoot Rift is considered to be the one of the main sources of the seismic activity that defines the New Madrid Seismic Zone (NMSZ) (Hildenbrand, et al., 1996). The rift is part of a southwest-trending failed rift system overlain by the south-plunging Cretaceous and Tertiary sediments of the Mississippi Embayment. Figure 3.3 shows the approximate location of the Reelfoot Rift beneath the Mississippi Embayment. The Reelfoot Rift has been mapped by gravity and magnetic surveys, and exhibits 1.6 to 2.6 km of structural relief on the magnetic basement (Shedlock and Johnston, 1994). The bounding and axial faults of the rift appear to be major contributors to the seismic activity in the NMSZ (Hildenbrand, et al., 1996). Figure 3.4 is a shaded relief magnetic map of the NMSZ, showing the Reelfoot

Rift, recorded earthquakes, major igneous bodies, and the Commerce Geophysical Lineament (CGL).

The CGL is a linear magnetic anomaly that trends northeast and parallels the Reelfoot Rift (Figure 3.4). The CGL appears to be related to a series of faults that outcrop near the town of Commerce, MO. Sedimentary deposits as young as 12,000 years old have been broken by fault movement in that area (Hildenbrand, et al., 1996). The CLG is a poorly understood structure, but is believed to be part of a zone of faulting over 150 miles long, and may represent a significant seismic risk for future NMSZ earthquakes.

3.3. NEW MADRID SEISMIC ZONE

The New Madrid Seismic Zone, located within the upper Mississippi Embayment, is the most seismically-active area in the United States east of the Rocky Mountains. The extent of the NMSZ is defined by the clustered areas of high seismic activity, mainly related to the Reelfoot Rift and large igneous bodies within the upper Mississippi Embayment (Figure 3.4). Figure 3.5 shows the areas of the NMSZ with the most seismic activity, as well as the zone's location relative to the Mississippi Embayment and Crowley's Ridge.

The seismic activity that defines the NMSZ generally has earthquake epicenters between 5 and 15 km deep. The area of greatest seismic activity lies mostly in Precambrian basement rocks within the Reelfoot Rift and near the large igneous intrusive bodies underlying the Mississippi Embayment. There are three major trends in the seismic activity monitored in the NMSZ since 1974. A northeast-trending zone from Marked Tree, AR, to Caruthersville, MO exhibits right-lateral strike-slip movement which appears to be coincident with the Paleozoic Blytheville Arch. A northwest-trending zone extending from Ridgely, TN, through the Lake County uplift, and on to New Madrid, MO, follows the southwest-dipping Reelfoot reverse fault and a large igneous body (Figure 3.4). The third zone trends northeast from New Madrid. This trend appears to be caused by right-lateral strike-slip motion along one of the Reelfoot Rift's northwest bounding faults.

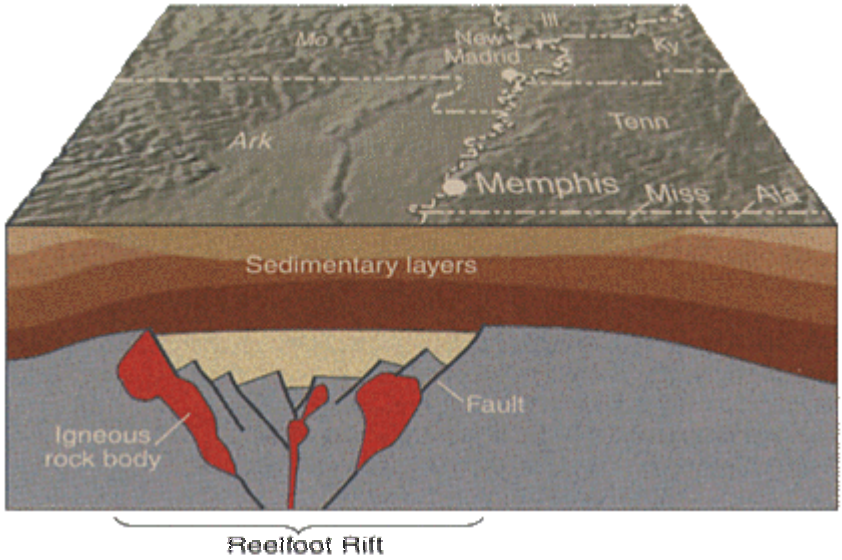

Figure 3.3 Block diagram of the upper Mississippi Embayment showing the location of the Reelfoot Rift relative to the Mississippi Embayment and the present-day Mississippi River. (from Hildenbrand, et al., 1996)

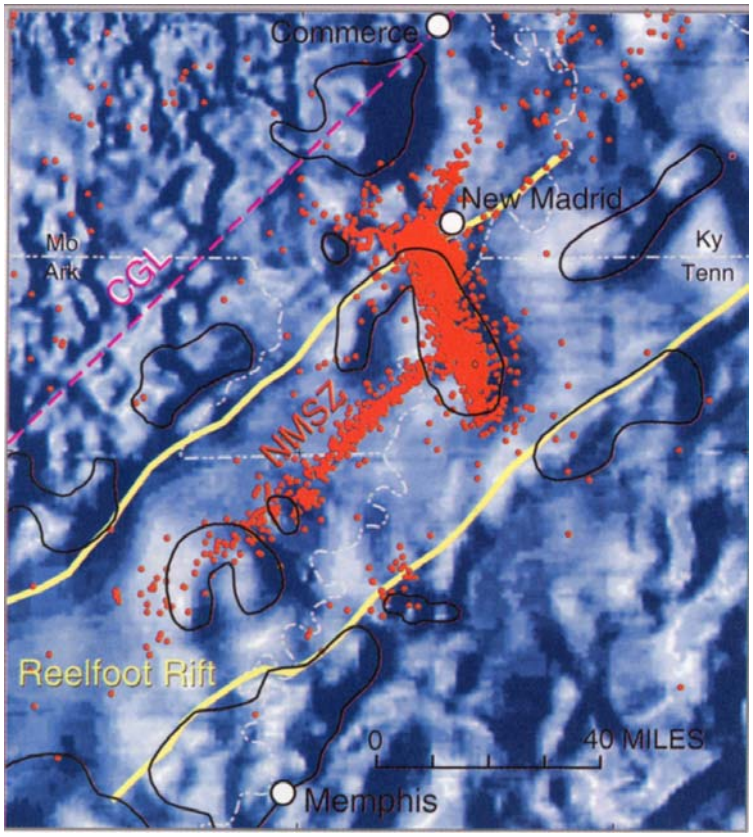

Figure 3.4 Shaded relief magnetic map of the NMSZ region. The Reelfoot rift can be seen as a relatively smooth area in the center of the figure. The igneous bodies associated with the rift and seismic activity in the NMSZ are outlined in black, while recorded earthquake epicenters are shown as red dots. The Commerce Geophysical Lineament (CGL) is indicated by a pink line paralleling the rift to the north. (from Hildenbrand, et al., 1996)

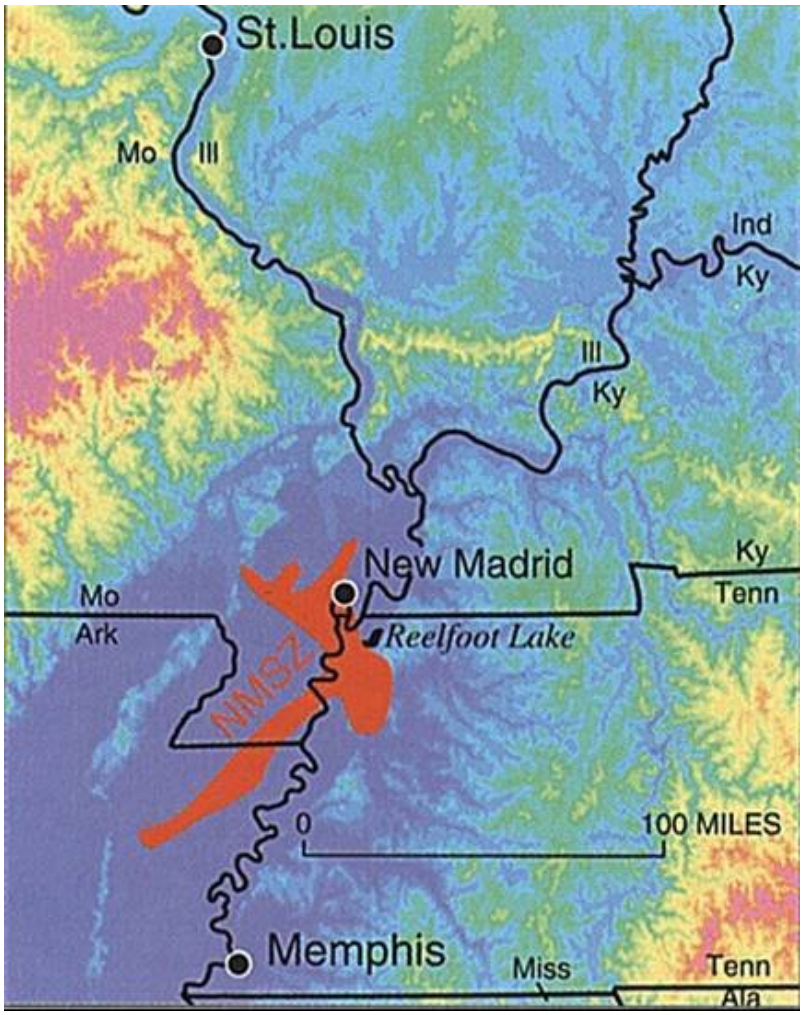

Figure 3.5 Map showing the main seismically-active area of the NMSZ, in red; the upper Mississippi Embayment, in dark blue, extending from the lower left of the map to the center; and Crowley's Ridge, the light blue area within the upper Mississippi Embayment. (from Hildenbrand, et al., 1996)

3.3.1. Seismic History

3.3.1.1 Paleoseismicity Although the New Madrid earthquakes of 1811 and 1812 are the best known seismic activity in the NMSZ, Native American traditions have recorded several previous earthquake shocks that allegedly "devastated" the region (Fuller, 1912). Fuller noted ground cracks with trees over 200 years old growing in them, suggesting an older series of earthquakes than the 1811-1812 sequence. Fuller also found faults

extending through the Lafayette gravel in the Chickasaw Bluffs and on Crowley's Ridge that appeared to pre-date the 1811-12 New Madrid earthquakes.

Using paleoliquefaction and archeological evidence, Tuttle and Schweig (1995) determined that two, possibly three prehistoric earthquakes, occurred near Blytheville, AR in the past 5000 to 6000 years. One sand blow crater in the area was dated between A.D. 800 and 1400, and another between A.D. 800 and 1670. According to Tuttle and Schweig, prehistoric liquefaction features in the Blytheville area suggest recurrence intervals of hundreds of years for earthquakes large enough ($m_b \geq 6.2$) to cause liquefaction. The prehistoric liquefaction features found were equal to or larger than the liquefaction features formed by the 1811-1812 earthquakes. This suggests that the prehistoric earthquakes may have been of similar sizes and type to the 1811-1812 earthquakes.

Kelson, et al., (1994), found evidence of three prehistoric earthquake events in the last 2400 years while studying the Reelfoot scarp. Saucier (1991) also identified paleoliquefaction features in the NMSZ. Paleoliquefaction features found near Reelfoot Lake were interpreted as being formed by two large prehistoric earthquakes that occurred within the past 1500 years.

3.3.1.2 Historical Seismicity

3.3.1.2.1 1811-1812 Earthquake Sequence Beginning on December 16, 1811, a series of large earthquakes shook the NMSZ. The initial shock on December 16th was followed by at least two, and as many as four, other major shocks. The two largest of the subsequent shocks occurred on January 23, and February 7, 1812. The February shock was the largest of the earthquake series. The approximate epicentral locations and magnitudes of the five largest earthquakes are shown on Figure 1.1. Between December, 1811, and March, 1812, the upper Mississippi Embayment experienced approximately 2000 earthquakes of surface wave magnitude (Ms) 3.0 or greater (Nuttli, 1973; Knox and Stewart, 1995). Five of the shocks have been estimated to have Ms between 8.0 and 8.8 (Nuttli, 1973). Aftershocks strong enough to be felt continued through 1817.

The earthquakes were felt over an area of 5 million km^2 (Van Arsdale, 1997), more than any other earthquake in American history. The area experiencing a Modified

Mercalli Intensity (MMI) (Table 3.1) of V or greater was approximately 2.5 million km^2 (Nuttli, 1973). This area of strong shaking is two to three times greater than the area affected by the 1964 Alaska earthquake and 10 times larger than the area affected by the 1906 San Francisco earthquake (Stover and Coffman, 1993). Figure 3.6 is a map showing the Modified Mercalli Intensities experienced during the December 16, 1811 earthquake. No intensities are shown west of the Mississippi River because the area was mostly unsettled, and eyewitness accounts of damage and effects were unavailable. The total estimated area of MMI V is based on the geology and topography west of the Mississippi River.

The December 16th earthquake was so severe that it awakened people as far away as Pittsburgh, PA, and Norfolk, VA. The felt areas of the three largest earthquakes extended to the gulf coast to the south, the Atlantic coast to the southeast, and to Quebec, Canada, in the northeast. Major topographic changes, including large ground fissures, sand blows, sunk lands, caving of river banks, and disappearing islands in the Mississippi River affected an area between 78,000 and 130,000 km^2 (von Hake, 1974; Stover and Coffman, 1993).

Table 3.1 Modified Mercalli Intensity Scale (from Richter, 1958)

MMI Value	Description of Shaking	Full Damage Description
I.		Not felt. Marginal and long period effects of large earthquakes.
II.		Felt by persons at rest, on upper floors, or favorably placed.
III.		Felt indoors. Hanging objects swing. Vibration like passing of light trucks. Duration estimated. May not be recognized as an earthquake.
IV.		Hanging objects swing. Vibration like passing of heavy trucks; or sensation of a jolt like a heavy ball striking the walls. Standing cars rock. Windows, dishes, doors rattle. In the upper range of IV, wooden walls and frames creak.
V.	Light	Felt outdoors; direction estimated. Sleepers wakened. Liquids disturbed, some spilled. Small unstable objects displaced or upset. Doors swing, close, open. Shutters, pictures move, Pendulum clocks stop, start, change rate.
VI.	Moderate	Felt by all. Many frightened and run outdoors. People walk unsteadily. Windows, dishes, glassware broken. Knickknacks, books, etc., fall off shelves. Pictures off walls. Furniture moved or overturned. Weak plaster and masonry D cracked. Small bells ring (church). Trees, bushes shaken (visibly or heard to rustle).
VII.	Strong	Difficult to stand. Noticed by drivers. Hanging objects quiver. Furniture broken. Damage to masonry D, including cracks. Weak chimneys broken at roof line. Falls of plaster, loose bricks, stones, tiles, cornices. Some cracks in masonry C. Waves on ponds; water turbid with mud. Small slides and caving along sand or gravel banks. Large bells ring. Concrete irrigation ditches damaged.
VIII.	Very Strong	Steering of cars affected. Damage to Masonry C; partial collapse. Some damage to masonry B. Fall of stucco and some masonry walls. Twisting, fall of chimneys, factory stacks, monuments, towers, elevated tanks. Frame houses moved on foundations is not bolted down; loose panel walls thrown out. Decayed piling broken off. Branches broken from trees. Changes in flow or temperature of springs and wells. Cracks in wet ground and on steep slopes.
IX.	Violent	General panic. Masonry D destroyed; masonry C heavily damaged, sometimes with complete collapse; masonry B seriously damaged. General damage to foundations. Frame structures, if not bolted, shifted off foundations. Frames racked. Serious damage to reservoirs. Underground pipes broken. Conspicuous cracks in ground. In alluvial areas sand and mud ejected.
X.	Very Violent	Most masonry and frame structures destroyed with their foundations. Some well-built wooden structures and bridges destroyed. Serious damage to dams, dikes, embankments. Large landslides. Water thrown on banks of canals, rivers, lakes. Sand and mud shifted horizontally on beaches and flat land. Rails bent slightly.
XI.		Rails bent greatly. Underground pipelines completely out of service.
XII.		Damage nearly total. Large rock masses displaced. Lines of sight and level distorted. Objects thrown into the air.

Masonry A: good workmanship, mortar, and design; reinforced, especially laterally, and bound together by using steel, concrete, etc.; designed to resist lateral forces.

Masonry B: good workmanship and mortar; reinforced, but not designed in detail to resist lateral forces.

Masonry C: ordinary workmanship and mortar; no extreme weaknesses like failing to tie in at corners, but neither reinforced nor designed against horizontal forces.

Masonry D: Weak materials, such as adobe; poor mortar; low standards of workmanship; weak horizontally

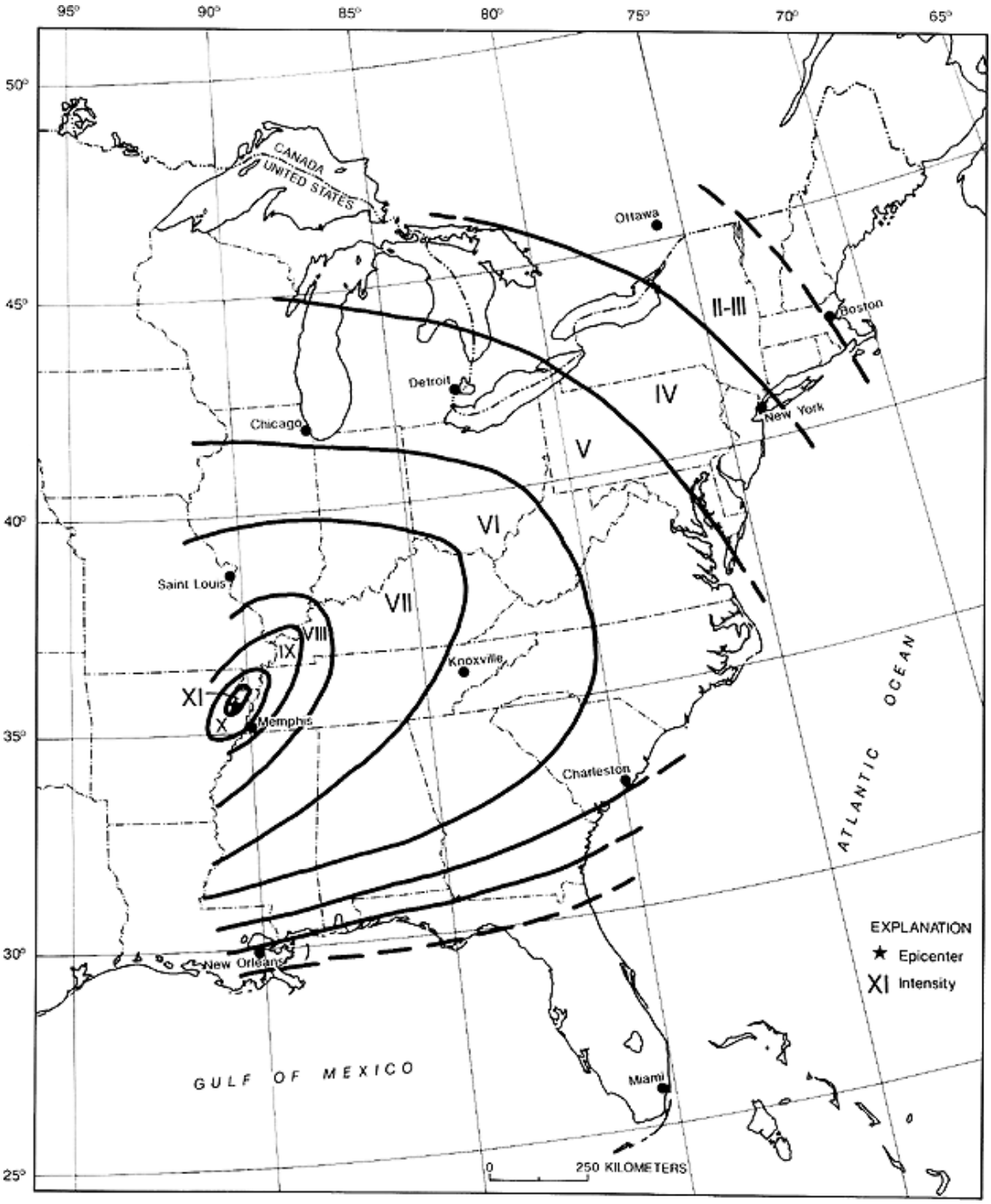

Figure 3.6 Map showing Modified Mercalli Intensities for the December 16, 1811 earthquake (from Stover and Coffman, 1993).

3.3.1.2.2 1895 Charleston, MO, Earthquake On October 31, 1895, an M6.7 earthquake centered near Charleston, MO, shook a large portion of the central and eastern United States. It was the largest earthquake to occur in the Mississippi Embayment since the New Madrid earthquakes. Structural damage and liquefaction phenomena were reported along a line from Bertrand, MO, in the west to Cairo, IL, in the east. Many sand blows were observed in an area southwest of Charleston and south of Bertrand. Isolated occurrences of sand blows also were reported north and south of Charleston (Stover and Coffman, 1993).

Severe damage occurred in Charleston, Puxico, and Taylor, MO; Alton and Cairo, IL; Princeton, IN; and Paducah, KY. The earthquake caused extensive damage to almost all the buildings in the commercial section of Charleston. At Cairo, east of Charleston, most buildings lost chimneys or windows. The courthouse, library, and a church in Cairo, IL, sustained extensive damage, and the brick walls of many buildings in the downtown area were badly damaged. Other damage include a cracked pier on an Illinois Central Railroad bridge over the Ohio River at Paducah and downed chimneys at Gadsden, AL; Evansville and New Waverly, IN; Covington, Spottsville Depot, and Uniontown, KY; St. Louis, MO; and Memphis, TN (Stover and Coffman, 1993). Figure 3.7 shows the area affected by strong shaking during the 1895 Charleston, MO, earthquake compared to the area of effect from the 1994 Northridge, CA, earthquake. Earthquakes emanating from the central United States tend to transmit seismic energy over much greater distances than similar size shocks in California because the basement rocks are more continuous and dense, allowing them to propagate seismic energy at greater velocities with less damping than crustal units underlying most of the western United States. The Modified Mercalli Intensities for the earthquake are mapped on Figure 3.8. By 1895 there were numerous reports of shaking intensity reported from west of the Mississippi River as compared to the 1811-1812 earthquakes because the region west of the Mississippi River had become more populated.

Earthquakes the size of the 1895 Charleston, MO earthquake (M_s 6.8) are believed to have a recurrence interval of 75 years ± 15 years (Hamilton and Johnson, 1990; CUSEC, 1999). This suggests that a similar size earthquake should have occurred sometime between 1950 and 1980. This moderate size earthquake may well be overdue,

or the 1895 event may have been a large aftershock in the wake of the 1811-12 earthquake sequence.

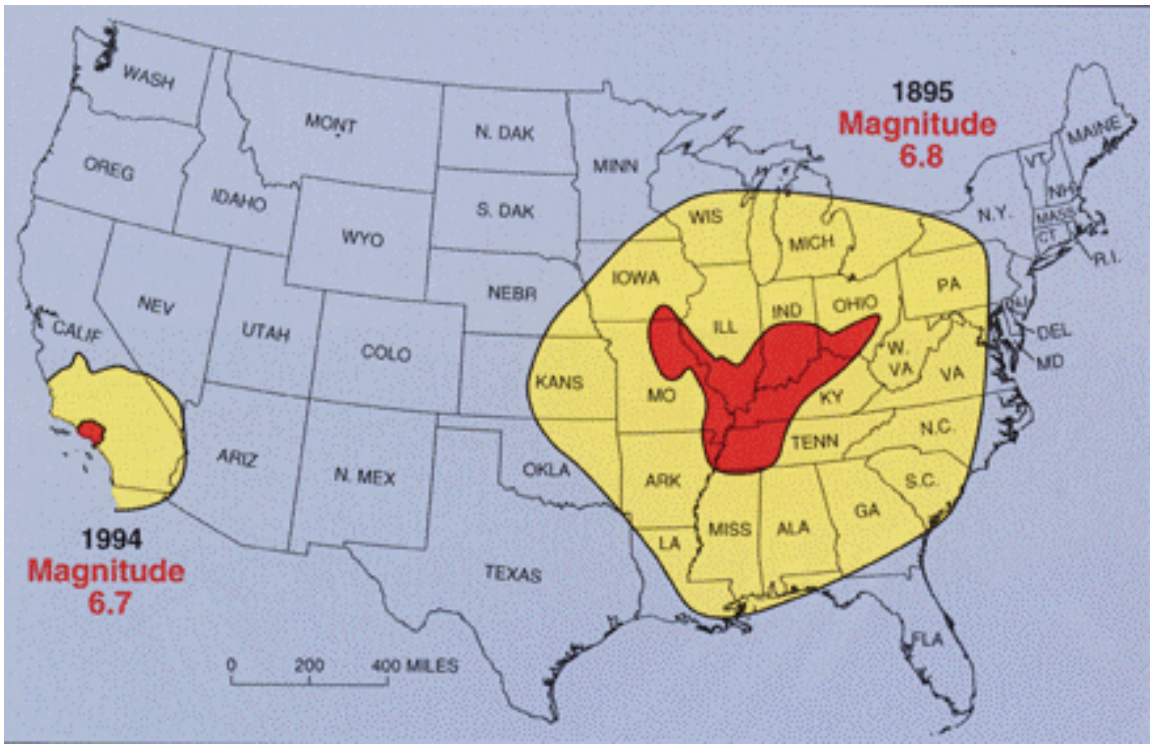

Figure 3.7 Map comparing the areas impacted by the M 6.7 1994 Northridge, CA earthquake and the M 6.8 1895 Charleston, MO earthquake. Areas in red show the greatest impact, MMI V or greater, and areas in yellow show extent of felt effects. (from Schweig, et al., 1995)

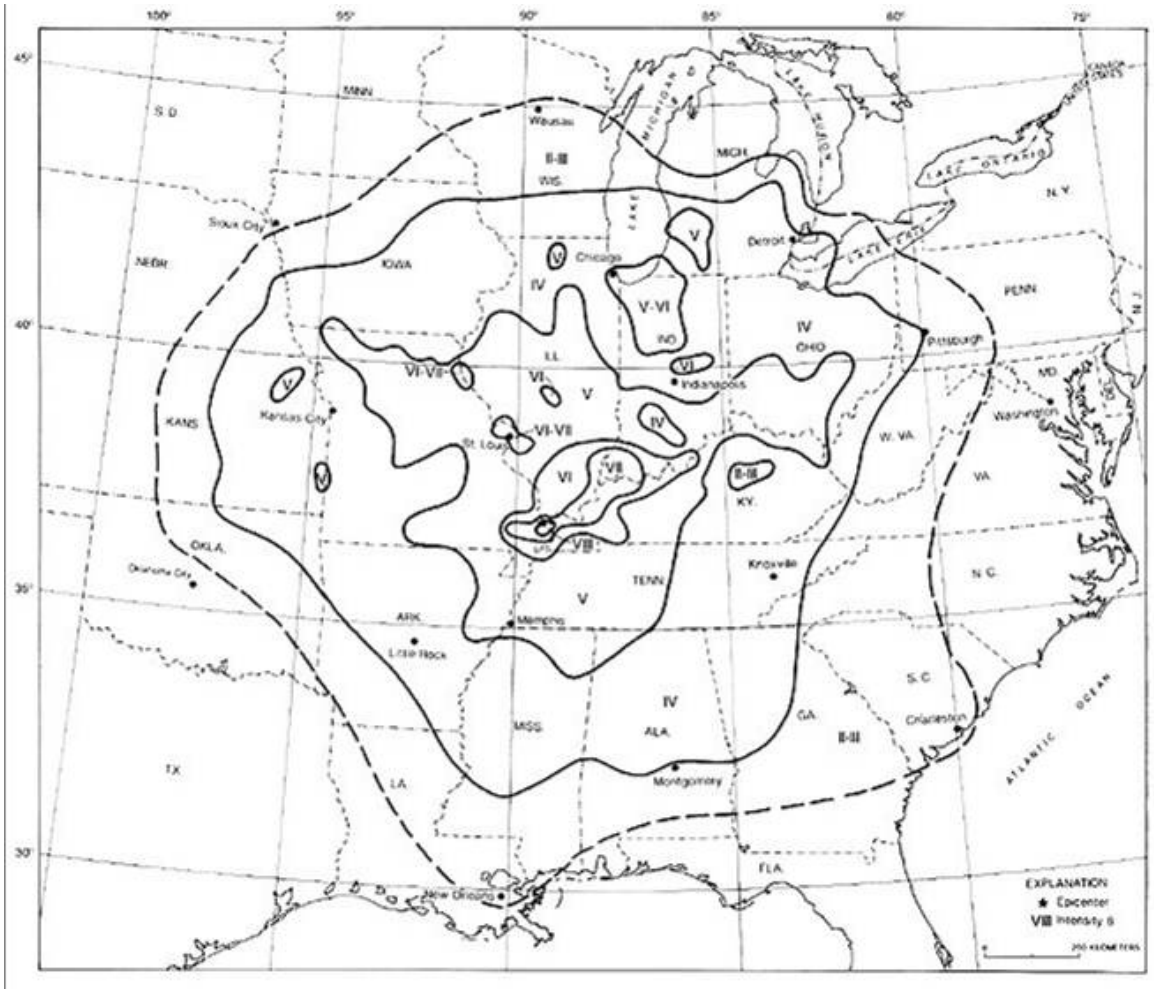

Figure 3.8 Modified Mercalli Intensity map for the M 6.8 1895 Charleston, MO, earthquake (from Stover and Coffman, 1993).

3.3.1.3 Current and Historic Seismicity Very little written record exists of seismic activity in the NMSZ prior to the 19th Century. However, Native American traditions speak of several earthquakes in the upper Mississippi Embayment (Fuller, 1912; von Hake, 1974). The first written record of seismic activity in the NMSZ was noted in 1699. A French missionary on a voyage down the Mississippi River reported feeling a distinct tremor on Christmas Day 1699 while camped in the area of what is now Memphis, Tennessee (von Hake, 1974).

Between 1838 and 1976 approximately 18 earthquakes with a body wave magnitude (Mb) of 5.0 or greater have been recorded in the NMSZ (Steckel, 1992).

From 1974 to 1978, 741 earthquakes were detected by seismograph stations in the NMSZ (Boyd and Schumm, 1995). Figure 3.9 is a map showing the locations of all detected earthquakes in the NMSZ from 1974 to 1995, and Figure 3.10 shows the seismic record for the NMSZ from 1990 to 2003. These seismic records indicate that the NMSZ is still a seismically active area with the potential for damaging earthquakes.

The four largest earthquakes in the NMSZ other than the 1811-12 New Madrid and 1895 Charleston, MO earthquakes have been recorded in 1843, 1917, 1934, and 1968. On January 4, 1843, a M 6.3 earthquake occurred near Marked Tree, AR, which caused notable damage to masonry chimneys and walls in Memphis, TN. One building reportedly collapsed as a result of the ground shaking. The ground surface sank at some places near New Madrid, MO and there was an unverified report that two hunters were drowned during the formation of a lake. The total felt area included for the 1843 earthquake included at least 1,036,000 square kilometers (van Hake, 1974; NEIC, 2003). A moderate earthquake on April 9, 1917, in the Ste. Genevieve - St. Mary's, MO area was reportedly felt over a 518,000 square kilometer area, from Kansas to Ohio and Wisconsin to Mississippi. In the epicentral area windows were broken and plaster cracked. A second shock of lesser intensity was felt in the southern part of the area. The small railroad town of Rodney, MO, experienced a strong earthquake on August 19, 1934. At nearby Charleston, windows were broken, chimneys collapsed or were damaged, and articles were knocked from shelves. Similar effects were observed at Cairo, Mounds and Mound City, IL, and at Wickliff, KY. The area of destructive intensity included more than 596 km^2. The November 9, 1968, earthquake centered in southern Illinois was the strongest in the central United States since 1895. The M 5.5 shock caused moderate damage to chimneys and walls at Hermann, St. Charles, St. Louis, and Sikeston, MO. The felt areas include all or portions of 23 states (von Hake, 1974).

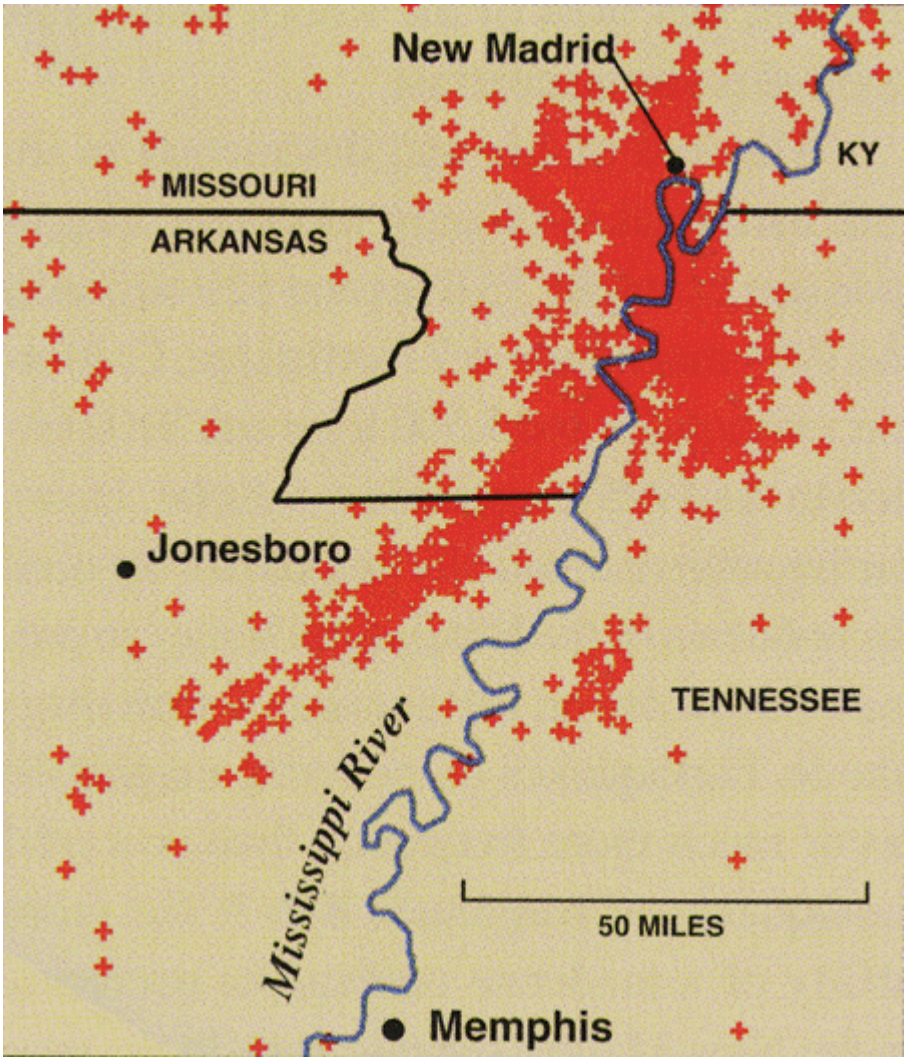

Figure 3.9 Map showing locations of NMSZ earthquakes from 1974 to 1995 (from Schweig, et al., 1995)

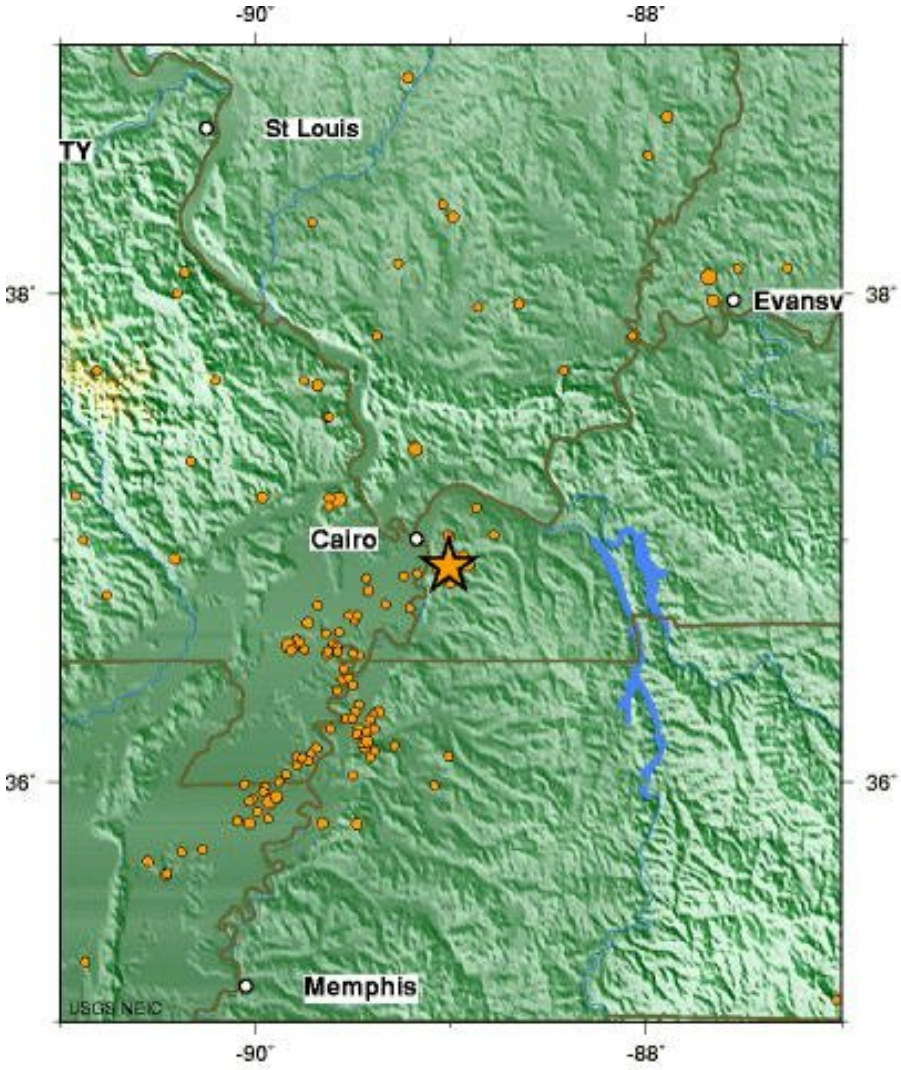

Figure 3.10 Shaded relief map of the upper Mississippi Embayment and NMSZ showing locations of recorded earthquakes from 1990 to 2003. The large star indicates an M4.5 earthquake that occurred in western Kentucky in 2003. (NEIC, 2003)

3.4. CROWLEY'S RIDGE

The most prominent topographic feature in the Upper Mississippi Embayment is Crowley's Ridge. Crowley's Ridge is a semi-continuous elevated upland lying west of the Mississippi River (Figure 3.11). The ridge extends from the Thebes Gap – Cairo, IL, area in the north to Helena, AR, approximately 380 km (236 mi) to the south (Figure 1.4). The ridge is 32 km (20 mi) wide at its widest point and up to 90 m (295 ft) high in some areas. However, some portions of the ridge exhibit only two to three meters of relief.

Crowley's Ridge appears to have been formed by a combination of Plio-Pleistocene deposition, late-Quaternary faulting (Figure 3.1), and Holocene Mississippi River erosion (Cox, 1988; Van Arsdale, 1992; Saucier, 1994; Boyd and Schumm, 1995). The western escarpment was eroded by the Pleistocene proto-Mississippi River, and, to the north, by the St. Francis River. The eastern escarpment has been eroded by the Holocene and present-day Mississippi River, as well as the St. Francis River in Arkansas. The northern portion of the ridge consists mainly of Paleozoic and Mesozoic rock capped by Plio-Pleistocene sediments (Figure 3.2) (Steckel, 1992; Santi and Neuner, 2002). The southern portion of the ridge is formed by Eocene sediments underlying Plio-Pleistocene sands and gravels (Figure 3.1) (Fisk, 1944; Guccione, et al., 1986; Saucier, 1994a, 1994b). Most of the ridge is capped by multiple Pleistocene loesses, including the Peoria Loess, and Loveland and Roxanna silts (Guccione, et al., 1986; Saucier, 1994a, 1994b; Ding, 1991). The loess is only a thin veneer on the northern portion of the ridge, but thickens considerably to the south (Leighton and Williams, 1950). Figure 3.11 is a photograph of a large theater-head headscarp on Crowley's Ridge showing the loess, gravel, paleosol stratrigraphy. In this area the loess is only 4 m (13 ft) to 10 m (32 ft) thick, but at the far southern end of Crowley's Ridge, between Marianna and Helena, AR, the loess can reach up to 43 m (140 ft) thick (Guccione, et al., 1986).

Over the years Crowley's Ridge has been subdivided into several segments when referred to in the geologic literature, including Dexter and Sikeston Ridges, and the Bloomfield and Benton Hills (Figure 1.4). Sikeston Ridge extends north from New Madrid approximately 37 km (23 mi). The ridge varies in width from 0.8 km (0.5 mi) to 1.9 km (1.2 mi) wide in the north to a fairly consistent 4 km (2.5 mi) wide in the southern 18 km (11 mi) of the ridge. Sikeston Ridge exhibits approximately 6 m (20 ft) of relief along its entire length. The eastern and western edges of the "ridge" tend to be relatively straight, suggesting some element of structural control (Boyd and Schumm, 1995). The Benton Hills segment of Crowley's Ridge is at the far northern portion of the ridge, and consists mainly of Paleozoic and Mesozoic sedimentary rock, possibly related to the rocks of the Ozark highlands to the northwest (Steckel, 1992). The total relief on the Benton Hills is about 68.5 m (225 ft).

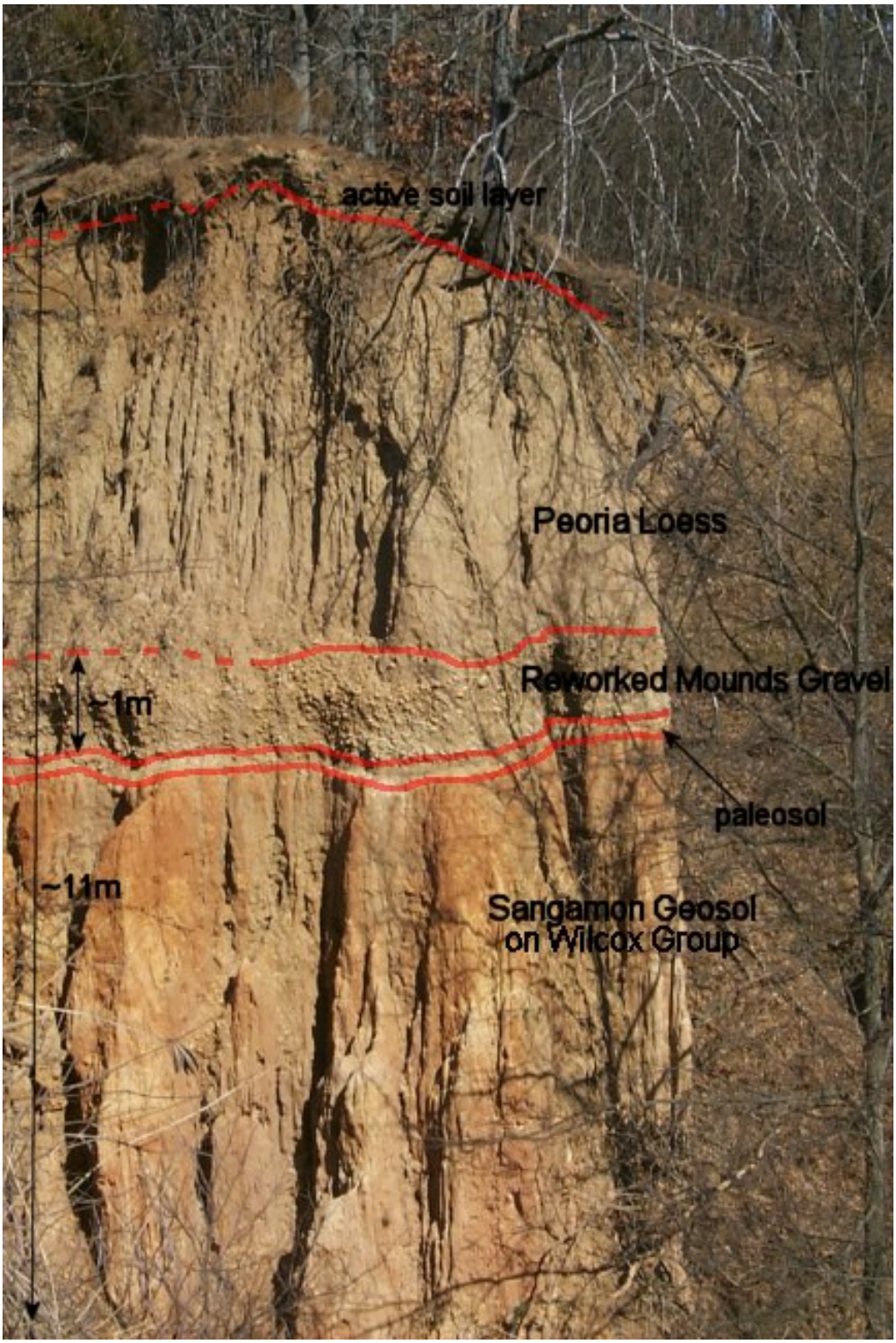

Figure 3.11 Photograph of an active theater-head headscarp on Crowley's Ridge near Valley Ridge, MO. Peoria loess can be seen overlying a gravel layer identified as reworked Mounds gravel. Underlying the gravel is a Sangamon Geosol on the Eocene Wilcox Group. The height of the scarp is approximately 11 m.

3.5. DEMONSTRATION QUADRANGLES

The preliminary screening of the 52 USGS 7.5 minute quadrangles covering Crowley's Ridge showed that the LaGrange, West Helena, and Helena, AR, quadrangles exhibited numerous areas of topography consistent with seismically-induced landslippage. Preliminary studies of these quadrangles using the topographic mapping protocol succeeded in identifying more than 200 definite and probable landslides, including translational block slides, earth flows, shallow retrogressive slumps and slump complexes, and lateral spread features, mostly along the eastern erosional escarpment of Crowley's Ridge. Previous studies in the area indicated, at most, eight landslides and shallow retrogressive landslide complexes within the LaGrange quadrangle (Ding, 1991; McFarland, 1992). An active landslide headscarp (Figure 3.12) within the Valley Ridge quadrangle was found during a field investigation by Jim Palmer of the Geological Survey and Resource Assessment Division (GSRAD) of the Missouri Department of Natural Resources (MoDNR). David Hoffman, also of GSRAD, relayed the Mr. Palmer's discovery and suggested further investigation of the Valley Ridge quadrangle. Study of the topographic map of the Valley Ridge quadrangle indicated a large number of potential landslides, many of which were confirmed during subsequent field reconnaissance with Messrs. Palmer and Hoffman.

Due to the high number and variety of probable landslides identified in the LaGrange, West Helena, Helena, and Valley Ridge quadrangles, these four quadrangles were chosen as demonstration quadrangles for this project. Screening of the quadrangles using the topographic mapping protocol to determine areas of likely landslide activity, followed by field investigation of the suspected sites, has identified numerous landslides in these areas. Sections 4 and 5 explain in detail the methodology for using the topographic mapping protocol and the ensuing field work.

4. METHODOLOGY

4.1. TOPOGRAPHIC MAPPING PROTOCOL

In an effort to identify possible seismically-induced earth movement along Crowley's Ridge related to either the 1811-12 earthquakes or paleoseismic events, the feasibility of recognizing landslide and lateral spread features using topographic mapping protocols has been studied. The protocol uses drainage and topographic keys to recognize anomalous site characteristics typical of various landslide forms, including lateral spreads, slump-earthflows, translational block slides, shallow retrogressive slump complexes, and theater-head slump-flow complexes. As with the use of stereopair aerial photos, some background information on the bedrock geology, underlying structure, and landslide mechanisms commonly exhibited in the area are needed before beginning any program of reconnaissance-level landslide inventory mapping.

This research indicates that topographic maps can easily be exploited for landslide hazard mapping, with certain limitations of scale and cartographic information quality affecting the end product. The employment of topographic mapping protocols as a reconnaissance method has the potential to revolutionize landslide inventory mapping by its use as a screening tool across large tracts of land. One of the major goals of this research was to test the validity of topographic protocols to identify landslide features across test areas selected along various portions of Crowley's Ridge, which extends over 240 mi (Figure 1.4). The test areas included the LaGrange, West Helena, Helena, and Stubbs Island, AR, and the Valley Ridge, MO, 7.5-minute topographic quadrangles. The end product of any reconnaissance landslide inventory mapping is a map showing specific slopes or areas exhibiting evidence of having been subject to mass slope movement(s), which can only be verified through site-specific field investigation. The identification of these seismically-induced landslide features is a necessary first step in making people aware that such hazards exist in the NMSZ and that such features could be expected to re-activate during future earthquakes.

4.1.1. Anomalous Topographic Expression The primary method evaluated for identifying landslides was anomalous topographic expression. Different types of geologic source materials tend to exhibit characteristic geomorphic expression based on

their physical properties, such as lithology, structure, bedding thickness, and joint spacing. The screening process begins with an examination of topographic patterns, searching for anomalies and inconsistencies which do not appear on adjacent slopes or changes which do not appear to be typical of underlying lithologic and structural contacts. In some cases, deranged or parallel drainage patterns allow large features, such as detachment complexes and landslides to easily be discerned. The most common forms of anomalous topographic expression associated with landsliding are described below. Various combinations of the topographic indicators are used to distinguish between different types of landslides, as described in Subsection 4.2.

1. Divergent contours: Contours that curve upslope immediately above contours that curve downslope. Divergent contours often suggest removal of material (deflation) from the upper portion of a landslide and deposition (inflation) in the lower portion of the slope, along the same fall-line, and perpendicular to the overall trend of the elevation contours (Figure 4.1).
2. Crenulated contours: Contours that exhibit waviness or scalloping not otherwise associated with the underlying geologic material and/or structure. Crenulated contours are often diagnostic of terrain underlain by repeated sequences of superposed landslippage (Figures 4.1 and 4.2).
3. Arcuate headscarp evacuation areas: Steep-sided, curvilinear features at the upslope boundary of a landslide formed by removal and transportation of slide material downslope (Figure 4.1).
4. Isolated topographic benches: Relatively broad, flat areas below the headscarp evacuation area formed by back-rotation of slump surfaces or infilling of pull-apart grabens (Figure 4.1)
5. Extended topographic ridges or isolated topographic knobs: Often formed by deep-seated translational movement of slide mass pulling the end of the ridge downslope (Figure 4.2).
6. Sudden up- or down-slope turns in hillside contours: Sharp changes in topography that do not appear related to underlying geologic structure or material changes. Often caused by downslope movement of an isolated portion of hillside (Figure 4.2).

7. Stepped topography: A often curvilinear and/or en-echelon series of topographic benches related to repeated episodes of retrogressive slumping, infilled headscarp grabens, or lateral spreading.
8. Fan profiles: Fan-like geomorphic features that do not exhibit the typical degrading profile of an alluvial fan are likely the depositional lobes of debris flows, earth flows, or lateral spreads.

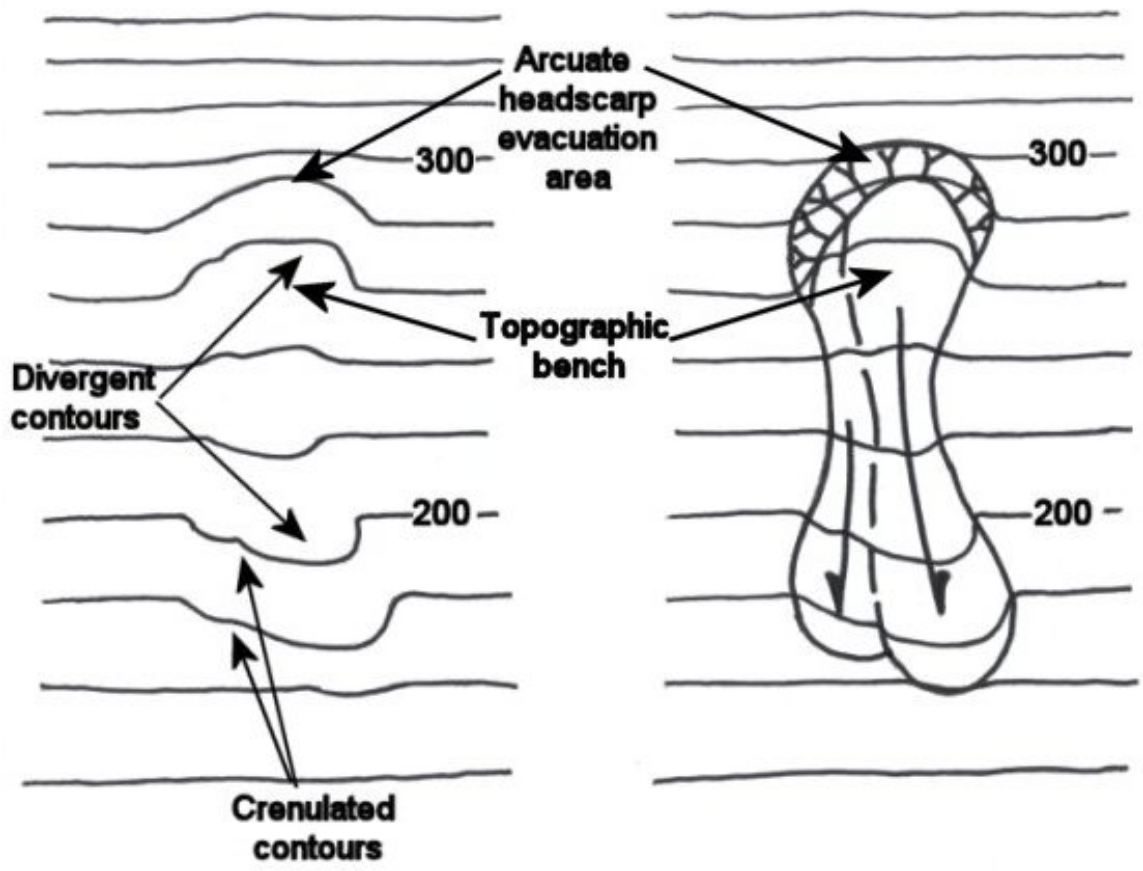

Figure 4.1 Illustration showing topographic anomalies used in landslide identification. The illustration shows a typical set of coalescing earth flows, although the anomalies may be related to other landslide types as well.

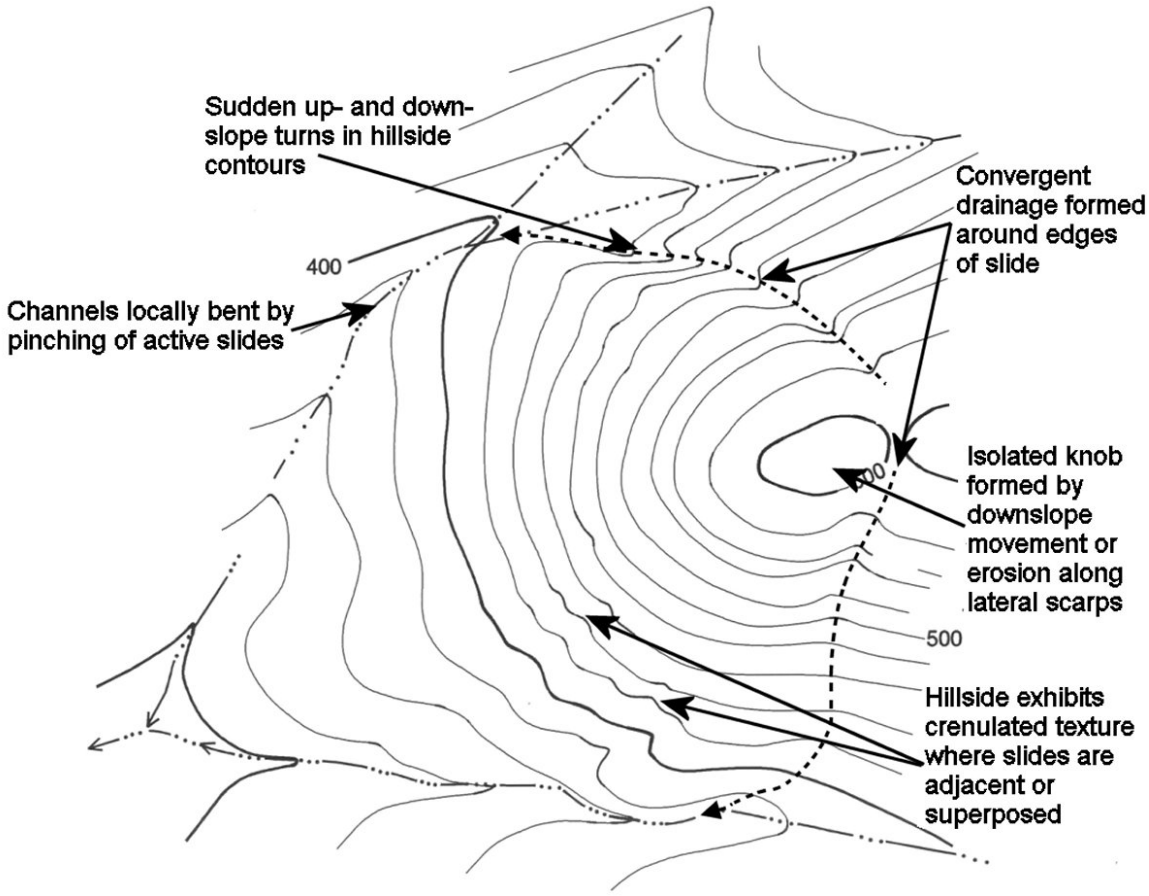

Figure 4.2 Illustration of anomalous topography associated with landsliding. The illustration shows a large translational slide with smaller earth flows and slumps on the slide mass. Figure 4.22 shows a mapped version of this slide complex.

4.1.2. Anomalous Drainage Patterns Closely related to anomalous topographic expression is the identification of past landslides through examination of anomalous drainage patterns. The drainage pattern of an area is a function of the underlying geologic material as well as any jointing or structural features (folding, faults and joints). Anomalous drainage patterns are any which do not appear similar to the drainage network developed within reasonable proximity of the area being evaluated. If distinct variations occur which cannot simply be attributed to marked lithologic changes or structural contacts, it may indicate that the drainage patterns have been altered by landsliding. Some anomalous drainage forms that may indicate landsliding are described below.

1. Convergent drainage: Gullies and small streams begin headward erosion toward each other along the lateral margins of a landslide (Figure 4.2).
2. Local bending of channels: Displacement and/or rerouting of stream channels as a result of landslide debris partially to fully blocking the stream channel (Figure 4.2)
3. Hydraulic jumps or other sudden changes in hydraulic grade lines: The gradient of a stream profile will decrease as the stream crosses landslides and landslide debris and then increase on the downstream side of the obstruction, rather than following a typical log-spiral shape (characterized by decreasing hydraulic grade with increasing watershed area downstream).
4. Ratio of drainage-basin area to fan size: Alluvial fan-like features with a drainage basin too small to supply the requisite sediment input may be the result of landsliding or lateral spreads (Figure 4.3). This is a comparative analysis between adjacent watersheds with similar characteristics. Larger watersheds will tend to respond more quickly to agents of geomorphic change because of increased stream power (Bull, 1991).

4.1.3. Aerial Photography and Remote Sensing Since the early 1950s evaluation of stereopair aerial photos has been the method most widely employed to identify various types of landslides (Liang, 1952; Liang and Belcher, 1958). Recognizing landslide features on stereopair aerial photos depends on a number of factors, including density of foliage and height of tree cover; age of the slope movements; time of year; and time of day the photos were imaged. For most landslides, a low sun angle from behind the headscarp forms long shadows and gives the best results (Figure 4.4).

The position of the sun's azimuth and consequent ground shadows are of paramount importance in discerning landslides on aerial photos. Figure 4.4 shows a northeast-facing slope in Moraga, California, at the upper left side of the image, imaged in 1946 with slight backlighting. Figure 4.5 is the same ridge imaged in 1984 with late morning sun shining directly on the slope. Although there appears to be increased vegetative cover in Figure 4.5, the earthflows are largely undiscernable. Five of the

Figure 4.3 The large fan-shaped feature shown above emanates from a watershed anomalously small to support such a large fan. The feature may be a debris fan, earthflow complex or lateral spread, if the ratio of the drainage basin size to the fan size is much smaller compared to drainage basin to fan ratios for similar watersheds along the same escarpment.

eight earthflows seen in Figure 4.4 had been reactivated in 1983, just a year prior to the imaging of Figure 4.5 (Rogers and Doyle, 2003). This comparison suggests that aerial photos may not be inclusive tools for landslide mapping, especially if limited to just one set of images.

Figure 4.4 – Vertical photo of Campolindo Ridge in Moraga, CA, taken in 1946 with oblique backlighting, which shows a series of dormant earthflows to good effect.

Figure 4.5 – The same view as the previous figure, but imaged in 1984, with morning sunlight shinning directly on the slope. The earthflows seen on Figure 4.4 were reactivated in 1983, but are not discernable on this image.

4.1.4. Scale Impacts A key factor in exploiting topographic information is the density and quality of the data. Small-scale maps, maps derived from high altitude/low ground resolution imagery, or maps of areas covered with heavy vegetation may tend to mask out details of smaller slides. Several physical features appear to bias topographic maps prepared from orthorectified stereopair aerial photography to the point of producing errors in surface topography. These factors include:

1. the severity of the topography being mapped;
2. the altitude of the source imagery;
3. the density of the ground cover over the slopes;
4. the height of the vegetation cover;
5. the time of year the images were made (trees with or without leaves);
6. the stereo model set-up techniques; and
7. the topographic control used for the map area.

Dense foliage, high trees and steep slopes may combine to produce topographic maps that are not spatially accurate on slopes because the mapping models use linear interpolation between visible control points to create contours. This means that slight nuances in the slope profile are often missed in preparing maps of heavily wooded slopes. Pyles and Froehlich (1987) discuss the impact of dense vegetation and high tree canopies on interpretation of aerial photographs for landslide mapping. Figure 4.6 illustrates the effect of tree height on aerial photographic mapping of landslides. Interference by the tree canopy may obscure all or part of landslides, depending on the location and orientation of the camera, the ground slope, tree height, and slide dimensions. In areas with a high, thick tree canopy, only large slides will be visible. Pyles and Froehich (1987) suggest that in unmanaged forest land, similar to what is found in the areas researched for this report, some landslides would have to be over two and a half acres in area to be recognizable at 1:24,000 scale. Since most topographic maps produced by the USGS are created from aerial photographs, errors in topographic interpretation due to tree canopy interference on the photographs is carried over to the topographic maps. The increasing use of Light Detection and Ranging (LiDAR), Laser Detection and Ranging (LADAR) and Interferometric Synthetic Aperture Radar (INSAR or IfSAR) methods for

imaging ground surfaces may alleviate many of the mapping problems inherent with utilizing visual photographic images for producing topographic maps discussed above.

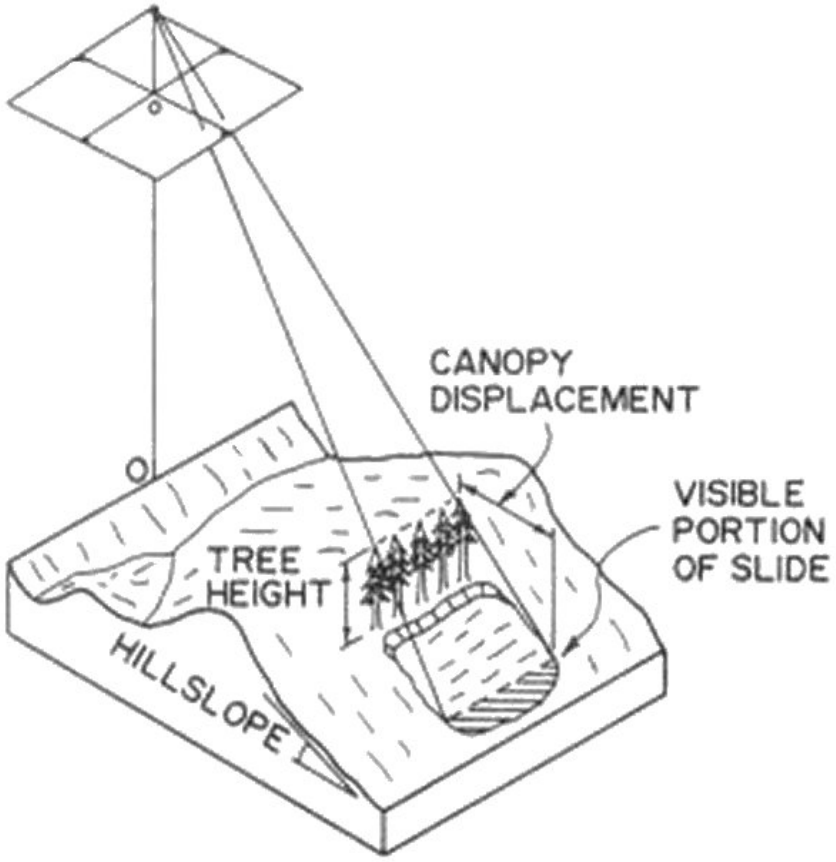

Figure 4.6 Illustration showing the impact of tree canopy interference on the identification and interpretation of landslides using aerial photography and topographic maps derived from aerial photography. Only a small portion of a landslide is visible due to displacement by the tree canopy (from Pyles and Froehlich, 1987).

4.1.5. Contour Intervals In general, the larger the map scale, the more precise the mapping can be, and small slides may be delineated with some degree of precision. A good guide is the "five-contour rule". If at least five contours cross an old slide feature, there is reasonable confidence that a landslide feature can be mapped. If the contour interval were 40 feet, this would mean the minimum size slide that could be discerned would need to be at least 4 x 40 feet, or 160 feet, which is the vertical space between 5

contours. That is a pretty typical threshold value for discerning most landslides on conventional USGS 7.5-minute topographic quadrangles with 40-feet contour intervals. The scale of discernable landslides decreases with increasing contour density. For example, a map with 20-foot contours should allow identification of earthflows with at least 80 feet of vertical relief, and a 10-foot contour maps should allow earthflows as little as 40-feet high to be discerned.

4.2. APPLICATION OF GEOGRAPHIC IMFORMATION SYSTEMS TO HAZARD IDENTIFICATION AND MAPPING

4.2.1. 7.5' United States Geological Survey Quadrangles 7.5-minute series USGS topographic quadrangles, which cover 7.5' of latitude and 7.5' of longitude, have been produced for the entire United States. These maps show the topography of an area as well as the major cultural features at 1:24,000 scale. The topographic maps of the Helena, AR, and Valley Ridge, MO, areas have a contour interval of 10 feet. Both paper and digital versions of the 7.5' quadrangles were examined for topographic and drainage anomalies during this project. First, the paper maps were examined to determine the likelihood of landslides on a particular map, and for initial identification of potential landslide sites.

After initial investigations identify landslides and the potential for landslides, digital versions of the topographic maps, or DRGs (Digital Raster Graphics), are input into a Geographic Information System (GIS). These DRGs are georeferenced, so that the GIS program will be able to determine the map coordinates of any location. The GIS allows the DRG to be viewed at a variety of scales to allow for more accurate mapping of landslides. In ArcGIS, a GIS program by ESRI, the 7.5' quadrangles can be viewed at a scale of 1:3,000 without excessive pixilation of the digital map (Figure 4.7). In the GIS program Global Mapper, by the company of the same name, the DRGs can be viewed clearly up to a 1:1,500 scale (Figure 4.8). Overlaying the DRGs on USGS Digital Elevation Models (DEMs) makes visualization of topography and identification of topographic and drainage anomalies easier.

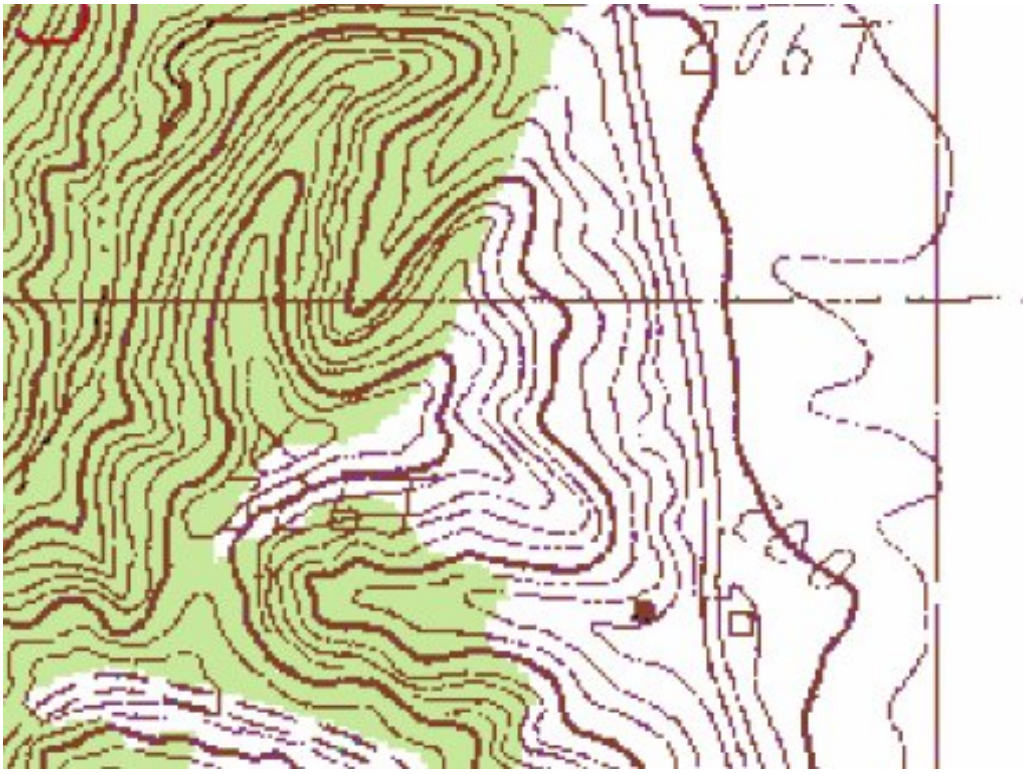

Figure 4.7 DRG image exported from ArcGIS at 1:3,000 scale.

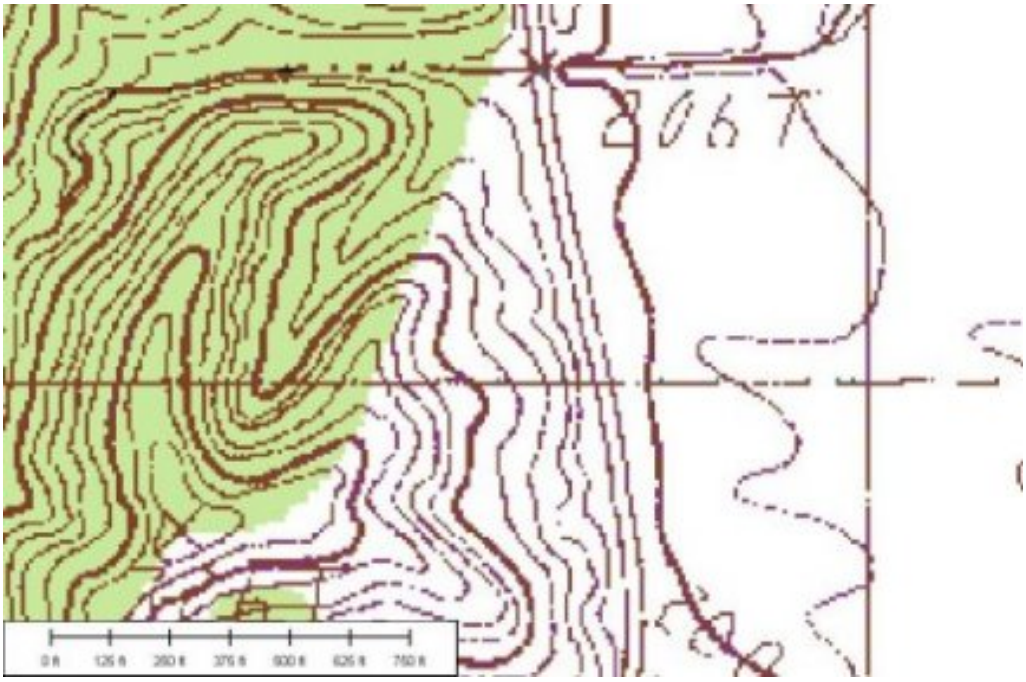

Figure 4.8 DRG image exported from Global Mapper at 1:1,500 scale, showing approximately the same area as in Figure 4.6.

4.2.2. United States Geological Survey Digital Elevation Models In addition to DRGs, the USGS routinely produces Digital Elevation Models (DEMs) of the same 7.5-minute quadrangles. DEMs are created using the topographic map of an area, overlaying a grid of either 30-meter or 10-meter squares, and georeferencing the map elevations at the grid intersections. Since DEMs have not only latitude and longitude for each point, but elevation as well, the DEMs can be input into GIS programs and DEM viewers to create 3D representations of topography.

4.2.2.1 30-meter Digital Elevation Models 30-m DEMs have been created by the USGS for the entire United States. These DEMs can be obtained from the USGS, state geological surveys, or from the internet. 30-m DEMs show a fairly coarse approximation of elevation. Elevation points are taken at 30 m intervals, so one pixel represents about 900 m^2 of ground area. The 30-m DEMs work best for examination of large areas of land at a fairly small scale. In areas of little relief, 30-m DEMs are useful, however, in areas of high relief, the 30-m DEMs do not provide a useful approximation of the topography for terrain analysis. Figure 4.9 shows a 30-m DEM in both standard DEM format and as a hillshade, or shaded relief, DEM. Shaded relief allows the topography of an area to be viewed in a pseudo-3D format. Hillshade images show the topography as it would look if a light source was shown on the area from a specific elevation and compass direction.

4.2.2.2 10-meter Digital Elevation Models 10-m DEMs are created using the same methodology as 30-m DEMs, but with a 10-m grid spacing. Therefore, each pixel represents 100 m^2 of ground area. This scale makes the 10-m DEMs more useful for mapping on a larger scale than 30-m DEMs. Unfortunately, very little of the United States is available on 10-m DEMs. For areas not already available as 10-m DEMs, the USGS will produce a new DEM, but the cost at the time of this research was $1000 per quadrangle. The 10-m DEMs used in this project were obtained through a cost-sharing program arranged with the USGS Mid-Continent Mapping Center in Rolla, MO. With their cooperation, 10-m DEMs of the four quadrangles in the Helena, AR, and one in Valley Ridge, MO, areas were compiled for use in this study.

Figure 4.10 shows a 10-m DEM, in both standard format and as a hillshade, of the same area as was shown in Figure 4.9. The altitude and azimuth for hillshade maps can be changed within GIS programs to highlight different features from different angles, as

shown in Figure 4.11. This eliminates one of the problems encountered with aerial photographs described above; sun angle causing obfuscation of slide features. During the course of this study it was discovered that overlaying the DRGs on the DEMs in both ArcGIS and Global Mapper makes it much easier to map terrain features. Figure 4.12 shows a Helena area DRG overlain on a DEM.

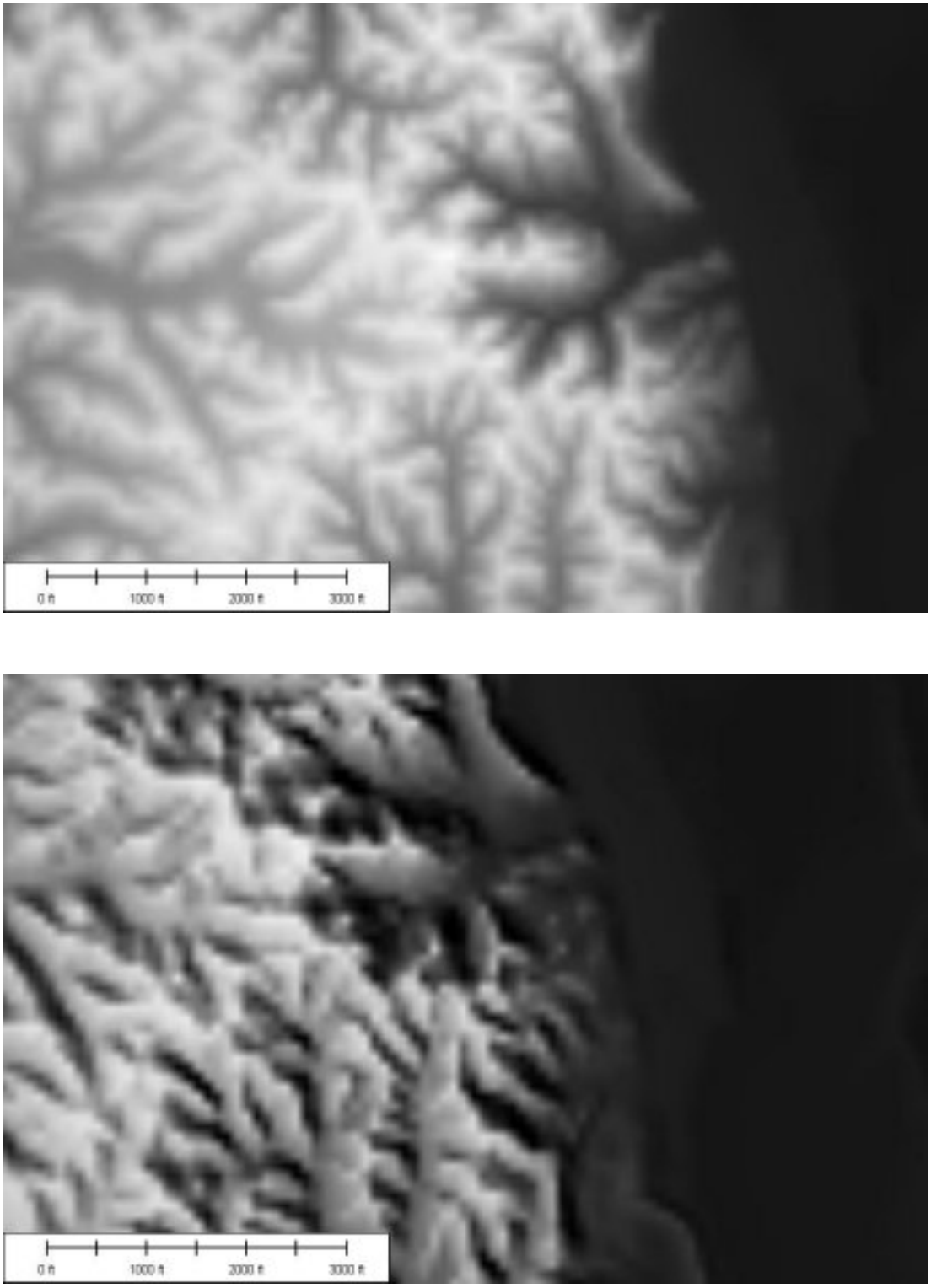

Figure 4.9 a) 30-m DEM in standard format exported from the GIS software Global Mapper. The area shown is just north of Helena, AR. b) Hillshade of the same area shown in a).

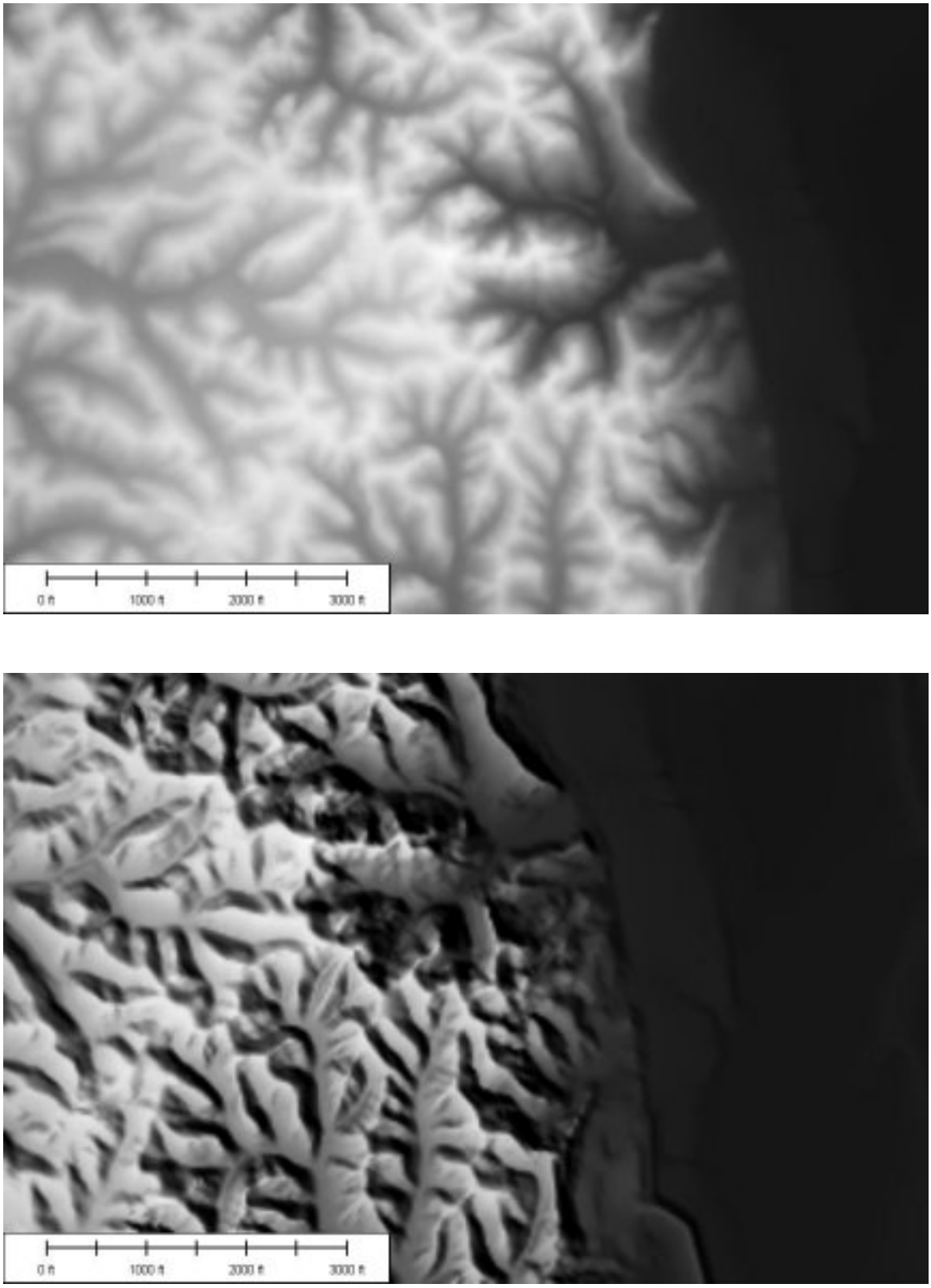

Figure 4.10 a) 10-m DEM showing an area on Crowley's Ridge just north of Helena. This is the same area as shown in Figure 4.8. b) Hillshade of the area shown in a). The light source is at an elevation of 55 m and an azimuth of 230°.

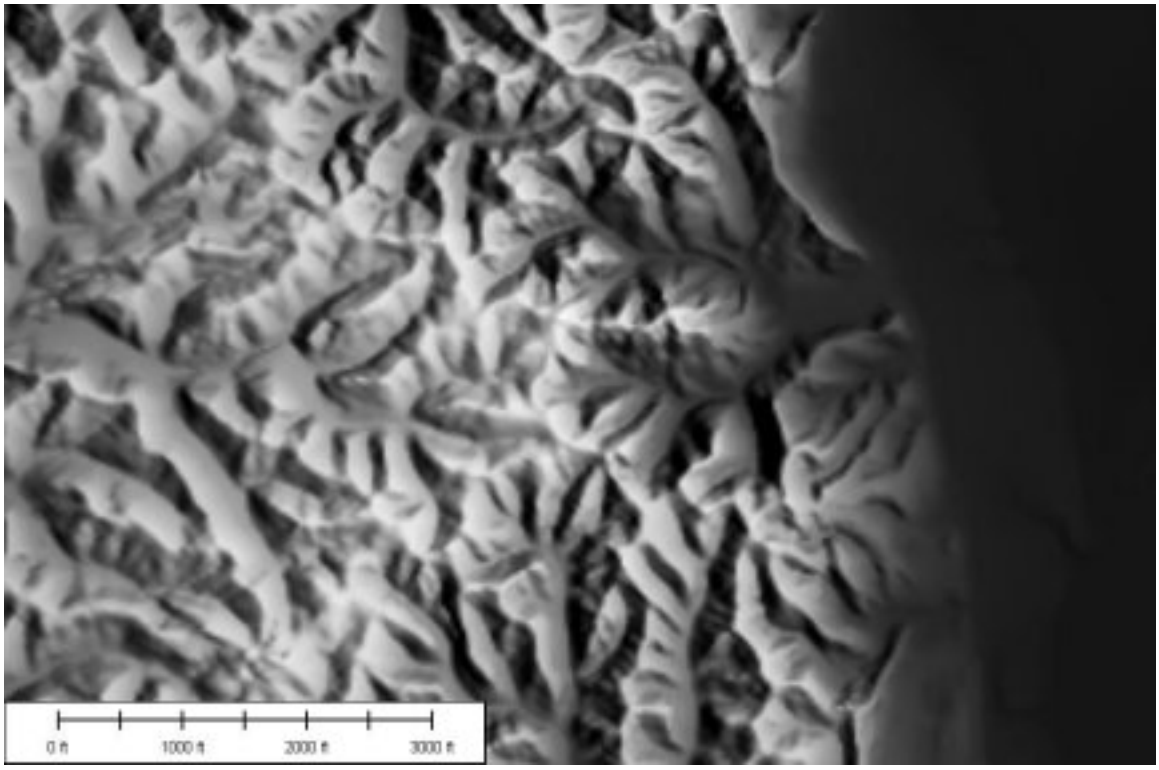

Figure 4.11 10-m DEM hillshade of the area in Figures 4.8 and 4.9 with the light source at an altitude of 55 m and an azimuth of 75°.

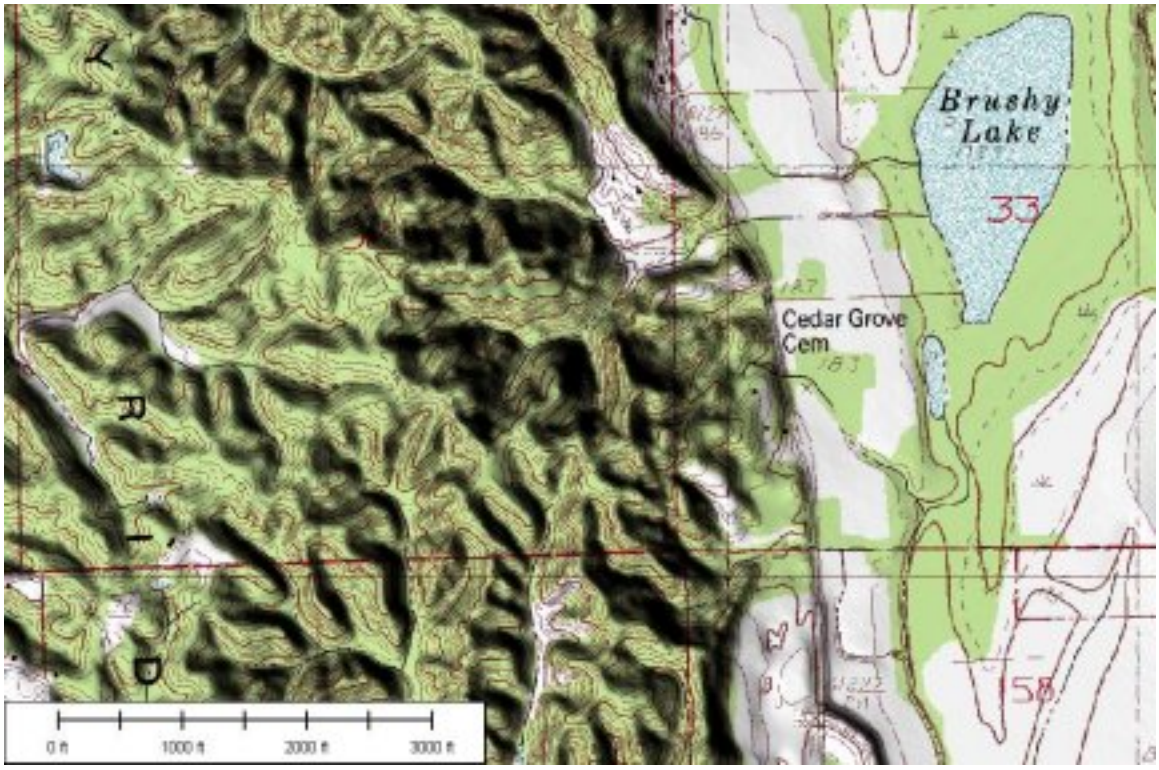

Figure 4.12 10-m DEM with DRG overlay created in Global Mapper. The area shown is the same area as in Figures 4.8, 4.9, and 4.10.

4.3. TOPOGRAPHIC EXPRESSION OF DIFFERENT LANDSLIDE TYPES

Five main landslide types had been identified along Crowley's Ridge near Helena, AR. The landslide types (lateral spreads, earthflows, translational block slides, slumps, and theater-head erosion complexes) and their associated topographic and drainage expression, are described below.

4.3.1. Lateral Spreads

4.3.1.1 Failure Mode Lateral spread features were first described in the geologic literature by Fuller (1912) in his landmark report on the 1811-12 New Madrid earthquakes. Although Fuller referred to the features he found in the NMSZ as "fissures", the mechanism for movement is the same as in lateral spreading. Figure 4.13 shows Fuller's sketch of a large graben formed by the lateral movement of a large block over "quick sand", towards an open channel. Today we realize that this "quick sand" was likely a confined sand seam which underwent liquefaction during earthquake shaking.

Unfortunately, there is no record of the exact locations of the "fissure" features described by Fuller.

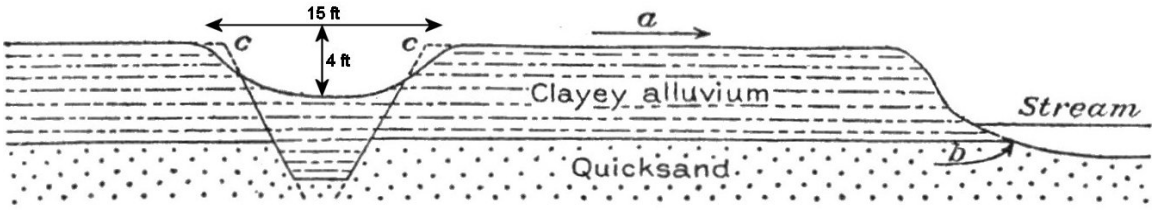

Figure 4.13 Fuller's (1912) sketch of a large "fissure" in the New Madrid Seismic Zone. The mechanism of formation described by Fuller is consistent with lateral spreading.

The term "lateral spread" was introduced by Varnes (1958) and subsequently used by Hansen (1966) and Seed and Wilson (1967) to describe the Turnagain Heights landslides which occurred in Anchorage during the 1964 Alaska earthquake. They discovered that the large flow slide was the result of liquefaction of discontinuous seams of cohesionless silt within the sensitive Bootlegger Cove formation, an uplifted estuarine clay. The liquefaction of the silt seams allowed large blocks of the overlying marine clay and surficial sand and gravel to be rafted towards Bootlegger Cove. Lateral spreads may cause the displacement of very large areas of ground and will often occur on very low angle failure surfaces. Previous to this investigation, no lateral spread features had been identified and named as such east of the Rocky Mountains.

The lateral spreads identified in the NMSZ are believed to have formed due to partial or total seismically-induced liquefaction of saturated confined sand, silt, and gravelly sand horizons underlying areas near or adjacent to channels or other natural depressions. The areas with the greatest potential for lateral spreading in the Upper Mississippi Embayment are:

1. along the margins of Crowley's Ridge where the channels of the L'Anguille, St. Francis, and Mississippi Rivers come within 0.60 km (0.375 mi) of the ridge;
2. areas adjacent to sweeping turns of the major river channels; and,
3. along levees and banks of large drainage ditches.

The main unit believed to have liquefied in lateral spreads on the margins of Crowley's Ridge is a Pliocene-age sand and gravel unit laid down as braided stream bar deposits in the area that was subsequently uplifted to become Crowley's Ridge (Guccione, et al., 1986). The Pliocene sand and gravel is underlain by Eocene basin-fill units and is overlain by deposits of Peoria Loess, Roxanna silt, and Loveland silt, which can reach thicknesses of 30 m (98 ft) or greater on the southernmost portion of Crowley's Ridge (Guccione, et al., 1986; Saucier, 1994a, 1994b), as shown in Figure 3.1. The loess acts a confining or semi-confining layer, nurturing the development of liquefaction during earthquakes.

4.3.1.2 Topographic Expression Topographic identification of lateral spread features was accomplished through examination of USGS 7.5-minute topographic maps, Digital Raster Graphics (DRGs) and GeoTIFF (georeferenced .tif files) images of the topographic maps, and 10m Digital Elevation Models (DEMs) of these same quadrangles. The major topographic indicators of a lateral spread feature may include:

1. divergent, or opposing, contours;
2. fan features much larger than could be supported by the local drainage area;
3. stepped features on fan surfaces;
4. headscarp evacuation grabens; and
5. arcuate, or theater-shaped, headscarps.

As divergent contours are the topographic anomaly common to several of the landslide types, identification of divergent contours must be combined with at least two of the other indicators to suggest the presence of lateral spreads. Large, arcuate headscarp areas and stepped features on the fan surface are the next most common topographic anomalies associated with lateral spread features.

Figure 4.14 shows two lateral spreads approximately 1.6 km (1 mi) north of Helena. The features exhibit several of the topographic indicators described above. Numerous other landslides, including earthflows, slumps, and translational block slides, have been mapped in the area using topographic s specific to the slide types. These slides are also shown on Figure 4.14.

Digital map data was input into the GIS programs ArcGIS, Global Mapper, and Terra Base II by MICRODEM. The maps generated from the data are then examined for topographic indicators of lateral spread features. Areas with topographic signatures that are suggestive of lateral spreading were highlighted for further examination using GIS programs followed by field reconnaissance. The use of the 10-m DEMs to create 3D and pseudo-3D images of the topography has greatly simplified the identification of the features. Figure 4.15 shows an oblique pseudo-3D view of a lateral spread from the Helena area with a large arcuate head scarp and evacuation graben at the edge of Crowley's Ridge.

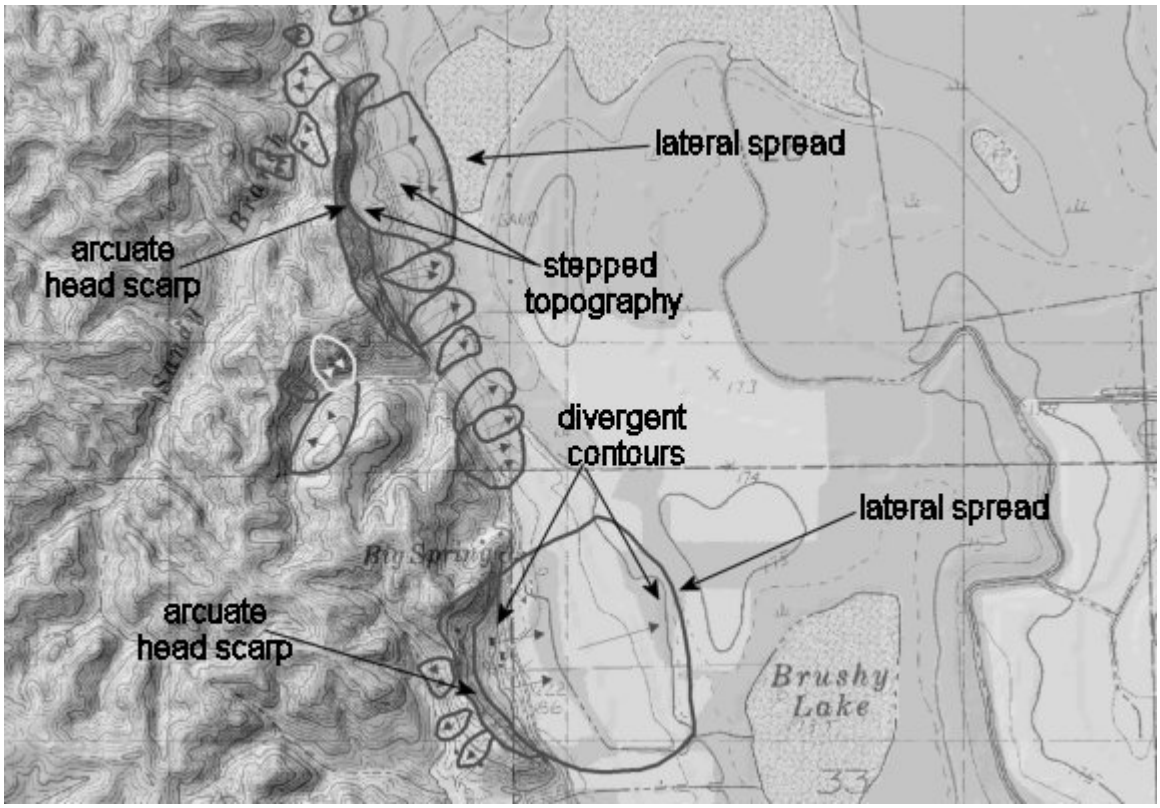

Figure 4.14 Two lateral spread features along Crowley's Ridge just north of Helena, AR, that show anomalous topographic expression typical of lateral spreads. Several other landslide types, including earth flows, slumps and translational block slides may also be seen in the figure.

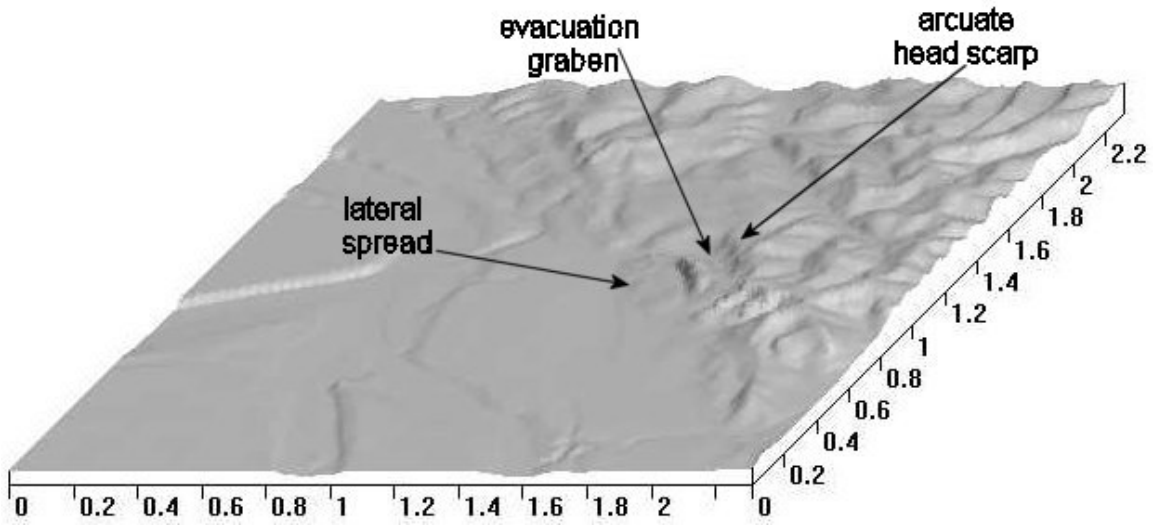

Figure 4.15 Oblique view of a lateral spread feature along Crowley's Ridge. A prominent arcuate head scarp and evacuation graben can be seen along the edge of Crowley's Ridge. Units are in miles.

Five prominent lateral spread features were identified in the Helena, AR, area through the use of topographic mapping protocols. All of the lateral spreads are on the eastern edge of Crowley's Ridge, and are located near the current channels of the L'Anguille, St. Francis, and Mississippi Rivers. These features tend to have a large arcuate headscarp created by down-dropped graben features and/or retrogressive slumps formed after initial movement of the distal portions of the lateral spread. The spreads have an average surface area of 0.31km^2 (0.12mi$^{2)}$, with the largest lateral spread identified having a surface area of 0.47 km^2 (0.18 mi^2) and a length of 717 m (0.45 mi). Figures 4.16 and 4.17 show a map and cross section through the largest lateral spread feature identified, located along the L'Anguille River near its confluence with the St. Francis River.

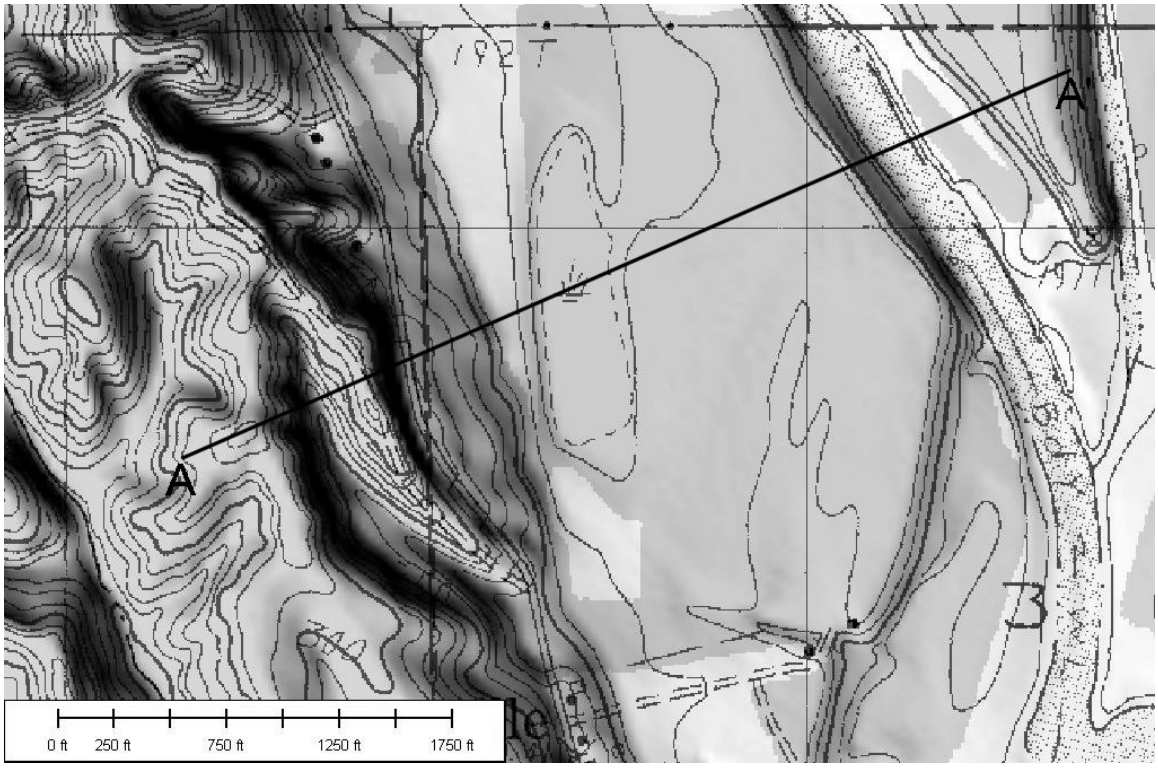

Figure 4.16 A portion of the LaGrange 10-m DEM overlaid with the LaGrange 7.5-minute DRG near Jeffersonville, AR.. A-A' is the location of the cross section shown in Figure 4.17. A large, arcuate head scarp feature may be seen in the center-left of the figure along the edge of Crowley's Ridge.

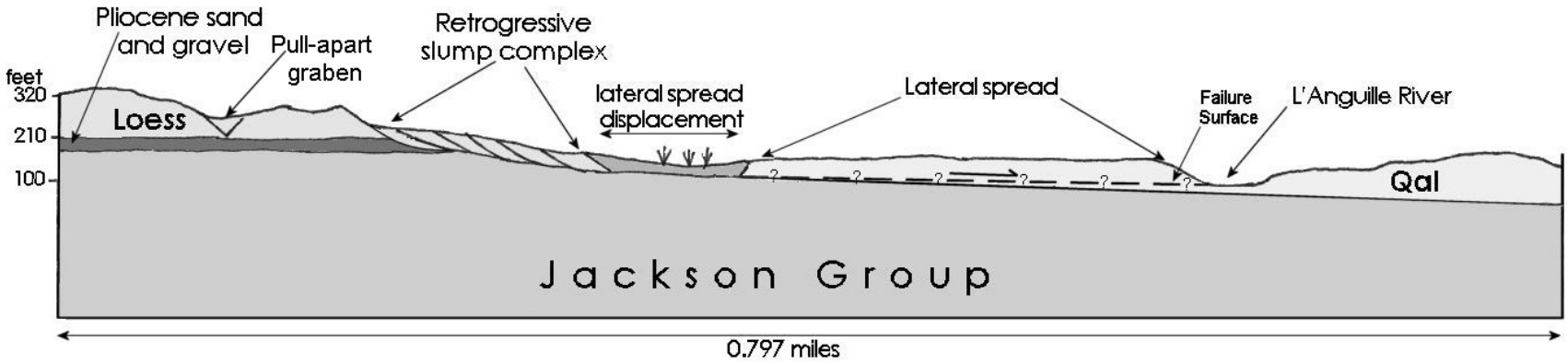

Figure 4.17 Cross section of the lateral spread feature along Crowley's Ridge that is mapped in Figure 4.16.

4.3.2. Earth Flows

4.3.2.1 Failure Mode Shallow earthflows are comprised chiefly of cohesive materials and are colloquially termed “mudslides”, “mud flows”, or “earth slides” by earlier workers (Kesseli, 1943; Forbes, 1947). For the purposes of this report, the generally accepted terminology, earthflow, originally posed by Varnes (1958) and subsequently reintroduced in Varnes (1978) and Cruden and Varnes (1993) will be used. Varnes introduced the term to describe soil-like material which exhibits behavior akin to the rheological model of a low viscosity fluid (Bruckl and Scheidegger, 1973 ; Selby, 1993).

Earthflows tend to concentrate in natural swales, as shown in Figure 4.18. Less often, smaller earthflows can occur on the flanks of natural swales, as shown conceptually, in Figure 4.19. Earthflows commonly begin as small rotational slumps, failing along log-spiral shaped rupture surfaces (Rendulic, 1935; Terzaghi, 1950). When these materials begin to translate downslope, fluid pressures are temporarily entrapped within the cohesive debris, causing excess pore pressures, which temporarily reduce interparticle friction to that approximating a viscous fluid (Hutchinson and Bhandari, 1971). As the material runs further downslope, the accompanying particle disintegration allows for some pore drainage, and as it drains the mass becomes increasingly viscous. Eventually, there occurs sufficient drainage so the mass regains interparticle friction/cohesion and comes to rest (Campbell, 1966). Cohesive debris deposited by earthflows can easily be mistaken for colluvium if it is not examined in the context of its depositional setting.

4.3.2.2 Topographic Expression Earthflows are the generally the easiest of the different slide types to identify. The following topographic indicators are used to identify earth flows:

1. divergent contours;
2. semi-circular headscarp evacuation areas; and,
3. necking-down, or narrowing, of the slide body at the transition between the inflation and deflation zones.

Their topographic expression is characterized by divergent contours within a natural swale or hill slope, as shown schematically in Figure 4.20. Whenever inward-shaped contours oppose outward-shaped contours, a repeating series of flow slides is usually indicated. The character of the depositional lobe, or toe, is dependent on several factors:

a) the cohesion of the parent material;

b) the fluidity/motion/inertia of the failed mass;

c) the slope gradient/channel constriction, and;

d) the degree of dissection affected by subsequent weathering processes.

Figure 4.18 Earthflows occupying the axes and flanks of colluvial-filled bedrock ravines near El Sobrante, CA, imaged in January 1993. Earth flows on Crowley's Ridge exhibit the same topographic expression, but are more difficult to visualize on aerial photographs due to the dense vegetation.

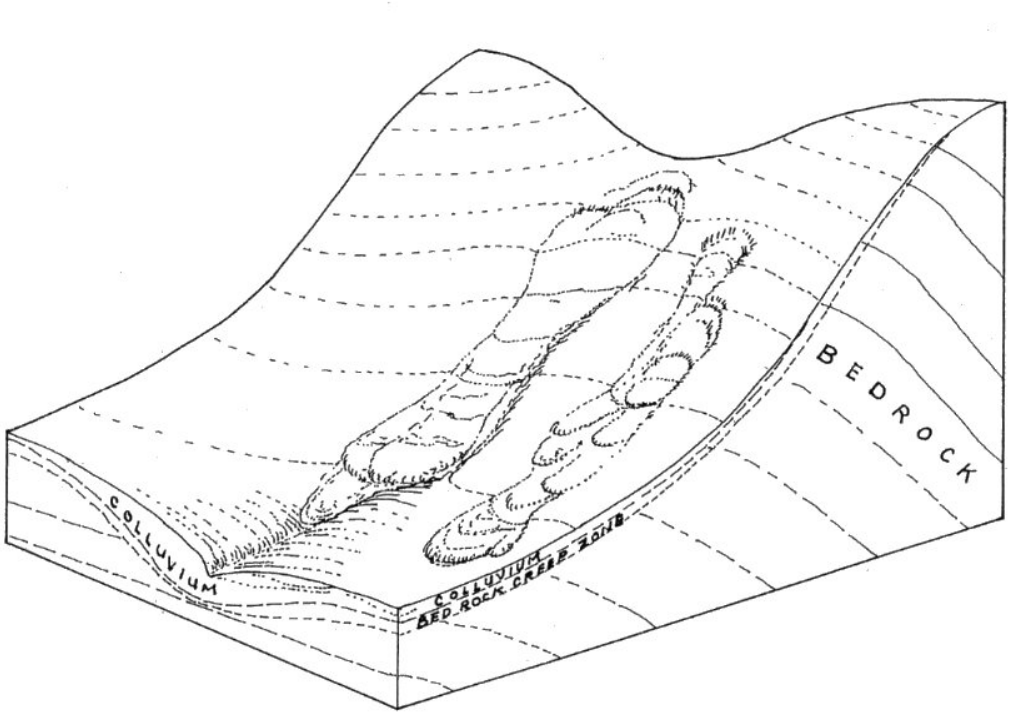

Figure 4.19 Block diagram illustrating how shallow earthflows commonly develop upon colluvial-filled bedrock ravines, when the colluvial material is dominantly cohesive.

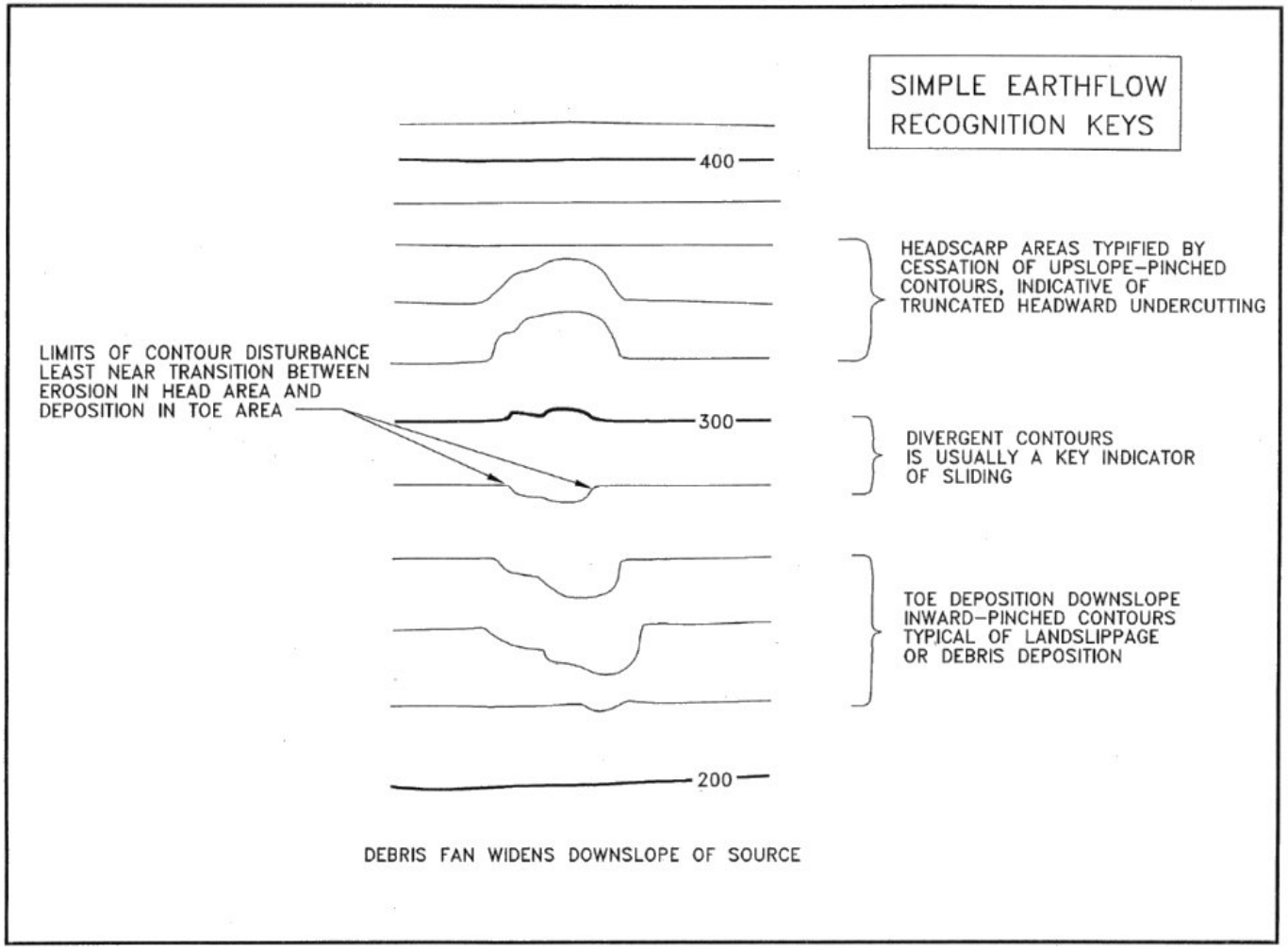

Figure 4.20 Topographic recognition keys for simple earth flows

4.3.3. Translational Block Slides

4.3.3.1 Failure Mode Varnes (1958) appears to have been one of the first workers to coin the term "block glide" to describe translational landslides which moved as a semi-coherent block upon a discrete failure surface, usually a pre-existing geologic discontinuity or contact (Miller, 1931; Leighton, 1969). Zaruba and Mencl (1982) and Varnes (1978) expanded the descriptor "translational slide" to encompass those manners of sliding which involve essentially planar surfaces and the sliding mass "translates" downslope as a semi-coherent mass. Such a classification would not include debris avalanches like the 1903 Turtle Mountain, Alberta or 1925 Gros Ventre, Montana events, where the material travels sufficiently far and fast so as to become disaggregated and flows, like a giant mass with reduced viscosity (Voight and Pariseau, 1979; Melosh, 1987).

4.3.3.2 Topographic Expression The topographic indicators for a typical translational landslide along Crowley's Ridge include:

1. extended ridges or isolated knobs;
2. convergent drainage; and,
3. sharp downslope turns in contour lines,

as illustrated in Figure 4.2. Many of the translational slides investigated are along the banks of streams, as shown in Figures 4.21a and 4.21b. These figures present a topographic expression and landslide map interpretation of translational sliding along an undercut stream bank. In translational slides, the length to width (L/W) ratio can be much lower than that for rotational slump-style failures, although this does not have to be the case. When such large slides initiate, they often block active stream channels, creating landslide dams. The channel generally excavates a bypass a short while later, displacing the thalwag (channel centerline), and perturbing the longitudinal gradient of the stream. The gradient perturbance is usually seen as a series of small riffles or rapids, depending on the size of the (landslide) disturbance, as well as the stream power exerted within the channel (Bull, 1991). The most common indicators of translational sliding blocking an old channel include:

a) perturbed geometry of channel turn;

b) presence of riffles at base of bank;

c) flat stream gradient upstream of riffles;

d) aggradation of channel with terrace deposits upstream of landslide;

e) narrowness of active channel across slide area;

f) relative lack of recent terrace deposits downstream of landslide; and

g) topographic expression of slide on slope above riffles.

Figure 4.22 a, b, c, and d presents topographic expression typical of bedrock translational slides as the slide remains dormant. First-order streams begin to incise more noticeably, and generally form convergent diagonals, diverging slightly from the natural fall-line of the ridge and contrasting with adjacent first-order streams. The erratic nature of the small first-order gullies sketched in Figure 4.22 are a key indicator of past sliding. Figure 4.23 shows translational landslides mapped along Crowley's Ridge in the Helena, AR, area.

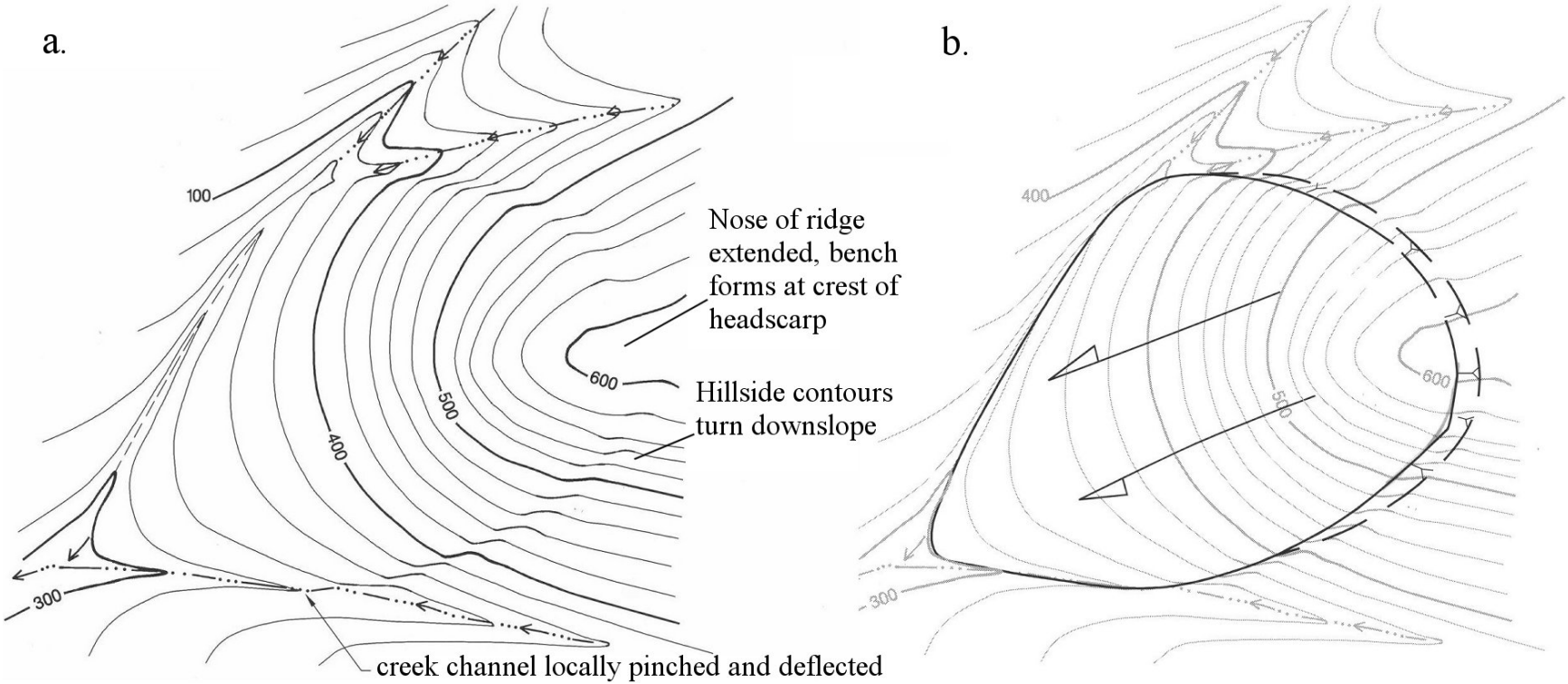

Figure 4.21 Topographic illustrations of a typical translational block slide. a) topography and topographic indicators for a translational block slide. b) mapped version of the slide in 4.21a.

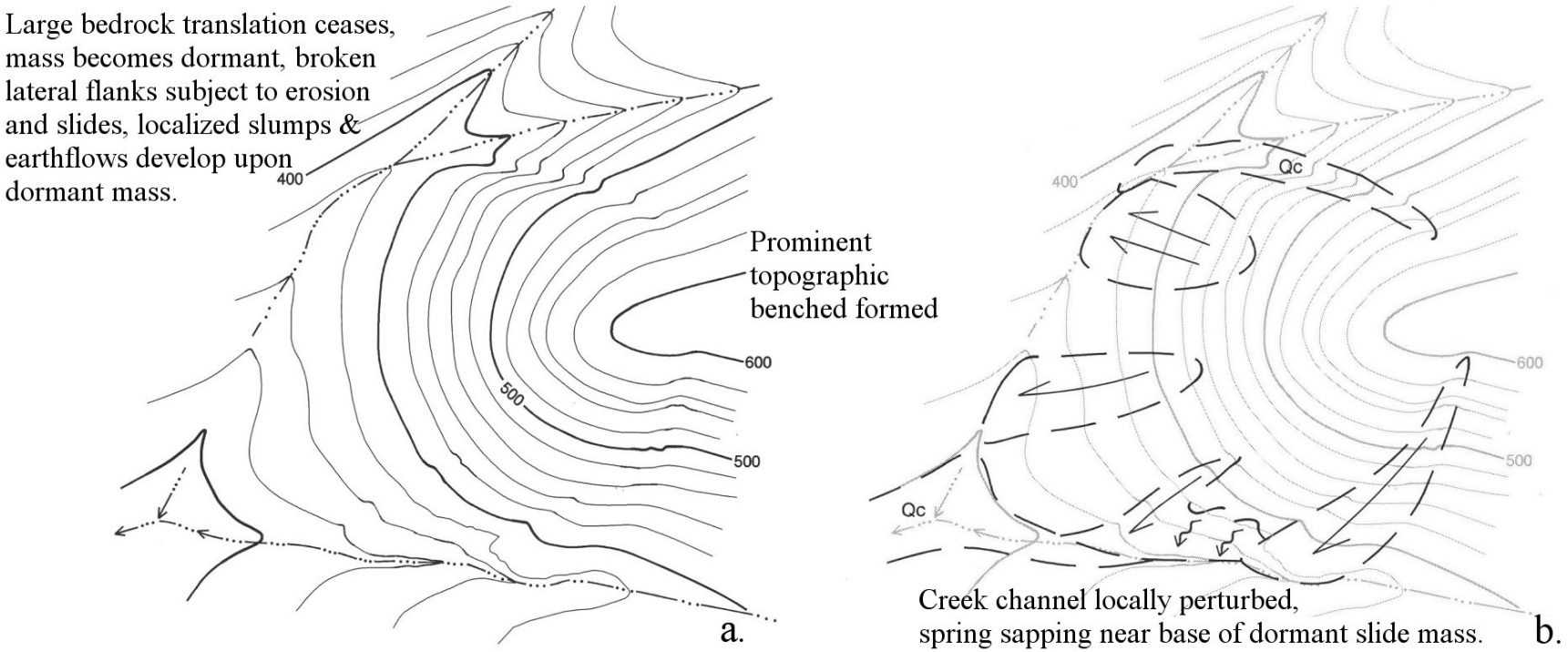

Figure 4.22 a) The translation slide shown in Figure 4.21 some time after initial movement. Erosion has occurred along flanks, and additional slumps and earth flows have formed on the translational slide mass. b) Erosional activity and mass wasting mapped on the original translational slide.

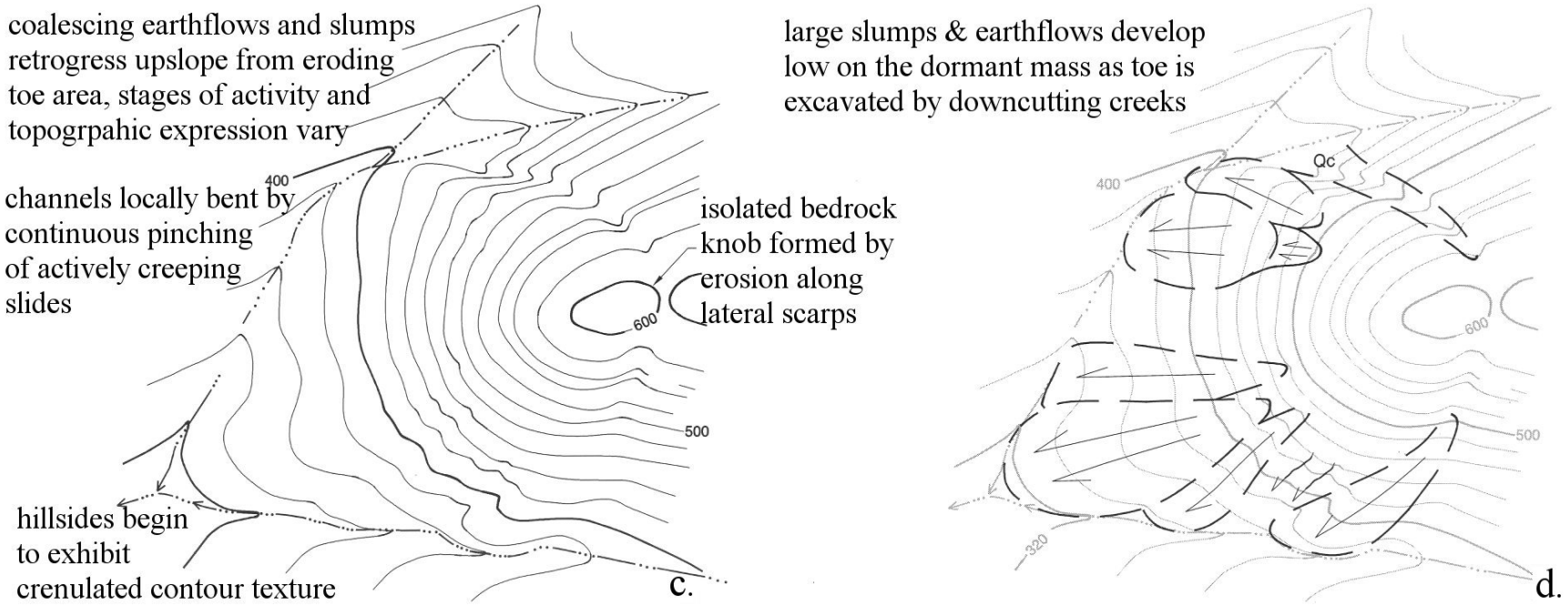

Figure 4.22 c) Continuing erosion and mass wasting begin to mask the underlying translational slide originally mapped in Figure 4.21. d) Map showing shallow slumps and earth flows that commonly develop on the parent translational slide.

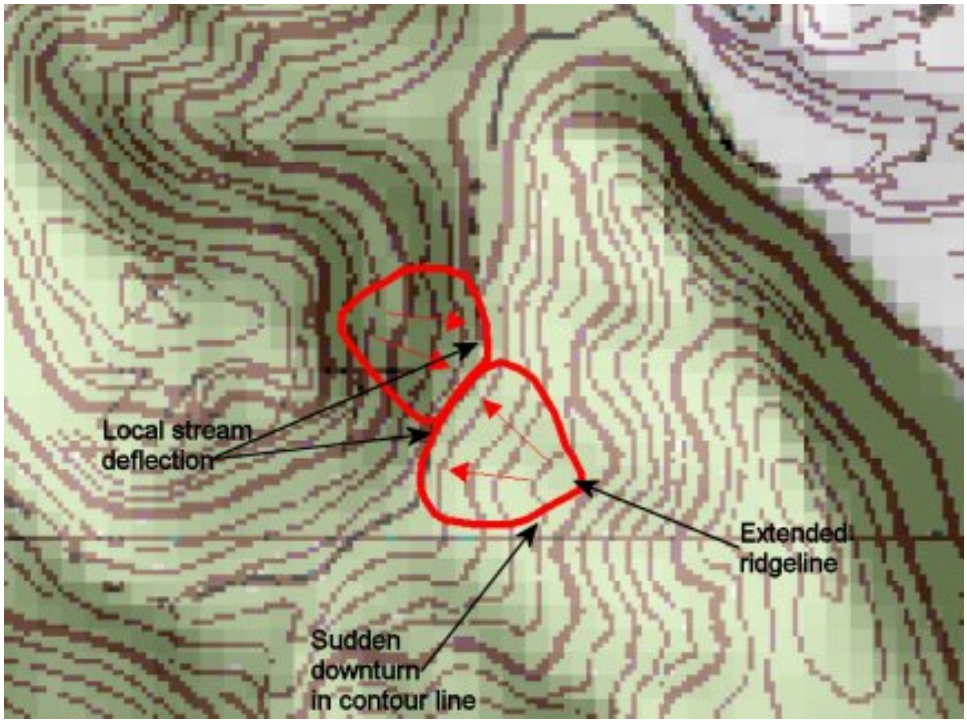

Figure 4.23 A pair of translational block slides mapped on Crowley's Ridge. The slide to the northwest is 60 m (197 ft) long, while the slide to the southeast is about 67 m (220 ft) long.

4.3.4. Slumps and Retrogressive Slump Complexes

4.3.4.1 Failure Mode An example cross section through a simple rotational slump is presented in Figure 4.24. It can be appreciated from this figure that, through simple rotation, a soil mass increases its own stability by lowering the relative position of the water table within the displaced body of material. In this manner, semi-homogeneous soil masses will tend to fail when sufficient pore pressure accumulates in the affected zone, within close proximity of the ground surface. Slumps generally occur after periods of sustained precipitation, when the inflow of water into the hill side exceeds the outflow, and a net build-up of pore water pressure occurs.

The geometry of rotational failures depends on the thickness and consistency of the soil or rock mass being affected. Statistically, the most common rotational slumps tend to form in homogeneous materials. Thick zones of soil, colluvium, and detritus

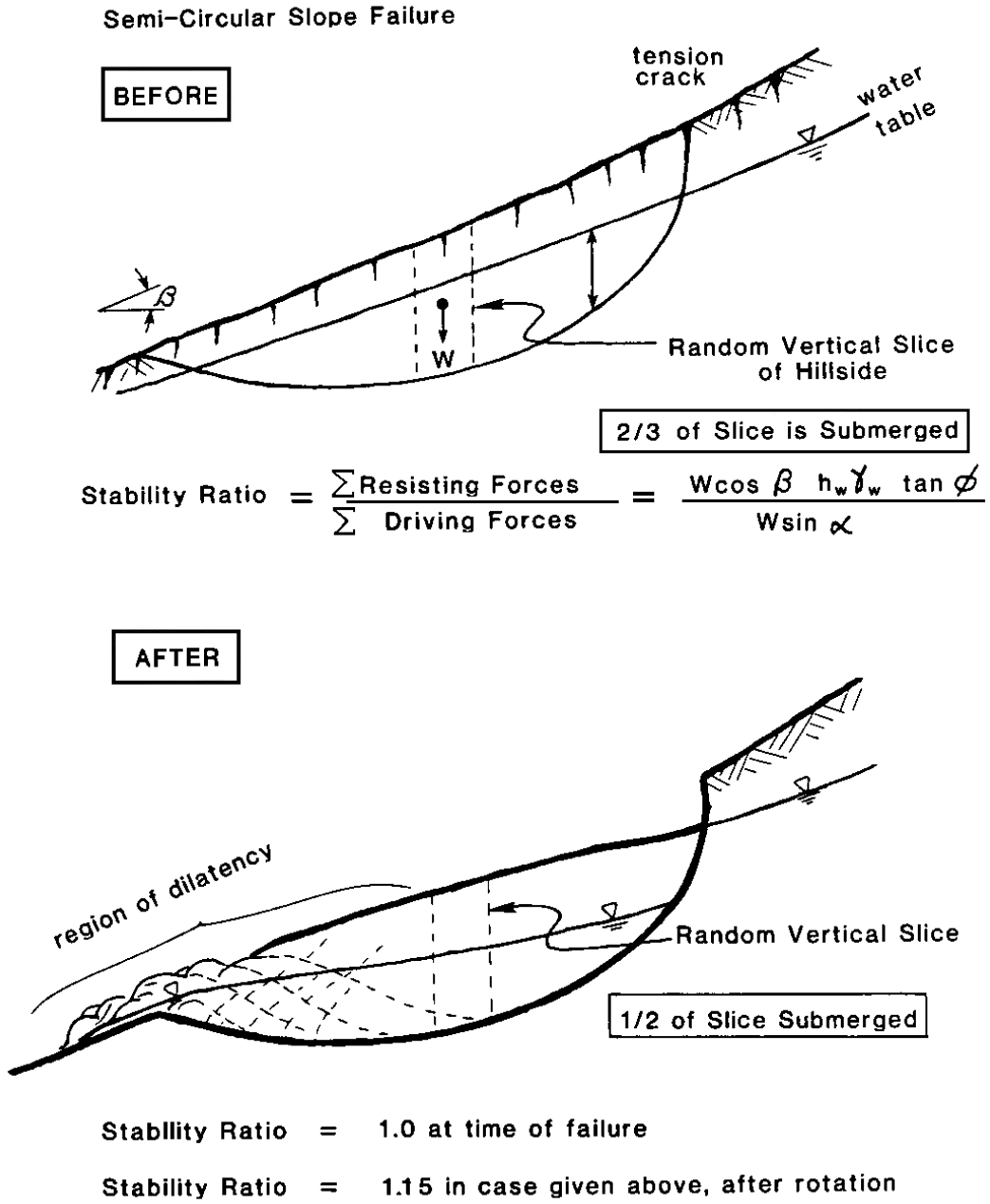

Figure 4.24 Mechanics of a rotational slump failure. The relative proportion of saturated soil in a random vertical slice is lessened by the rotation (from Dietrich and Rogers, 1989).

from the soil zone will tend to foster simple spoon-shaped slumps (Varnes, 1958). These are the most common slump features on Crowley's Ridge, due to the thick layer of homogeneous loess blanketing the ridge.

Fuller (1912) investigated and identified numerous slumps and slump complexes in both the eastern and western NMSZ. He noted many areas where large trees had been rotated backward, as is typical near the head scarp of a slump. An example of the rotation of trees on Crowley's Ridge slumps is shown in Figure 4.25.

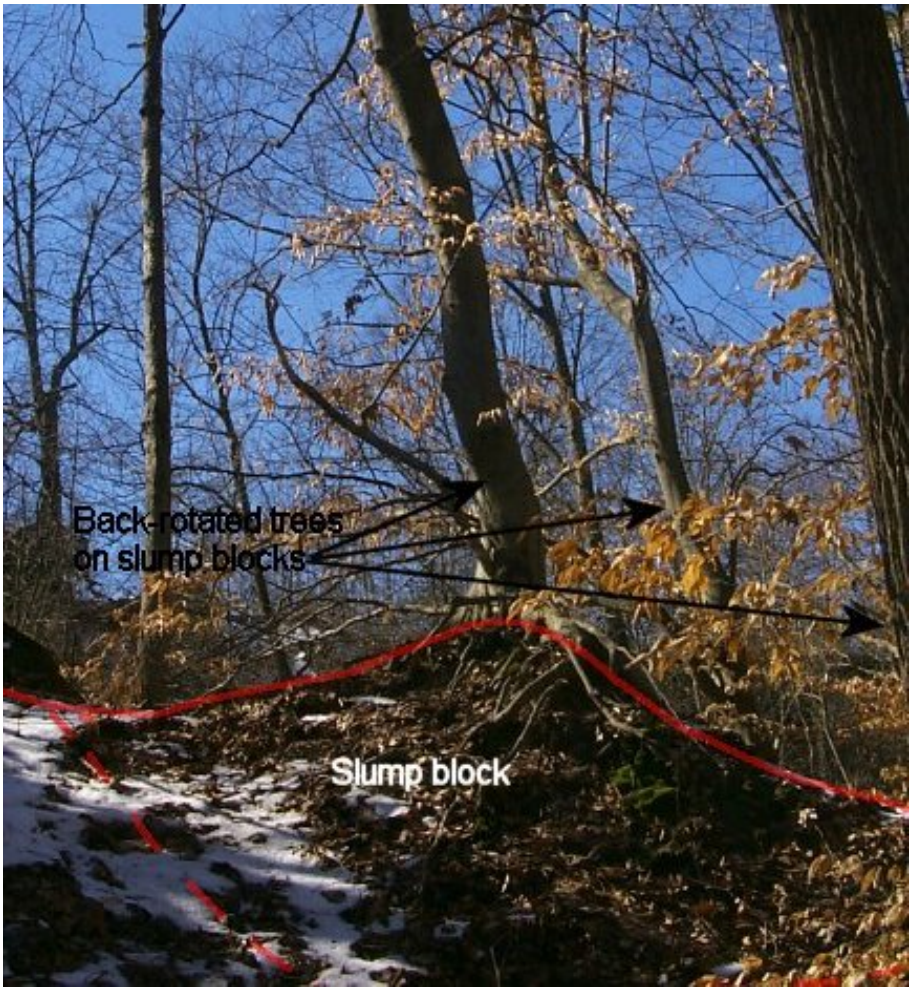

Figure 4.25 Crowley's Ridge slump showing back rotation of trees. The solid red line shows the slump block surface while the dashed red line is the projected failure surface.

A common type of slump failure found along Crowley's Ridge, and long recognized within bedrock and soil slumps (Zaruba and Mencl, 1982), is that of progressive, or retrogressive sliding (Bjerrum, 1966; Goodman, 1976). A typical example, identified on Crowley's Ridge by Ding (1991) is presented in Figure 4.26.

When one mass of material rotates downslope, it removes lateral support from the next adjacent mass upslope. It can be appreciated that, the further a block translates downslope, the more precarious becomes the stability of the next-adjacent block, up slope. In such a manner, block rotation can simply "migrate" up slope, as described by Strahler (1942). This mechanism of progressive failure is most troublesome in situations where an underlying zone of weakness exists (Hutchinson, 1969). Figure 4.27 shows a series of small retrogressive slumps along Crowley's Ridge.

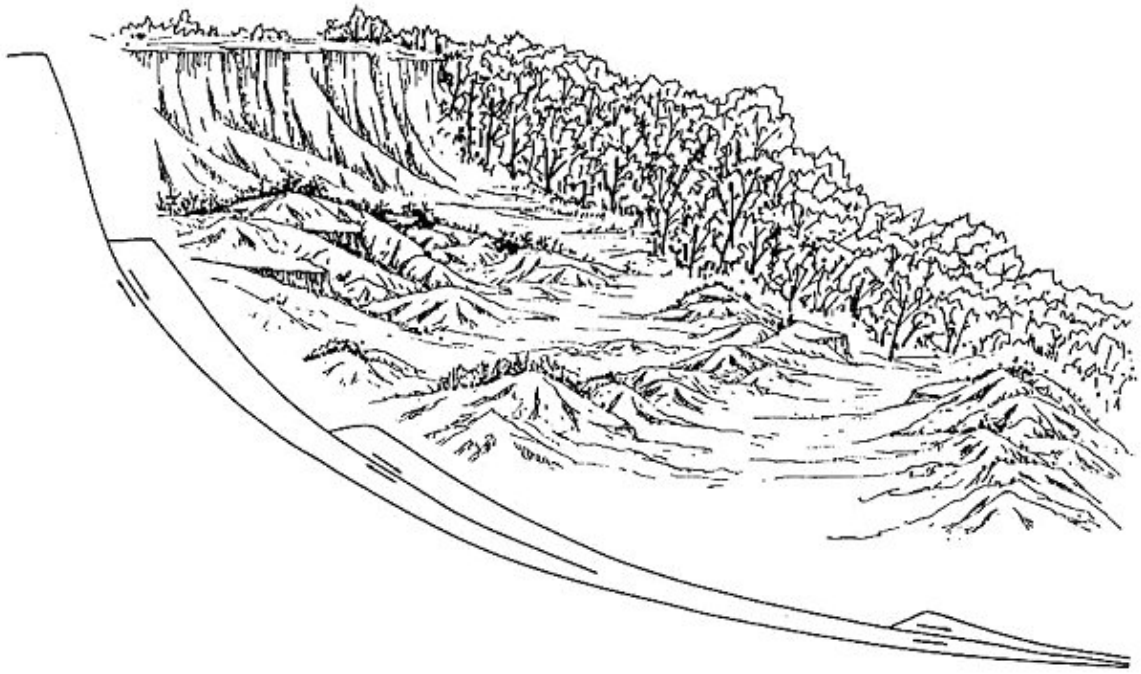

Figure 4.26 Sketch by Ding (1991) of a series of shallow retrogressive slumps along Crowley's Ridge.

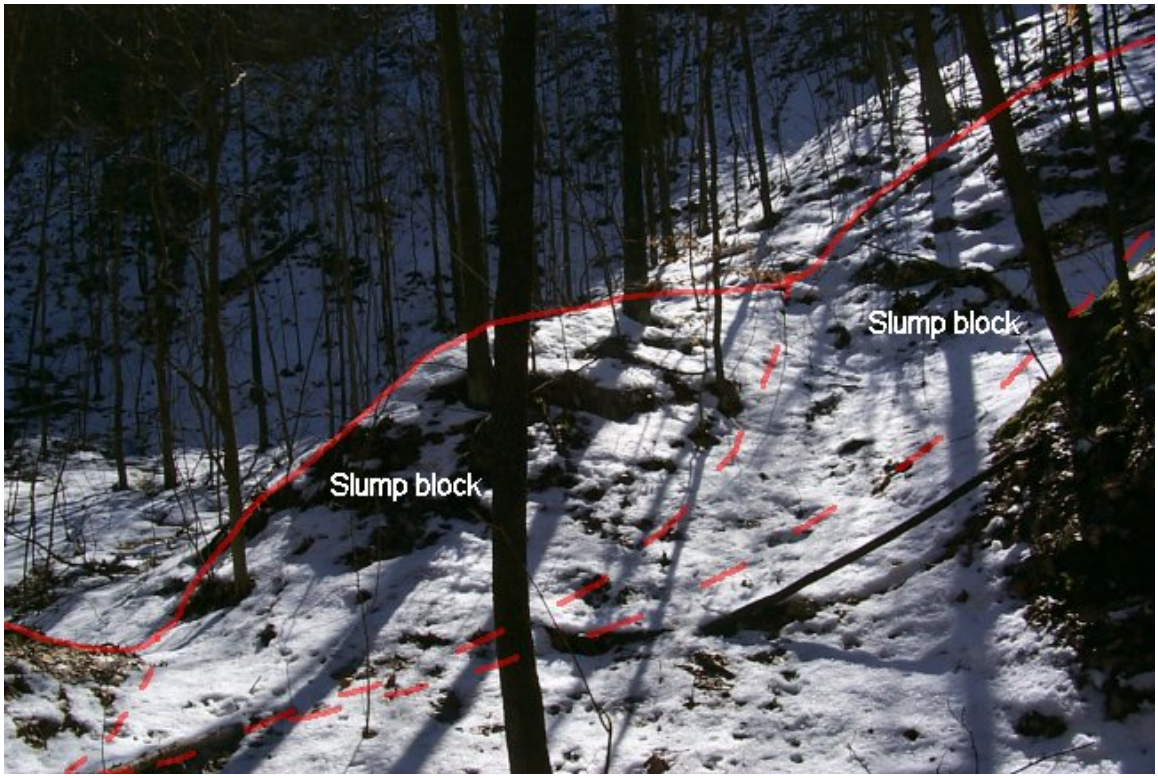

Figure 4.27 Series of small retrogressive slumps on Crowley's Ridge near Valley Ridge, MO. The surface of the slumps is outlined with a solid red line while the approximate failure surface is shown with a dashed red line.

4.3.4.2 Topographic Expression Shallow rotational slumps within the soil mass can be difficult to identify, depending on contour fineness, map scale, vegetative cover and age since occurrence. The main topographic indicators for a rotational slump or slump complex include:

1. asymmetric opposing contours;
2. pinching of or isolated breaks in contours;
3. topographic expression of back-rotated grabens, which form prominent benches; and
4. in the case of retrogressive slumping, the occurrence of en-echelon series of topographic benches, such as those sketched in section in Figure 4.26. In plan, these types of features often appear as a series of small terrasets (Sharpe, 1938), often infilling established channels.

In other instances, retrogressive blocks simply nurture the enlargement of a landslide complex. An example of a simple rotational slump is presented in Figure 4.28, which shows the topographic expression typical of a recent slump, the map interpretation of the slide, and typical recognition keys, such as asymmetric opposing contours absent any ravine above or below, and isolated contour breaks (pinching of contours) in the headscarp evacuation zone. Figure 4.29 shows topographic indicators typical of most rotational slumps, including a discernable topographic bench.

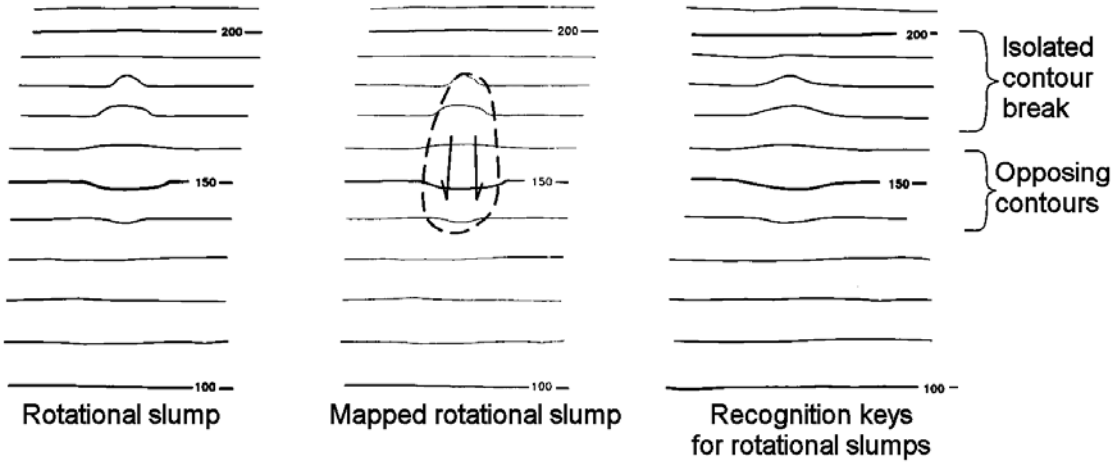

Figure 4.28 Topographic indicators for rotational slumps similar to slumps found on Crowley's Ridge.

4.3.5. Theater-head Erosion Complexes While theater-head erosion complexes are not actually landslides, they are common topographic features along Crowley's Ridge. The features are due in part to the highly erosive nature of the loess blanketing Crowley's Ridge. Theater-head erosion complexes typically have very steep-sided, amphitheater-like walls formed by repeated cleaving of blocks of loess. As the loess blocks drop they break apart and the disaggregated material is easily swept downstream, clogging the ephemeral first-order channels below. Figure 4.30 shows theater-head erosion complexes on Crowley's Ridge just north of Helena. The erosion that caused these features may

have been initiated by landsliding that disturbed the loess on Crowley's Ridge. However, some of the features could have been initiated by human activity, including road and levee construction and sand and gravel pit construction.

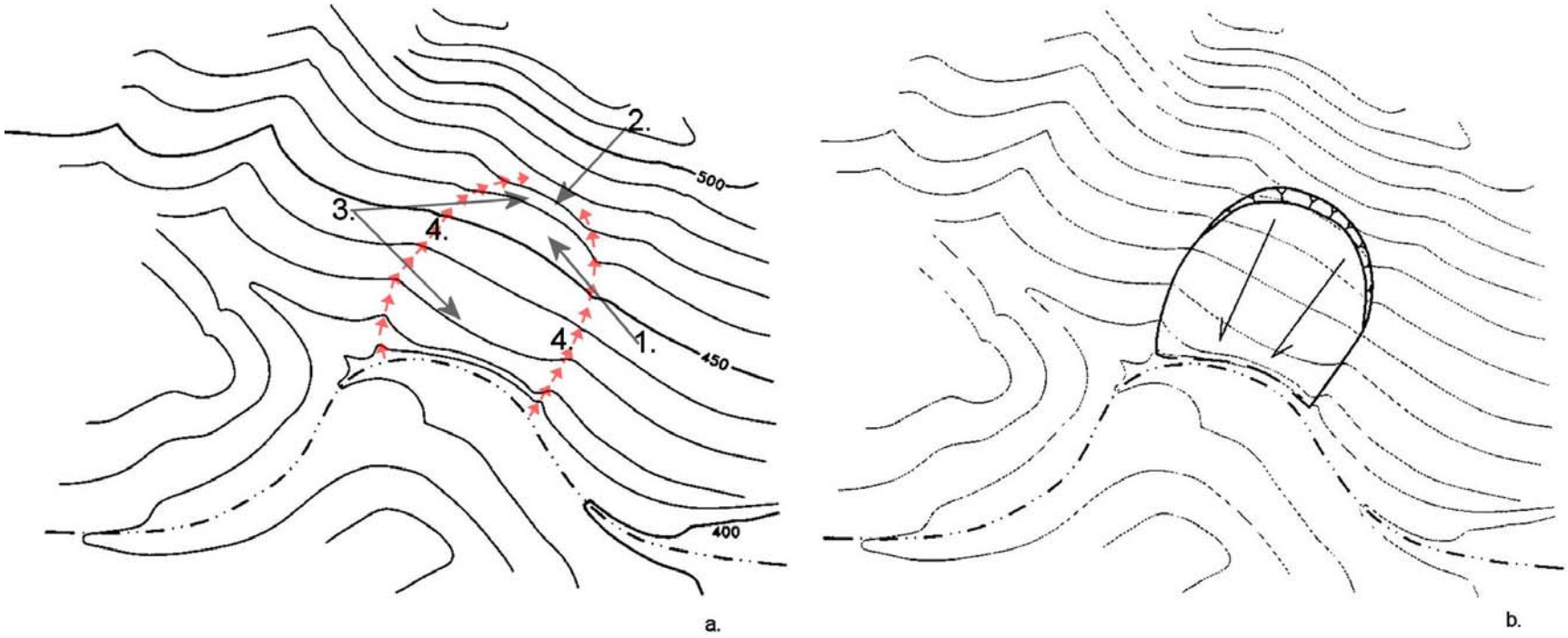

Figure 4.29 a. Topographic indicators for a typical slump on Crowley's Ridge, where toe erosion by a stream has precipitated the failure. 1. Topographic bench below head scarp. 2. Semi-circular headscarp evacuation area. 3. Divergent (or opposing) contours. 4. Headward erosion leading to the formation of convergent drainage along the edges of the slide. Arrows indicate direction of headward erosion. b. Illustration of how the slide identified in Figure 4.29 a. would be mapped.

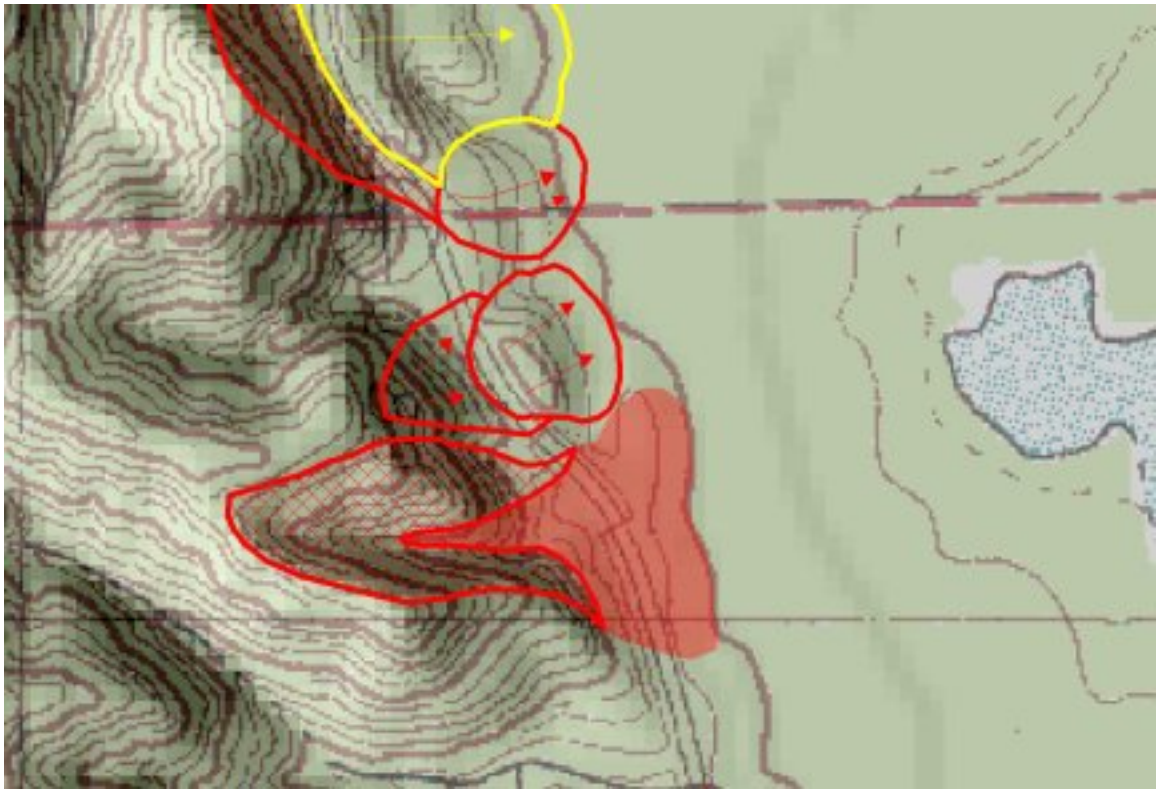

Figure 4.30 Theater-head erosion complex just north of Helena, AR, on the eastern escarpment of Crowley's Ridge. The erosional scarp is shown with red cross-hatches, while the depositional fan is shaded red. Just north of the theater-head complex is a retrogressive slump complex.

5. ANALYSIS OF LANDSLIPPAGE

5.1. FIELD WORK

5.1.1. Landslide Verification Once the topographic s were employed to tentatively identify areas of anomalous topography, field investigations were undertaken to verify the existence of actual landslides. Due to the highly vegetated nature of Crowley's Ridge (Figure 5.1) initial field investigations were conducted in early to mid spring. Field reconnaissance included looking for hummocky topography, head scarps, graben structures, deranged drainage, closed depressions, anomalous topographic benches, arcuate drainage and stepped or hummocky topography beneath the tree canopy. It was soon appreciated that the actual topography below the tree canopy was quite different from the topography mapped on the USGS 7.5-minute quadrangles, especially along the east-facing escarpment of Crowley's Ridge. The topographic maps of Valley Ridge, MO, and the Helena, AR, area were prepared from orthorectified stereopair aerial photography. Most of the steeply inclined slopes are masked by a dense tree cover. In areas with tall trees, the tree canopy tends to act as a reflective surface, making interpretation of the underlying topography difficult, as discussed in Subsection 4.1.4 and shown in Figure 4.6. The field work suggested that all too often, the topography of heavily vegetated hillslopes is interpolated linearly, between areas of bare earth, such as roads or ridgetops. Figure 5.2 illustrates how the thick tree canopy and tree height along the base of Crowley's Ridge has interfered with accurate mapping of topography. Errors in topographic mapping made it difficult to identify small landslides on topographic maps, but the larger landslide features are often discernable because they are of greater scale than the tree canopy.

Because of interference by the tree canopy with aerial photographs and small-scale topographic mapping, verification of the anomalous topographic features as actual landslides was very important. Field investigations were necessary to compare the topographic anomalies on the map to the physical features in the field, beneath the tree canopy. In most instances, the ground surface was much more uneven and hummocky than reflected on the topographic maps. These comparisons gave us a feeling for the

Figure 5.1 Photographs showing heavy vegetation on the slopes and at the base of Crowley's Ridge. a) within the Valley Ridge quadrangle, early February, 2003; and b) Helena, AR, mid March, 2003.

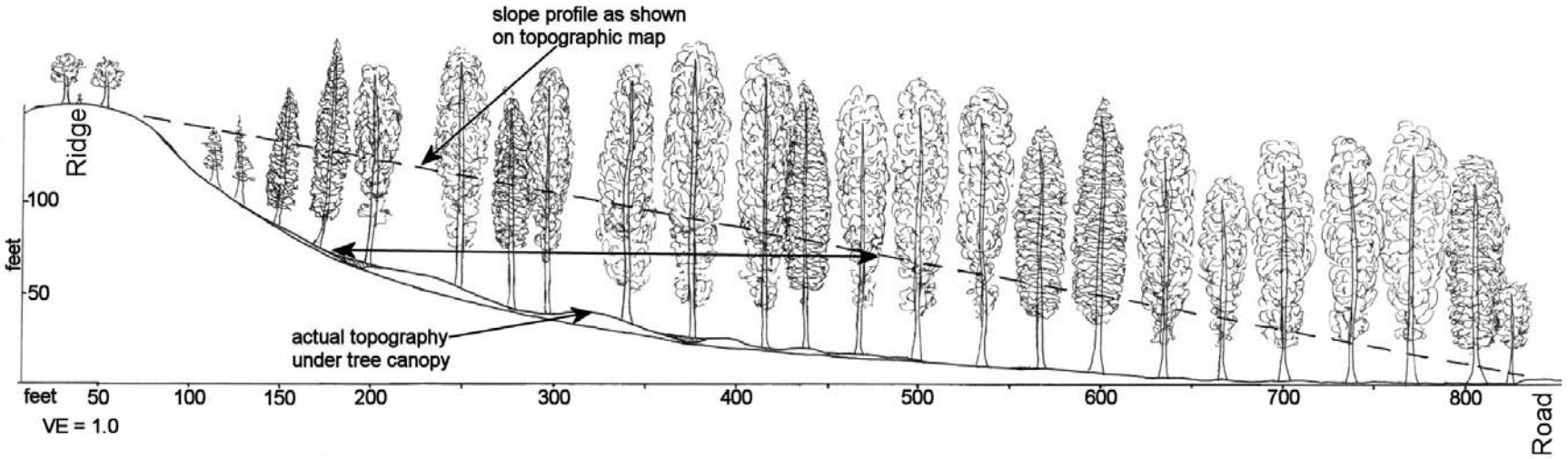

Figure 5.2 Illustration of the impact of vegetation on accurate mapping of topography along Crowley's Ridge. Due to the high tree height and the highly reflective surface formed by thick vegetation, the actual topography of the ridge side slopes cannot be seen on aerial photographs used to create the topographic maps. The only points that can be seen clearly are the ridge top and the road at the base of the ridge. On the topographic maps, the area between the ridge top and road is mapped with a straight-line interpretation (dashed line), which does not accurately represent the topography under the tree canopy.

inherent inaccuracies on USGS topographic maps and ideas on how to map areas that were not easily accessible on foot.

Initial field reconnaissance of the Valley Ridge quadrangle began in early February, 2003. The Valley Ridge quadrangle was suggested by Dave Hoffman and Jim Palmer of MoDNR GSRAD after Mr. Palmer discovered the headscarp of an active theater-head erosion complex along Crowley's Ridge in Morris State Park, near Campbell, MO. The field reconnaissance included Mr. Hoffman and Mr. Palmer, and Jim Vaughn (GSRAD retired), who were familiar with the site and the local geology. Professor J. David Rogers and Kevin James, a graduate student, of the Department of Geological Engineering at the University of Missouri – Rolla also assisted in the field investigations. While many of the larger landslides in the Valley Ridge quadrangle were identifiable using the method of topographic s, it was soon discovered that countless smaller landslides were not identifiable on the 1:24,000 scale topographic maps. It would appear that the smaller slides are not reflected on the USGS topographic maps because of their scale in comparison with the tree heights and density of overgrowth, as well as the original scale of the stereopair aerial photos from which the maps were made. The field investigation of the Valley Ridge quadrangle showed that the topographic mapping protocols proved accurate for the larger landslides in the Valley Ridge area, usually features more than 91.5 m (300 ft) long. Most of the smaller landslides could not be identified using topographic anomalies. However, in most instances, theater-head erosion complexes could be identified on the topographic map.

Field investigations of the Helena, AR, area began in mid-March, 2003, with assistance of Dr. Rogers and Mr. James. Initial field reconnaissance efforts focused on areas of anomalous topography that had been identified by the mapping protocols prior to ever visiting the sites. Similar to the Valley Ridge quadrangle, numerous topographic indicators of past landslippage were obscured under the tree canopy on Crowley's Ridge. Field mapping began on the LaGrange quadrangle, but was subsequently extended to the adjoining West Helena and Helena quadrangles when the extent of landsliding in those adjoining areas became apparent. In the vicinity of Helena, AR, Crowley's Ridge has a much thicker cover of vegetation than in the Valley Ridge, MO area. Trees in this area reach heights of as much as 56 m (185 ft), which appears to have led to increased error on

the topographic maps, as described previously and shown in Figure 5.2. Despite these problems, most of the larger landslides occupy sufficient surface area to be discernable on the USGS topographic maps, because of their 3 m (10 ft) contour interval and increased resolution of aerial photographs imaged from lower altitudes. Most of the smaller landslides were obscured by the vegetation.

The largest landslides mapped in the Helena, AR, area were lateral spreads, which were easily identified using the topographic that had been suggested for them. After the suspected lateral spread features were investigated in the field and some measure of confidence acquired, geophysical methods were employed to amplify the characterization of such features, including approximation of length-to-depth and length-to width ratios of the slide masses. Electrical resistivity methods were selected as the method of choice to enable profiling of the landslide features, along trends normal and parallel to the inferred direction of motion. The resistivity profiles also attempted to delineate the likely position of the landslide rupture surfaces through the overlying silt and loess. Field investigations of lateral spread features, both reconnaissance and geophysical, searched for the presence of:

1. saturated cohesionless materials capped by low permeability materials;
2. proximity to adjacent buried channels or depressions;
3. prominent evacuation grabens formed by block movement that may subsequently have become be infilled;
4. sand dikes filled with liquefied cohesionless materials; and,
5. stepped topography, typical of repeated events which may have engendered ground lurching of selected zones towards old channels or natural depressions.

5.1.2. Geophysical Methods As stated above, the geophysical investigations focused on using electrical resistivity methods to confirm the lateral spreads identified with the topographic mapping protocols. The geophysical studies focused on the lateral spreads for three main reasons:

1. the location of the lateral spreads along the eastern edge of Crowley's Ridge made them easily accessible;
2. lateral spreads have the highest damage potential of the landslide types in the NMSZ due to their large areal extent; and

3. lateral spreads had not been previously identified in the NMSZ, and their mode of formation in the area is not completely understood.

For the other landslide types identified in the area, visual confirmation was sufficient to verify the existence and classification of the slides.

The geophysical surveys were run by Anthony Buccellato, a graduate student in UMR's Department of Geology and Geophysics, under the supervision of Dr. Estella Atekwana. Assisting in the surveys were Craig Kaibel and Conor Watkins, graduate students in Geological Engineering, and Garret Euler, and undergraduate student in Geophysics. Geophysical studies along Crowley's Ridge north of Helena, AR, began in May, 2003. Much of the area studied was within the St. Francis National Forest, however, portions of two suspected lateral spreads were situated on private land. Mrs. Catherine O. West of Marianna, AR, and Mrs. Frank Clancy, her son Frank Clancy, and their family of Helena, AR, generously allowed access to their property for geophysical surveys. Unfortunately, subsequent conversations with Mr. Clancy indicated that the topography believed to be a lateral spread was the result of an unmapped sand and gravel borrow pit from the mid-1930's, whose material was used to build the Mississippi River levee around Helena, AR.

Figure 5.3 shows a map of a large lateral spread near Marianna, AR, on which geophysical survey lines were performed. The data collected from the electrical resistivity surveys suggests that the failure surface of the lateral spread was at the contact between the loess and the underlying saturated Pliocene sand and gravel. The saturation of the sand and gravel made liquefaction along the contact zone plausable, and allowed rafting of the main lateral spread body easterly, toward the L'Anguille River channel. Following the movement of the main body, it would appear that a series of retrogressive slumps developed along the eastern margin of Crowley's Ridge, within the loess cover. Figure 5.4 a and b show cross-section C-C', near the center of the lateral spread, as developed from the resistivity survey data, and the interpretation of the data showing the series of retrogressive slumps. The main body of the lateral spread was not fully accessible due to the swampy nature of the suspected lateral spread. Several inches of standing water were present on the main body of the lateral spread, which made electrical resistivity surveys of the area impossible.

Figure 5.5 a is an electrical resistivity cross-section along line B-B' at the southern end of the lateral spread feature, as shown on Figure 5.3. An interpretation of the data is given in Figure 5.5 b. Again, a series of retrogressive slumps can be seen to the west of the main slump body. A large graben-like structure appears to exist on the western end of the cross-section. Due to the depth of the structure, it may be caused by a fault splay along the western edge of the lateral spread. This fault splay may be an offshoot of the eastern bounding fault along Crowley's Ridge (Figure 3.1), which, unfortunately, cannot be clearly discerned with the existing geophysical data (which is of insufficient depth).

The collected geophysical data confirmed the presence of a reasonably thick sand and gravel layer below the loess that blankets this portion of Crowley's Ridge. The presence of retrogressive slumping along the margins of the lateral spread, as suggested in Figure 4.16, was also confirmed. Investigations of other lateral spread features using electrical resistivity in the area are ongoing, and investigations using Ground Penetrating Radar (GPR) and seismic reflection and refraction surveys are being planned. The data gathered to date, however, strongly supports the identification of these large anomalous feature as lateral spreads, and fits well with the cross-sectional models developed for lateral spreads in the NMSZ, discussed in Section 4.

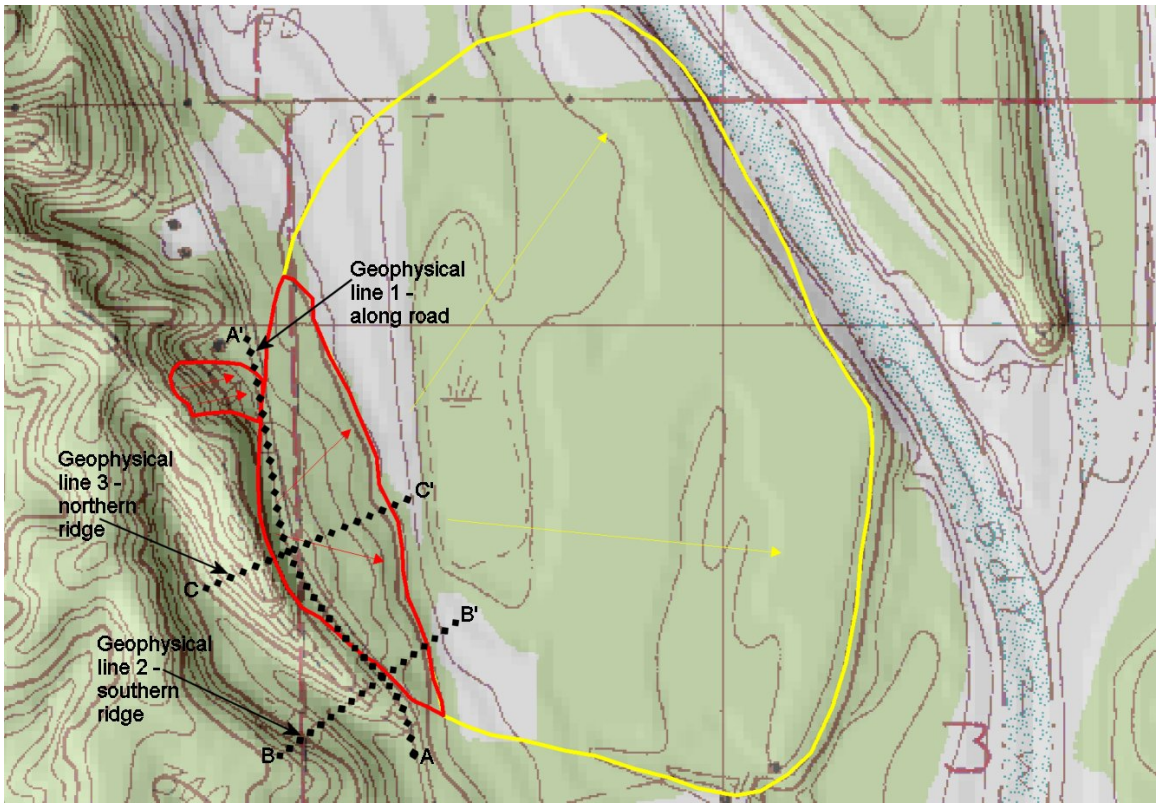

Figure 5.3 Map of a large lateral spread feature on Crowley's Ridge just south of Marianna, AR. The large area outlined in red is the upper portion of the lateral spread, characterized by a series of en-echelon retrogressive slumps, formed after initial movement of the main body of the lateral spread. The area outlined in yellow shows the suspected extent of the main body of the lateral spread. The dotted black lines show the locations of electrical resistivity surveys profiling the upper area of the lateral spread.

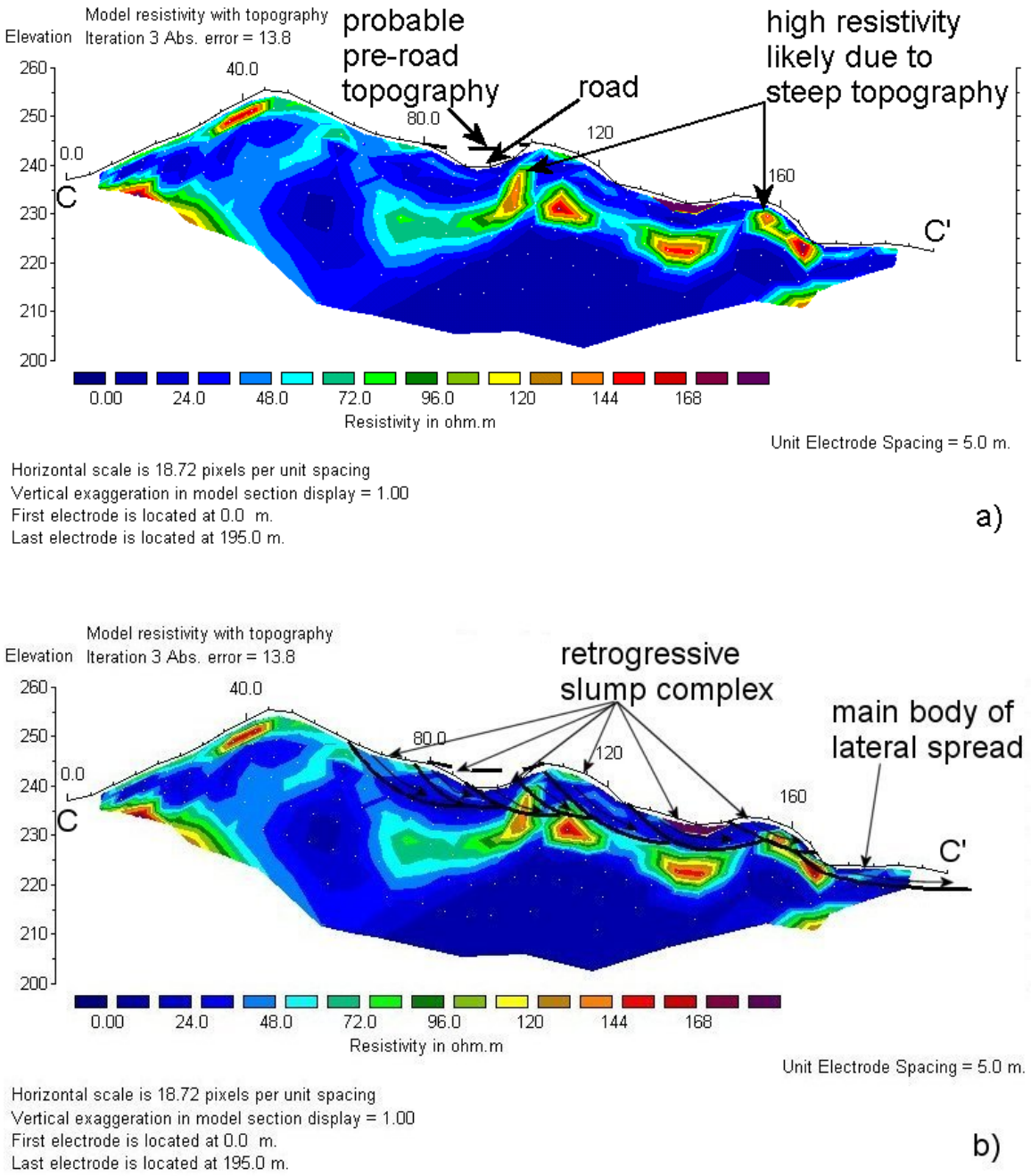

Figure 5.4 a) Electrical resistivity data collected along line C-C' (vertical exaggeration of 1:1) on the lateral spread shown in Figure 5.3. Blue areas indicate materials with low resistivity, such as silts and clays. Orange and red areas indicate higher resistivity, such as sands and gravels. Two areas of anomalously high resistivity are indicated. These high values are likely the result of the overlying steep topography. b) Interpretation of the geophysical data showing a series of retrogressive slump blocks and the westernmost portion of the main lateral spread body.

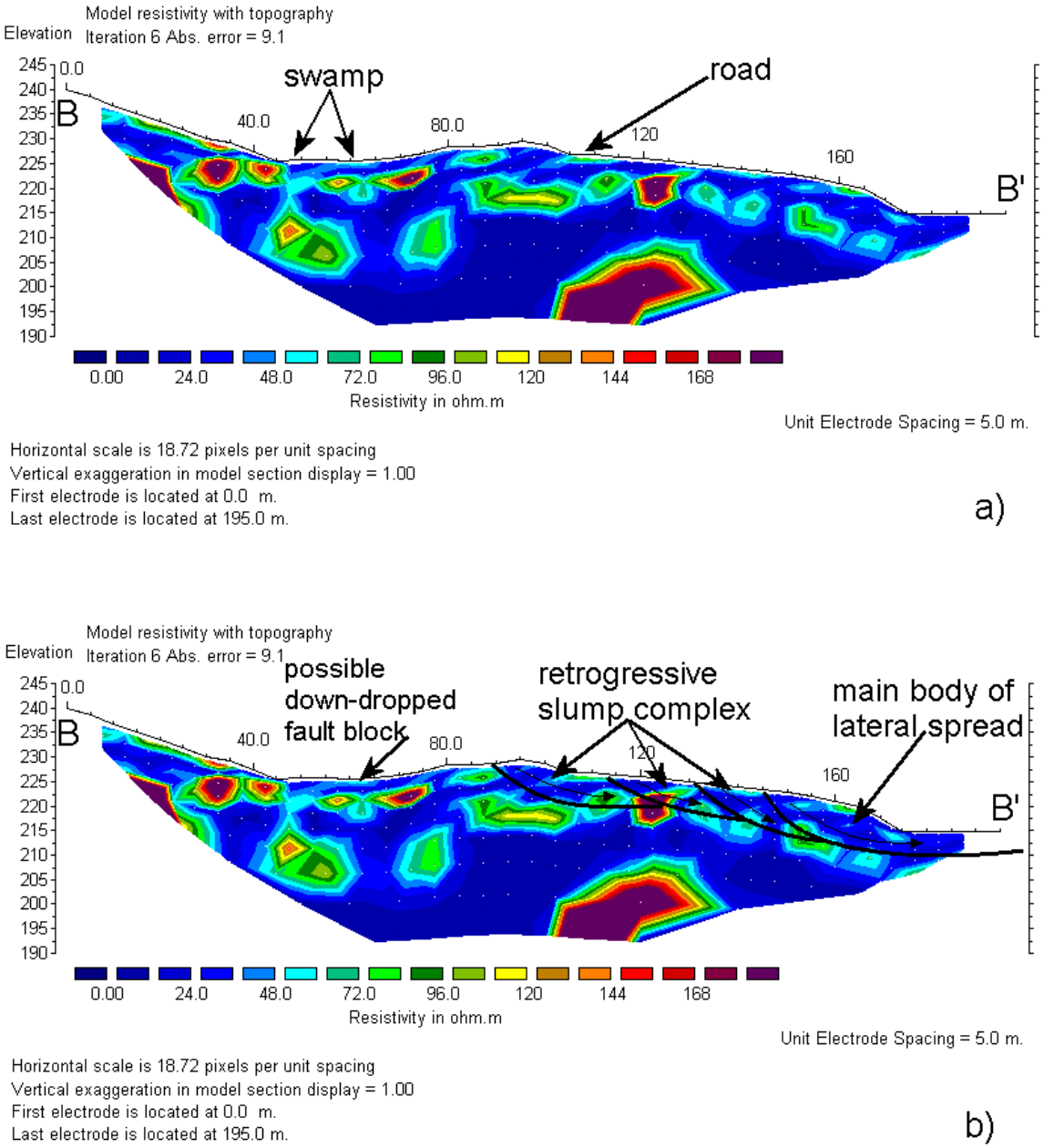

Figure 5.5 a) Electrical resistivity data collected along line B-B' (vertical exaggeration 1:1) at the southern end of the lateral spread shown in Figure 5.3. The western (left) end of the line begins on Crowley's Ridge, crosses a swamp, and then up onto the ridge again before leaving the ridge and crossing into the floodplain of the L'Anguille River. b) Interpretation of the geophysical data for the southern geophysical line. A series of retrogressive slumps area again seen on the eastern flank of Crowley's Ridge, just upslope (west) of the main body of the lateral spread. The depression occupied by the swamp may be a down-dropped fault block related to the east-bounding fault that elevated Crowley's Ridge.

6. RESULTS

6.1. SEISMIC ANALYSIS OF THE MAPPED LANDSLIDES

The landslides mapped in the areas of interest for this report were likely caused by intensive ground shaking associated with the 1811-1812 New Madrid earthquakes. The landslides investigated for this report all appear to be of the same age, based on several factors, including:

1. degree of erosion on the main slide features, including headscarps and toe deposits;
2. the comparable rates and degrees of scarp retreat between slides of similar type and size;
3. similar density of vegetation growing on the slide surfaces; and,
4. the degree of activity on the slides.

Most of the landslides mapped in this project, with the exception of the theater-head features, show little sign of activity in at least the past several decades. No instances of large-scale landsliding have been recorded in the area in recent history. The landslide activity that has been recorded is small-scale and related to stream downcutting and human activity. The lack of recent activity, as well as the other factors described above, suggest that the landslides investigated for this report formed at more or less the same time. A large, regional event, such as the New Madrid earthquakes, is the most likely explanation for the formation of such a wide variety of landslide types over a large area at the same general time.

While investigating landslides along the Chickasaw Bluffs in the eastern NMSZ, Jibson and Keefer (1994) performed seismic slope stability back-analyses of two representative landslides; a translational block slide and an earthflow. They concluded that both of these slides could only have failed under dynamic loading conditions, most likely related to the 1811-1812 earthquakes. The slides studied by Jibson and Keefer (1994) were of similar types, sizes, morphology, and apparent age to the landslides mapped for this study. The landslides studied by Jibson and Keefer also formed in Pleistocene loess lying unconformably on the Pliocene Lafayette gravel, above the Eocene Jackson formation; a geologic setting nearly identical to that of the Helena area.

Jibson and Keefer (1994) used split-spoon and piston core samples of the loess and underlying gravel to determine the geotechnical properties of the materials involved in the landsliding, including soil unit weight and shear strength. Static, or aseismic, and dynamic tests were conducted on models of the pre-landslide bluffs to determine slope stability, using data taken from samples recovered in the undisturbed bluffs near the two landslides, as well as stratigraphic information obtained from their subsurface exploration program. The static slope stability back-analysis were modeled using the computer program STABL, with five different groundwater conditions:

1. a water table at the top of the bluff, in the loess;
2. a water table perched on top of the Lafayette gravel;
3. a water table at the top of the Jackson Formation;
4. a water table at the base of the bluffs; and,
5. a water table sloping upward, from the base of the bluffs to the top of the Jackson Formation, with a perched water table on the Jackson Formation which saturates the gravel (Jibson and Keefer, 1994).

The scenario with the water table at the top of the bluffs was found to be the most critical. The factor of safety (FS) for this groundwater condition was 1.32, indicating the bluffs were stable under even the most adverse aseismic conditions imaginable. For the bluffs to fail under aseismic conditions, there would need to be an artesian water pressure greater than 10 m above the top of the bluff, which is not likely, given the existing regional geology (Jibson and Keefer, 1994).

Using Newmark analyses and the STABL program, Jibson and Keefer (1994) also modeled the behavior of the loess bluffs under dynamic, undrained conditions. The most critical failure surfaces generated by STABL correlated closely with the observed failure surfaces of the slides selected for back-analysis by Jibson and Keefer. Further analysis of the landslides under dynamic loading indicated that the landslides could only be triggered by significant ground motions, similar to those of the 1811-1812 earthquakes (Jibson and Keefer, 1994). The results determined by Jibson and Keefer on landslides similar in type and morphology to the landslides mapped in this project, and the nearly identical geologic conditions, suggest that the landslides mapped in the western NMSZ are also the result of the 1811-1812 New Madrid earthquakes.

6.2. SUMMARY OF LANDSLIDE DATA

Of the 254 definite and probable landslides and theater-head erosion complexes mapped on the LaGrange, Stubbs Island, Helena, and West Helena quadrangles, 98 were slumps or retrogressive slump complexes, 66 were block slides, 52 were earth flows, 20 were theater-head erosion complexes, and 18 were identified as lateral spreads. The Valley Ridge quadrangle had 429 slumps and retrogressive slump complexes, 93 block slides, 124 earth flows, and 21 lateral spreads. The largest of the mapped slides is the Jeffersonville lateral spread, with a surface area of 517,888 m^2. The smallest slide mapped is an earthflow on the LaGrange quadrangle, with an area of approximately 900 m^2.

Figure 6.1 shows graphs of the distribution of the landslides types, not including theater-head erosion complexes, for both the Helena-area quadrangles and the Valley Ridge quadrangle. The high number of slumps compared to the other slides types is likely a factor of the relatively homogeneous characteristics of the loess covering Crowley's Ridge, as rotational slumps tend to form in homogeneous material. The higher number of slides on the Valley Ridge quadrangle is likely due to the fact that the quadrangle is located much closer to the epicenters of the 1811-1812 earthquakes, and would therefore experience more severe ground shaking.

On the Valley Ridge quadrangle, the slides were relatively evenly distributed across Crowley's Ridge, with 50.7% of the slides on the eastern half of the ridge, and 25% along the eastern escarpment. This is likely due to the fact that the Valley Ridge quadrangle is located much closer to the epicenters of the 1811-1812 earthquakes. Higher intensity ground shaking in the area would create a more even distribution of landslides over the region than in more distant areas, and allow failure on shallower slopes. Slopes on Crowley's Ridge in the Valley Ridge quadrangle range from near 0° in the bottoms of some of the stream valleys to vertical in areas of recently eroded loess bluffs. The landslides generally occur on slopes greater than 15°, with 53.7% (358) of the mapped slides partially or fully on slopes of 45° or greater. Figure 6.2 shows the distribution of the different landslide types on slopes of Crowley's Ridge in the Valley Ridge quadrangle.

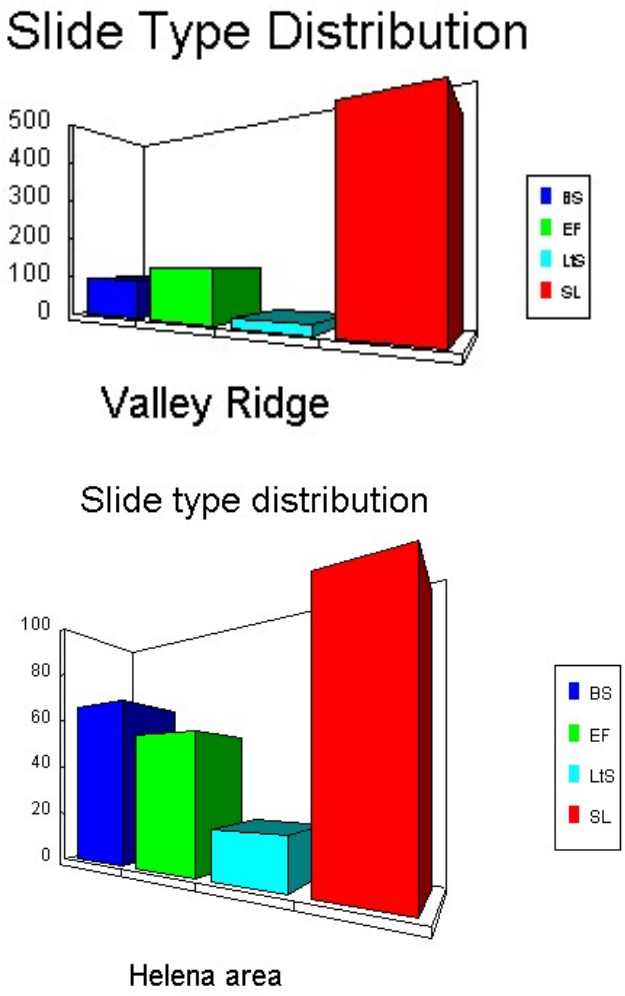

Figure 6.1 Landslide distribution by type for the Helena area quadrangles and Valley Ridge quadrangle. The dark blue bars represent block slides (BS); the green, earth flows (EF); the light blue, lateral spreads(LtS); and the red, slumps (SL).

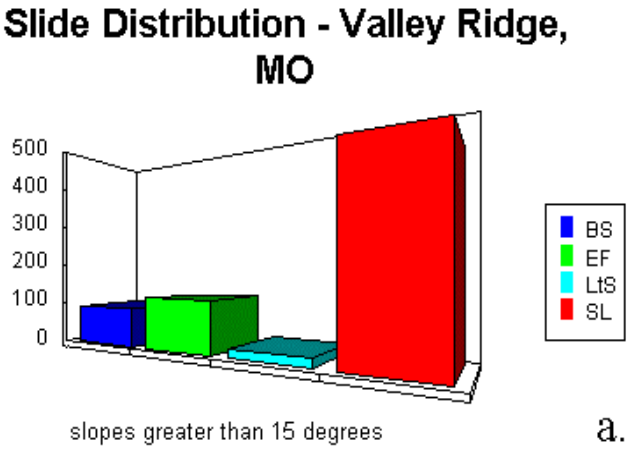

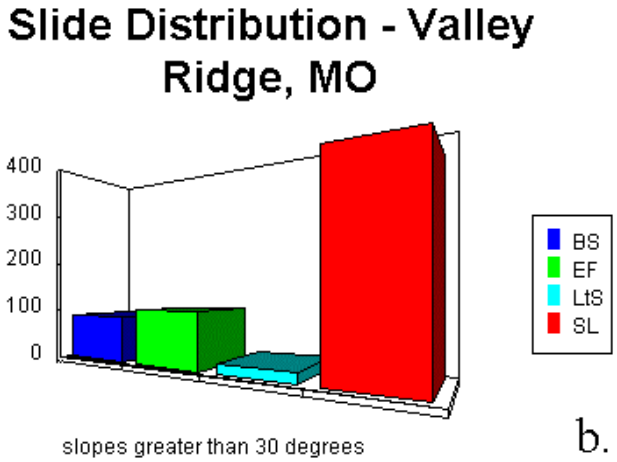

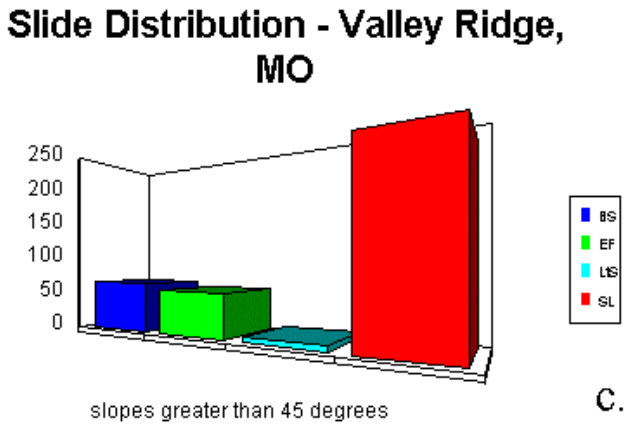

Figure 6.2 Distribution of slides with respect to degree of slope for the Valley Ridge quadrangle. a) distribution of landslides on slopes 15° or greater; b) distribution of landslides on slopes 30° or greater; c) distribution of landslides on slopes of 45° or greater. BS – block slide, EF – earthflow, LtS – lateral spread, SL – slump

In the Helena area, the slopes on Crowley's Ridge range from nearly flat in the stream valleys, to near vertical in the loess bluffs. However, the eastern escarpment of Crowley's Ridge is much higher and steeper than that exposed in the Valley Ridge quadrangle. The landslides in the Helena area are much more concentrated along the eastern escarpment of Crowley's Ridge, with about two-thirds (65.8%) of the slides on the eastern escarpment, and 82.9% of the landslides on the eastern half of Crowley's Ridge. The concentration of the landslides on the eastern side is likely ascribable to the steeper slopes along that escarpment, because of erosion by the Mississippi, St. Francis, and L'Anguille Rivers and likely tectonic control by the Commerce Geophysical Lineament (Hildenbrand, et al., 1996). The late Wisconsin-age loess blanketing the eastern side of Crowley's Ridge in the Helena appears to be fed by pervious Pleistocene-age gravels lying beneath the loess, similar to the situation described by Jibson and Keefer (1994) along the Chickasaw Bluffs, where the loess is underlain by the Lafayette gravel. This stratigraphy tends to make slope failures along the eastern escarpment more probable. Unlike the Valley Ridge area, the landslides in the Helena area occurred on much higher slopes. This difference can be ascribed to several possible factors:

1. the greater distance between Helena and the epicenters of the 1811-12 New Madrid earthquakes;
2. the expected decrease in dynamic strength parameters (effective cohesion and effective friction) with increasing slope height; and,
3. the significant variance in average annual rainfall between the Helena area (55 inches) and the Valley Ridge area (36 inches).

97% (227) of the landslides in the Helena area developed partially or fully upon slopes inclined 65° or higher; with 73% (171) of the landslides on slopes greater than 75°! Figure 6.3 shows the distribution of the various landslide types on slopes in the Helena area.

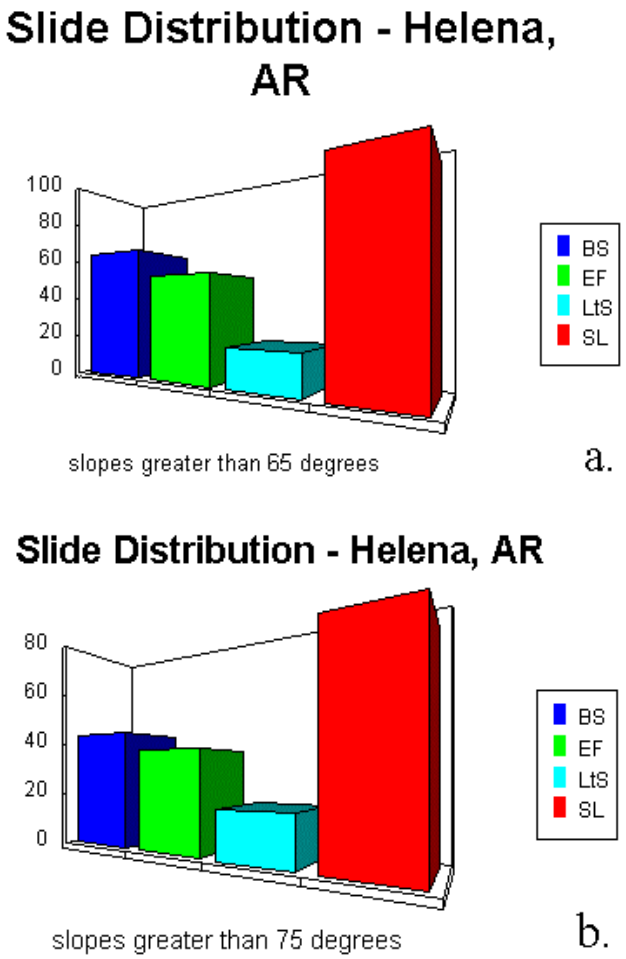

Figure 6.3 Distribution of landslides with respect to slope inclination for the Helena, AR area. a) distribution of landslides on slopes 65° or greater; b) distribution of landslides on slopes 75° or greater. BS – block slide, EF – earthflow, LtS – lateral spread, SL – slump

6.3. LANDSLIPPAGE MAPS

Landslide inventory maps of the 1:24,000 scale Valley Ridge, MO, and LaGrange, West Helena, and Helena, AR, 7.5-minute USGS topographic quadrangles were created in the Geographic Information Systems (GIS) program ArcGIS by ESRI. Once tentative identification of the slides was made on paper maps, these areas were field checked to verify the likely existence of past landslippage, using high resolution enlargements of the quadrangle DRG files with shaded topography. Once these target sites were confirmed, the approximate areal limits of the landslides were input into ArcGIS. The landslides were created as polygons, with attached attribute tables

containing the data pertinent to each slide, including type, confidence level in the landslide identification, and surface area of the landslide.

Five different types of landslides were identified and mapped on the Valley Ridge and LaGrange/Helena/West Helena quadrangles, as described in Section 4: translational block slides (BS), earthflows (EF), slumps and retrogressive slump complexes (SL), theater-head erosion complexes (TH), and lateral spreads (LtS). Numerous slide features on both the Valley Ridge and Helena area quadrangles were composite slides, exhibiting characteristics of more than one slides type (IAEG, 1993a; 1993b). For example, a large number of slides that were slumps at the head of the slide began to behave as earth flows at the base of the slide. Rather than create more feature classes for the composite slides, they were labeled with the dominant landslide type.

Slides were also defined by the level of confidence in the identification of the feature, based on the geomorphic expression observed in the field. Confidence levels are given as either definite (D) or probable (P), after the nomenclature developed by Jibson (1985), Jibson and Keefer (1988, 1994) and used by Ding (1991) in the New Madrid Seismic Zone. Definite slides are landslides mapped with a high degree of confidence. Probable slides fit most of the criteria developed for landslide identification using the topographic expression protocol, but of insufficient geomorphic definition to be absolutely sure of their existence. Figure 6.4 shows the distribution of definite versus probable slides for the three Helena area quadrangles and the Valley Ridge quadrangle. Each landslide feature delineated on the quadrangles is labeled according to the slide type, while the confidence level is shown by the color outlining the features. Landslides with a definite confidence level are shown in red while slides with a probable confidence level are shown in yellow. Figure 6.5 presents a portion of the Helena area landslide map, illustrating the form of the landslide inventory maps.

Plates 1 and 2 show index sheets of the Valley Ridge, MO and LaGrange-West Helena-Helena, AR quadrangles. Plate 2 also includes the Stubbs Island, AR quadrangle. No landslides were mapped on the Stubbs Island quadrangle, which does not extend into Crowley's Ridge, but several landslides on the edges of the Helena, West Helena, and LaGrange quadrangles are located close to the Stubbs Island quadrangle (the four quadrangles come together very close to some mapped landslide complexes). The

rectangular areas indicate map areas enlarged for viewing the mapped landslides. The numbers inside the rectangular areas on the index sheets correspond to enlarged maps of the respective quadrangles in Appendix A (Valley Ridge) and Appendix B (LaGrange-West Helena-Helena). The topographic maps in the appendices are presented at a scale of 1:8,000 scale (1 inch = 667 feet).

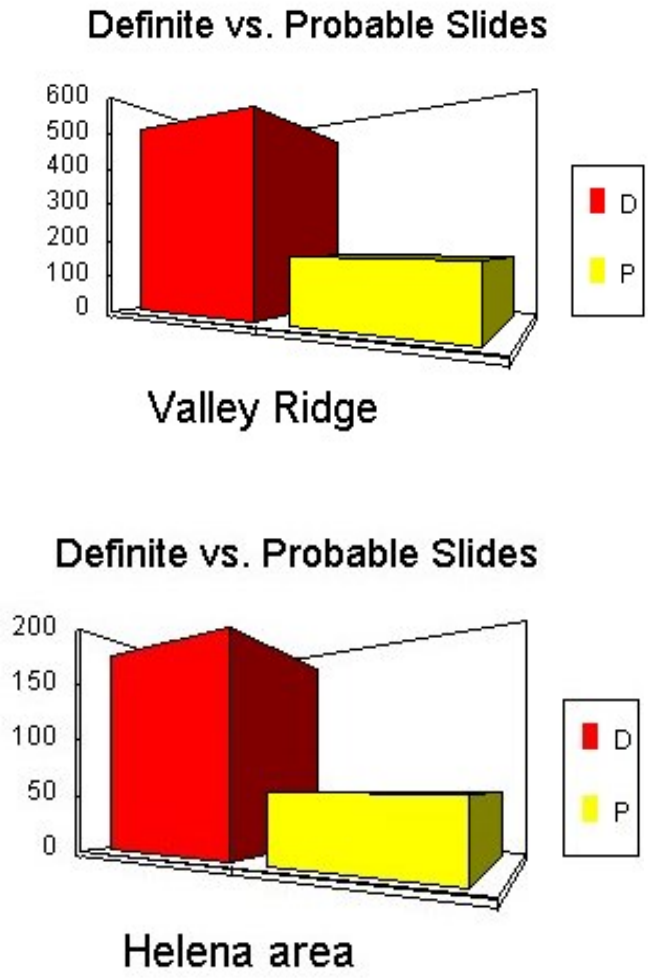

Figure 6.4 Graphs showing comparison between numbers of definite and probable landslides identified on the Helena, AR area quadrangles and the Valley Ridge, MO quadrangle. Red indicates definite slides (high confidence in identification) and yellow indicates probable slides (somewhat lower confidence in identification).

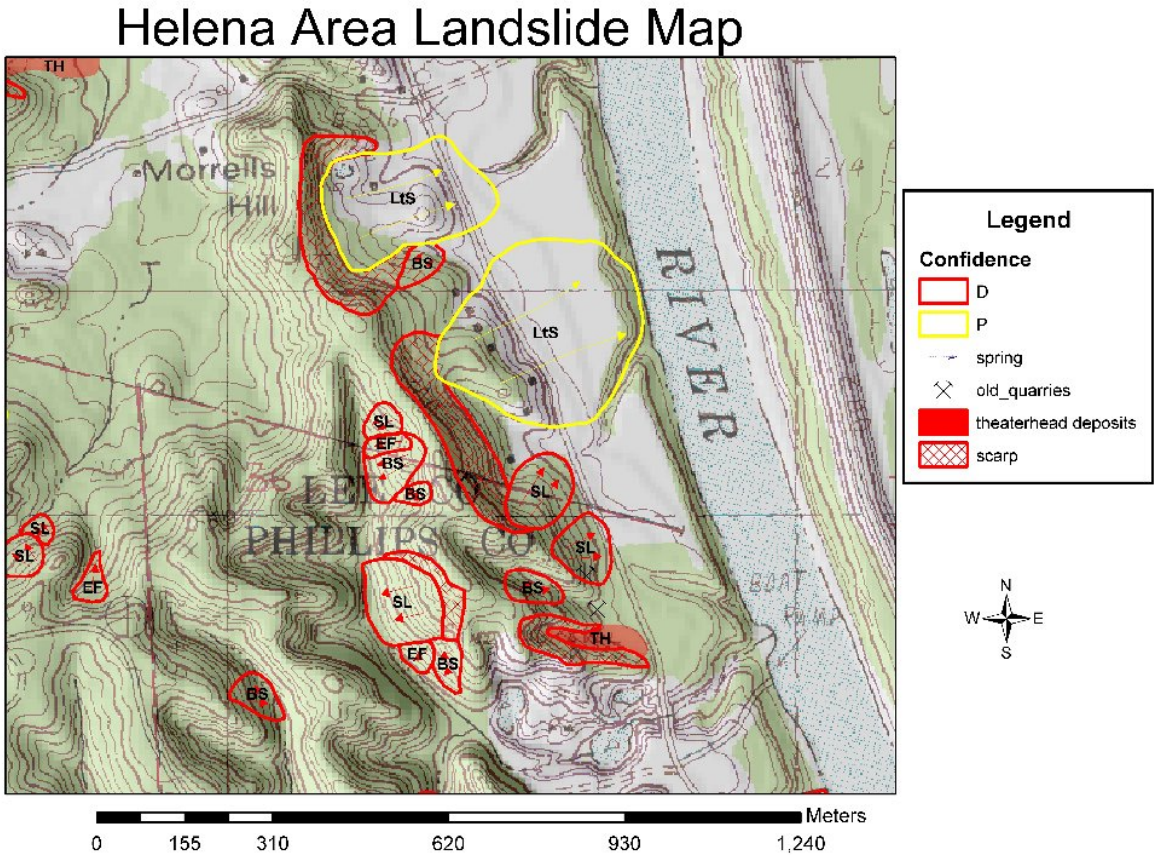

Figure 6.5 Portion of the landslippage map near Helena, AR, as shown in Appendix B. The map shows both definite (red) and probable (yellow) landslides. Arrows indicate direction of movement. The landslide type is labeled within the slide outline: BS (translational block slide), EF (earthflow), SL (slumps and retrogressive slump complexes), TH (theater-head erosion complex), LtS (lateral spread). Cross-hatched areas are scarps of both landslides and theater-head deposits.

7. IMPACTS OF LANDSLIPPAGE ON INFRASTRUCTURE

The potential for seismically-induced lateral spreads, slope failures and ground settlement is very high in the NMSZ. Widespread ground movement would severely impact the Upper Mississippi Embayment of southeast Missouri, eastern Arkansas, and western Tennessee and Kentucky and southern Illinois. Potential damage to transportation routes as well as other infrastructure features, such as communications, pipelines and their associated facilities, water supply, and sewage treatment facilities by seismically-induced landslippage is a matter of concern for community planners and the emergency management agencies of all states near the NMSZ.

Of the landslide types described in this research, lateral spreads have the greatest potential to cause major damage to infrastructure in the NMSZ. Lateral spreads, as discussed in Section 4, tend to occur on relatively shallow slopes, where landslippage would not normally be predicted (Seed and Wilson, 1967). Lateral spreads also impact a much larger area than other landslide forms mapped in the NMSZ. Several of the lateral spreads mapped adjacent to Crowley's Ridge near Helena, AR, have a surface area greater than 0.30 km^2. These large features can cause severe damage to transportation, pipeline, and other infrastructure by disrupting or destroying long segments of the infrastructure. Other, smaller landslippage forms may damage only a small segment of a road, drainage ditch, or pipeline, allowing for rapid repair, but damage by lateral spreads may be difficult to repair due to the large areal extent of impact.

The NMSZ and surrounding area was sparsely settled during the times of the 1811-1812 earthquakes, as well as the 1895 Charleston, MO, earthquake. At the time of the New Madrid earthquakes, Cincinnati, OH, and Louisville, KY, were the largest towns west of the Allegheny Mountains and the only large towns near the earthquake center. However, the damage caused by the earthquakes was so great, even with the sparse population, that in 1815 the United States Congress passed the first disaster relief act to assist settlers in the area with relocation. If similar large earthquakes were to occur today the damage in the central United States could be expected to be between $10 and $20 billion (Wheeler, Rhea and Tarr, 1994). Even for an earthquake the size of the 1895 Charleston, MO, earthquake (M_s6.7), the cities of St. Louis and Cairo, IL, would be

within the zone with MMI VII (Table 3.1), the zone of severe shaking. Memphis and Nashville, TN, Chicago, IL, and Little Rock, AR, would be in the area with MMI V. For a large 1811-1812 magnitude quake, the MMI VII would include St. Louis, Memphis, and Little Rock, and MMI V would reach to Knoxville, TN, Detroit, MI, Kansas City, MO, and Charleston, SC. The vast majority of the buildings in these areas were not built to withstand earthquake shaking, unlike structures in other seismically-active areas, such as California.

Figure 7.1 shows the portion of an infrastructure map developed by Wheeler, Rhea, and Tarr (1994) which includes the area immediately surrounding Crowley's Ridge. The locations of the five M8.0+ earthquakes of the 1811-12 New Madrid earthquake sequence have been added to the map. Numerous transportation routes and major pipelines can be seen in the vicinity of Crowley's Ridge and the Mississippi and St. Francis Rivers. These areas, as well as areas adjacent to the large drainage ditches that criss-cross the area, are highly susceptible to lateral spreading, in addition to other types of landslides.

7.1. TRANSPORTATION ROUTES

Numerous transportation routes cross Missouri and Arkansas in the vicinity of Crowley's Ridge and the Ozark Escarpment. These include Interstates 55, 155, and 40; U.S. Highways 45, 49, 51, 60, 61, 62, 63, 64, 67, 79 and 412; and mainline corridors and spurs of the Union Pacific and Burlington Northern-Santa Fe Railroads. U.S. Hwy 60 and Interstate 40 are major east-west highways that traverse the Little River Drainage District as well as Crowley's Ridge and/or the Ozark Escarpment. U.S. Highway 60 is also an emergency evacuation route for southeast Missouri. Planners have recognized that the danger of damage to or destruction of these transportation routes by seismically-induced landslippage in the event of an earthquake is extremely high (Hanley, 1992; Wheeler, Rhea and Tarr, 1994). The ability to identify areas with the potential for reactivation of previously existing seismically-induced landslippage and areas of potential new slope failures would prove valuable to both state and federal departments of transportation for future decisions about emergency access corridors, possible seismic retrofitting and disaster planning purposes.

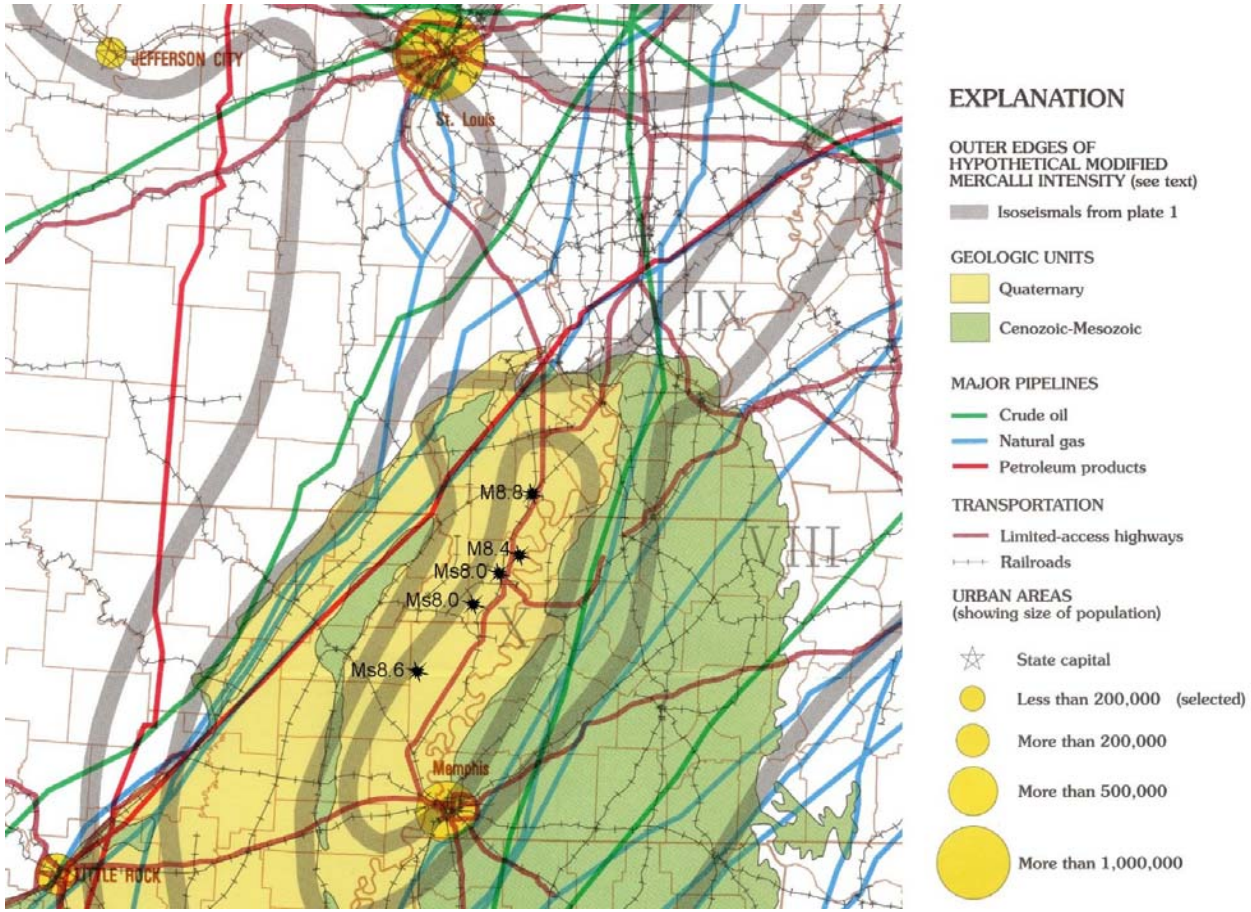

Figure 7.1 Portion of a map showing major infrastructure elements in the NMSZ, including pipelines, highways, and railroads. The approximate locations and magnitudes of the largest of the 1811-1812 earthquakes are shown. (adapted from Wheeler, Rhea, and Tarr, 1994).

A potential for damage to airports within the NMSZ exists as well. Memphis, TN and St. Louis, MO, have relatively large urban airports, with Memphis serving as the round-the-clock hub for Federal Express. Numerous towns in the western NMSZ also support small regional or local airports, many of which are critical to the agricultural industry in the region, which require six to nine passes by pesticide and fertilization dusting aircraft for each crop cycle. Runways, buildings, and fuel storage and distribution facilities may be damaged as a result of ground shaking, lateral spreads, and localized ground liquefaction. Partial or total closure of these facilities could affect disaster relief efforts in the event of a large earthquake.

One other major transportation route that has the potential to be impacted by seismic events and related landslippage in the NMSZ is the Mississippi River. Mississippi River barges carry a large volume of agricultural and manufacturing products each day. Descriptions of the effects of the 1811-1812 earthquakes (Fuller, 1912), describe caving of Mississippi River banks and alterations to channel physiography, including the sinking of river islands, and shallowing of areas of the river. Large lateral spread features have the potential to drastically narrow or shallow the Mississippi River, making commercial transportation difficult and possibly impacting the ability to move disaster relief personnel and supplies into the NMSZ.

7.2. WATER RESOURCES

7.2.1. Drainage Districts Southeast Missouri is at the upper reaches of what was once the largest bottom land hardwood forest in the United States. Extending through the flood plain of the Mississippi River and its tributaries, this forest covered 24 million acres from southern Illinois and Missouri south to coastal Louisiana. This wetland forest was created by the constant flooding of the Mississippi River flood plain, the 45+ average inches of yearly precipitation in the area, and runoff entering the flood plains from the Ozark highlands.

In 1907 state legislation was enacted to create special assessment districts to drain the Upper Mississippi Embayment. The first of these was the Little River District headquartered in Cape Girardeau. In order to drain the more than 550,000 acres in that district, engineers had to intercept runoff that originates in the Ozark Plateau and St.

Francois Mountains. This runoff was diverted through the 40-mile-long Headwaters Diversion Channel which extends from Greenbriar, in Bollinger County, to just south of Cape Girardeau, where it enters the Mississippi River.

Between 1914-1928 the Little River District excavated more than 900 miles of drainage ditches, up to 35 feet deep. The largest is the 100-mile-long Ditch No.1, which collects runoff from all other ditches in the district and carries it south into Arkansas, where it empties into the St. Francis River and later the Mississippi, 250 miles away. Dozens of similar drainage districts were subsequently formed to drain smaller areas, and by 1942, more than 1,200,000 million acres of wetlands were converted into farmland suitable for year-round row crops. The land reclamation carried out between 1910-42 allowed the agricultural development of southeast Missouri and eastern Arkansas for the first time, bringing approximately 235,000 new residents to the affected region. Today this region grows corn, wheat, soybeans, rice, cotton, grain, sorghum, vegetables, peaches, watermelons, and other fruits. This area forms Missouri and Arkansas' best producing counties for corn, soybeans, wheat and sorghum.

In 1890 the three largest towns in the Missouri Bootheel region were New Madrid, Caruthersville and Charleston, all associated with Mississippi River commerce. While these towns have remained about the same size, dozens of larger communities have sprung up in the reclaimed flood plains. The population of the reclaimed region presently stands about 250,000. This entire area was subjected to inundation and uplift during the 1811-12 earthquake sequence (Fuller, 1912). Much of this region would be subject to crippling flood damage if portions of the drainage ditches become inoperable, due to landslippage of the steep side slopes, liquefaction-induced slope failures and lateral spreading. These ditches have very low flow gradients, so are very susceptible to even modest flow obstructions (Steckel, 1992)

The side slopes of the deep drainage ditches exhibit marked evidence of paleoliquefaction. A repeat of the M_s 8.0 to 8.8 1811-12 earthquake sequence or even the M_s 6.5 1895 Charleston, Missouri earthquake, could be expected to cause liquefaction and lateral spreading of the drainage ditches and drop simply-supported highway bridges that cross these ditches. U.S. Highway 60 alone crosses seven major ditches, any of

which could be expected to experience slope failures that would undermine the bridge abutments (Anderson, et al., 2001).

7.2.2. Retention Structures Numerous small water retention structures and several large reservoirs, including Lake Poinsett, Bear Creek Lake, and Storm Creek Lake in Arkansas, and Lake Wappapello in Missouri, have been constructed on Crowley's Ridge and/or within the NMSZ. These structures have the potential to fail as a result of seismically-induced landslippage, lateral spreading, liquefaction-induced slope or bearing failure, or by overtopping caused by landslippage into the reservoirs. Failure of these structures would result not only in flooding downstream, but in a drastic reduction of available potable water for surrounding communities.

7.3. PIPELINES AND ELECTRIC POWER TRANSMISSION CORRIDORS

The upper Mississippi Embayment is a major corridor for the transportation of energy resources from Louisiana and Texas in the south-central U.S. to St. Louis, Chicago, Detroit, and the eastern seaboard. Numerous pipelines carrying natural gas, crude oil, and other petroleum products cross the upper Mississippi Embayment and the New Madrid Seismic Zone. In the western NMSZ, one major crude oil pipeline, three major natural gas pipelines, and one major pipeline carrying other petroleum products pass within 50 miles of Crowley's Ridge. Numerous other smaller associated pipelines also traverse the area (Wheeler, Rhea and Tarr, 1994). The petroleum product pipeline runs intermittently on Crowley's Ridge for approximately 100 miles, and one of the natural gas pipelines follows the western edge of Crowley's Ridge for the same distance.

Damage to these pipelines, or to their associated pumping and transfer stations, during a moderate to severe earthquake, would not only impact the immediate area, but would have the potential to disrupt energy supply to much of the north and eastern United States. A rupture on any part of the pipeline would disrupt flow along the entire length of the pipeline. Although shaking and bending caused by earthquake ground motion are usually not sufficient to rupture pipelines, large areas of liquefaction, landsliding, or lateral spreading could easily break any of the pipelines that cross such features. This is a very real risk for the pipelines that run near the Mississippi River and/or adjacent to Crowley's Ridge. While it is possible that structural damage to pipeline pumping and

transfer stations may be caused by ground shaking, landsliding, or lateral spreads, loss of power to the stations due to disruption of electrical transmission lines and power stations has the potential to impact large portions of the pipeline system.

Numerous electrical transmission corridors also cross Crowley's Ridge and the NMSZ. Several transmission lines in the Helena, AR, area cross large landslides and lateral spreads. Reactivation of the landslides, or formation of new slides in the area, may cause extensive damage to the existing power transmission corridors. This damage would impact not only the regional pipelines, but local sewage and water treatment facilities, emergency response networks, and even the ability of rural residents to obtain potable water from private wells.

8. CONCLUSIONS

A large number of seismically-induced landslides, including lateral spreads, earth flows, slumps, block slides, and theater-head erosion complexes, appear to exist along the eastern escarpment of Crowley's Ridge in the New Madrid Seismic Zone. 919 slides, both definite and probable, were mapped in the Helena-West Helena-LaGrange, AR, and Valley Ridge, MO, 7.5-minute quadrangles. This research suggests that the use of topographic expression can be effective method for the preliminary identification of active, dormant or even ancient landslides. Each type of landslide tends to exhibit characteristic topographic relief, anomalous hillside profiles, and anomalous drainage characteristics that allow for tentative identification. This method has the potential to become an important tool for rapid screening of large land areas for signs of past landslippage. While the accuracy of the method is somewhat dependent on the scale and resolution of topographic maps and digital elevation data, development of new and more accurate mapping methods, including Light Detection and Ranging (LiDAR), Synthetic Aperture Radar (SAR), and Interferometric Synthetic Aperture Radar (InSAR), will continue to improve the map data and accuracy of analysis using topographic expression and in the near future, quite possibly, computerized s.

Most of the landslides found appear to have moved about two hundred years ago, most likely triggered by ground shaking during the 2,000 earthquakes that befell the region in late 1811 and early 1812. The identification of so many different kinds of seismically-induced landslides in the NMSZ will likely play an important role in shaping how future studies of seismic hazards in the NMSZ are evaluated. All of the landslide types investigated have the potential to cause damage to engineering infrastructure through massive permanent ground movement. Lateral spread features appear to pose the greatest danger to engineered structures because they envelop large tracts of land, and would be difficult and expensive to mitigate. Highways, railways, transmission lines or buried pipelines traversing a lateral spread would all likely be severed. The other types of landslides identified in this study also have the potential to cause severe or extensive damage to transportation, utility, and drainage infrastructure within the NMSZ, but over a

more localized and limited area. For these reasons, the identification of slide types and their areal extent is important to hazard planning in the upper Mississippi Embayment.

9. FUTURE WORK

The LaGrange, West Helena, and Helena, AR, and Valley Ridge, MO, quadrangles are only four of the 52 7.5' USGS quadrangles that cover Crowley's Ridge. Future work should include the development of computerized topographic s and GIS programs including ArcGIS, Global Mapper, and TerraBase II to map the remaining 48 quadrangles in Missouri and Arkansas. The continuing work will be funded in part by the USGS NEHRP grant used to support the research discussed above. Additionally, further investigation into the use of geophysical methods including electrical resistivity, induced polarization, Ground Penetrating Radar, and seismic reflection/refraction methods is also planned.

Computer-based s would have to potential to evaluate enormous tracts of land and highlight anomalous topography and drainage features, allowing for these to be evaluated in more detail to determine their origins. The topographic s we have developed to date allow anomalous features to be identified using visual comparison. The reliability of this approach and the speed with which it can be applied depends in large part on the individual's experience and the data quality. More detailed topographic maps (scales between 1:24,000 and 1:3000), aerial photos and digital elevation models can elicit more detailed landslide inventory maps. The development of computerized s would have the potential to allow for identification of areas of anomalous topography and drainage over wide tracts of land in very little time, and, might diminish the operator experience variable. It would appear that operator experience is the single greatest variable in controlling the reliability and time expended to prepare landslide inventory maps. The U.S. Geological Survey has expressed interest in assisting in the development of such computers, and Dr. Curt Davis of the Electrical Engineering department at the University of Missouri – Columbia has been contacted about assisting in the development of the computer programs.

One of the major difficulties encountered in the project was the difference between the 1:24,000-scale topographic maps prepared by the USGS and the actual "bare earth" surface that exists beneath extensive tree canopies. The USGS quadrangles used in this study were derived from stereopair aerial photographs of highly vegetated hillside

areas. The dense canopy appears to create a reflective surface that requires USGS cartographers to employ over-simplified interpolation models, which assume near-linear slopes beneath the trees. In many instances, we found this interpretation to be overly erroneous, having Root Mean-Square Errors (RMSE) in excess of 180 feet, which is 18 times the contour interval. This value appears to be about equal to the height of the tree canopy in those same mismapped areas. Future investigations using new and more accurate mapping methods, including Light Detection and Ranging (LiDAR), Synthetic Aperture Radar (SAR), Band-C Interferometric Synthetic Aperture Radar (INSAR), and Band-P Synthetic Aperture Radar (SAR) may prove valuable in determining the actual "barer earth" topographic surface beneath the vegetation. Band-P SAR and INSAR data has the potential to "see" through most types of vegetation down to the actual ground surface. The use of INSAR and SAR scanners may enable more accurate representations of topography in highly vegetated areas than traditional orthophoto-derived topographic maps have been, heretofore, able to produce. Accurate topographic models would allow for more accurate identification of anomalous topographic features normally associated with landslippage. Unfortunately, Band-P SAR interferes with radio transmissions, making it difficult to obtain permission from the Federal Communications Commission (FCC) to make Band-P SAR data acquisition flights.

The identification of past landslide features and investigation into their locations and modes of formation in the NMSZ will play an important role in future studies of seismic hazards in the region. These ground disturbances have the potential to cause extensive damage to transportation, utility, and drainage infrastructure within the NMSZ.

REFERENCES

Anderson, N., Baker, H., Chen, G., Hertell, T., Hoffman, D., Luna, R., Munaf, Y., Prakash, S., Santi, P., and Stephenson, R., 2001, Earthquake Hazard Assessment Along Designated Emergency Vehicle Priority Access Routes: Prepared by University of Missouri-Rolla for the Missouri Department of Transportation Geotechnical Group, Research, Development and Technology, Final Report RDT REDT01-009, 369 p.

Bjerrum, L., 1966, Mechanism of Progressive Failure in Slopes of Overconsolidated Plastic Clays and Clay Shales, Third Terzaghi Lecture, Norwegian Geotechnical Institute, Oslo, Norway.

Boyd, K.F. and Schumm, S.A., 1995, Geomorphic Evidence of Deformation in the Northern Part of the New Madrid Seismic Zone: U.S. Geological Survey Professional Paper 1538-R, 35 p.

Bruckl, E., and Scheidegger, A.E., 1973, Application of the Theory of Plasticity to Slow Mudflows: Geotechnique, v. 23, no. 1, pp. 101-107.

Bryan, K., 1940, Gully Gravure-A Method of Slope Retreat: Journal of Geomorphology, v. 3, pp. 89-107.

Bull, W.B., 1991, Geomorphic Response to Climatic Change, Oxford University Press, New York, 326 p.

Campbell, A.P., 1966, Measurement of Movement of and Earthflow: Soil and Water, March 1966, pp. 23-24.

Cedargren, H. R., 1989, Slope Stabilization With Drainage: Ch. 8 in Seepage, Drainage and Flow Nets, 3rd Ed.: John Wiley & Sons, New York, pp. 292-336.

Cox, R.T., 1988, Evidence of Quaternary Ground Tilting Associated with the Reelfoot Rift Zone, Northeast Arkansas: Southeastern Geology, v. 15, p. 618-621.

Cruden, D.M., and Varnes, D.J., 1996, Landslide Types and Processes, *in* Landslides: Investigation and Mitigation, Turner, A.K., and Schuster, R.L., eds., Transportation Research Board Special Publication 247, pp. 36-75.

CUSEC, 1999, Central United States at Risk: A Strategic Plan for Reducing the Unacceptable Risk From an Earthquake in the Central U.S.; Central United States Earthquake Consortium, Memphis, TN, 27 p.

Davis, W.M., 1909, Geographical Essays: Dover Publications, Inc., reprinted 1954, 777 p.

Dietrich, W.E., and Rogers, J.D., 1989, Mass Wasting and Slope Failure: in Landform Development, Ch. 42, *in* Hydrogeology: Geology of North America, Back, Rosenshein and Seaber, eds., Geological Society of America, DNAG volume O-2, p. 383-400.

Ding, Zheng, 1991. An Investigation of the Relationship Between the 1811-1812 New Madrid Earthquakes and Landslides on Crowley's Ridge, Arkansas; unpublished Masters Thesis, Memphis State University, Memphis, Tennessee.

Fisk, H.N., 1944, Geological Investigation of the Alluvial Valley of the Lower Mississippi River; Mississippi River Commission, US Army Corps of Engineers, 70 p. 33 pl.

Forbes, H., 1947, Landslide Investigation and Correction: Transactions of the American Society of Civil Engineers, v. 112, pp. 377-442.

Fuller, Myron L., 1912, The New Madrid Earthquake (A Scientific Factual Field Account); U.S. Geological Survey Bulletin 494, reprinted by The Center for Earthquake Studies, Cape Girardeau, MO.

Goodman, R.E, 1976, Methods of Geological Engineering in Discontinuous Rocks, West Publishing, New York, 472 p.

Guccione, M.J., Prior, W.L., and Rutledge, E.M., 1986, The Tertiary and Quaternary Geology of Crowley's Ridge: A Guidebook; Guidebook 86-4, Arkansas Geological Commission, Little Rock, AR.

Hamilton, R., and Johnston, A.T., 1990, Tecumseh's Prophecy: Preparing for the Next New Madrid Earthquake; U.S. Geological Survey Circular 1066.

Hanley, Paul, 1992, Reducing Earthquake Hazards in the Central U.S.: Critical Facilities: prepared for the U.S. Geological Survey by the Department of Urban and Regional Planning, University of Illinois, Urbana-Champaign,.

Hansen, W.R., 1966, Effects of the Earthquake of March 27, 1964 at Anchorage, Alaska; U.S. Geological Survey Professional Paper 542-A, 68 p.

Hildenbrand, T.G.; Langenheim, V.E.; Schweig, E.; Stauffer, P.H., and Hendley II, J.W., 1996, Uncovering Hidden Hazards in the Mississippi Valley, U.S. Geological Survey Fact Sheet 200-96, Center for Earthquake Research and Information, The University of Memphis, Memphis, TN.

Hutchinson, J.N., 1969, A Reconsideration of the Coastal Landslides at Folkestone Warren, Kent, Geotechnique, Vol. 19, No. 1, p. 6-38.

Hutchinson, J.N., and Bhandari, R.K., 1971, Undrained Loading, A Fundamental Mechanism of Mudflows and Other Mass Movements: Geotechnique, v. 21, no. 4, pp. 353-358.

International Association of Engineering Geology Working Party on the World Landslide Inventory, 1993a, A Suggested Method for Describing the Activity of a Landslide: Bulletin of the International Association of Engineering Geology, No. 47, pp. 53-57.

International Association of Engineering Geology Working Party on the World Landslide Inventory, 1993b, Multilingual Landslide Glossary: Bi-Tech Publishers, Richmond, British Columbia, 59 p.

Jibson, R.W., 1985, Landslides Caused by the 1811-12 New Madrid Earthquakes: Ph.D. dissertation, School of Earth Science, Stanford University, 232 p.

Jibson, R.W., Keefer, D.K., 1988, Landslides Triggered by Earthquakes in the Central Mississippi Valley, Tennessee and Kentucky; USGS Professional Paper 1336-C, 24 p.

Jibson, R.W., Keefer, D.K., 1994, Analysis of the Origin of Landslides in the New Madrid Seismic Zone; USGS Professional Paper 1538-D23 p.

Keaton, J.R., and DeGraff, J.V., 1996, Surface Observation and Geologic Mapping, *in* Landslides: Investigation and Mitigation, Turner, A.K., and Schuster, R.L., eds., Transportation Research Board Special Publication 247, pp. 178-227.

Kelson, K.I., Simpson, G.D., Haradan, C.C., Lettis, W.R., Van Arsdale, R.B., and Harris, J.B., 1994, Multiple Holocene Earthquakes Along the Reelfoot Fault, Central New Madrid Seismic Zone; *in* Proceedings of the Workshop on Paleoseismology; USGS Open File Report 94-568, p.92-93.

Kesseli, J.E., 1943, Disintegrating Soil Slips of the Coast Ranges of Central California: Journal of Geology, v. 51, pp. 342-352.

Knox, B.R., and Stewart, D.M., 1995a, The New Madrid Fault Finders Guide: Gutenberg-Richter, Marble Hill, MO, 179 p.

Knox, B.R., and Stewart, D.M., 1995b, The Earthquake America Forgot: 2,000 temblors in five months: Gutenberg-Richter, Marble Hill, MO, 377 p.

Leighton, F.B., 1969, Landslides and Hillside Development; *in* Engineering Geology in Southern California, Proctor, R., and Lung, R., eds., Special Publication of the Los Angeles Section of the Association of Engineering Geologists, Arcadia, CA, p. 149-190.

Leighton, M.M., and Williams, H.B., 1950, Loess Formations of the Mississippi Valley: Journal of Geology, Vol. 58, No. 6, pp. 599-623.

Liang, T., 1952, Landslides – An Aerial Photographic Study: Ph.D. dissertation, Cornell University, 274 p.

Liang, T., and Belcher, D.J., 1958, Airphoto Interpretation: *in* Landslides and Engineering Practice, Eckel, E.B., ed., Highway Research Board Special Report 29, pp. 69-92.

McFarland, J.D., 1992, Landslide Features of Crowley's Ridge; Arkansas Geological Commission, Information Circular 31, Little Rock, Arkansas.

Melosh, H.J., 1987, The Mechanics of Large Rock Avalanches; *in* Debris Flows/Avalanches: Process, Recognition, and Mitigation, Reviews in Engineering Geology, Volume VII, Costa, J.E., and Wieczorek, G.F., eds., Geological Society of America, Boulder, CO, p. 41-51.

Miller, W.J., 1931, The landslide at Point Fermin, CA: Scientific Monthly, v. 32, p. 464-69

Nuttli, O.W., 1973, The Mississippi Valley Earthquakes of 1811 and 1812 – Intensities, ground motion, and magnitudes; Seismological Society of America Bulletin, v. 63, p. 227-248.

Penck, W., 1927, Die morphologische Analyse: Stuttgart (translated as Morphological Analysis of Land Forms, London, Longmans), 371 p.

Pyles, M.R., and Froehlich, 1987, Rates of Landsliding as Impacted by Timber Management Activities in Northwestern California, Discussion and Reply, Bulletin of the Association of Engineering Geologists, Vol. XXIV, No. 3, pp. 425-431.

Rendulic, L., 1935, Ein Beitrag zur Bestimmung der Gleitsicherheit: Der Bauingenieur, v. 16, pp. 230-233.

Rib, H.T., and Liang, T., 1978, Recognition and Identification: *in* Landslides: Analysis and Control, R.L. Schuster and R.J. Krizek, eds., Transportation Research Board Special Report 176, pp. 34-80.

Richter, C.F., 1958, Elementary Seismology; W.H. Freeman and Company, San Francisco.

Rogers, J. D., 1980, Factors Affecting Hillslope Profile: Current Topics in Geomorphology, U.C. Berkeley, unpublished manuscript, U.C. Water Resources Center Archives, Berkeley, 67 p.

Rogers, J. D., 1994, Report Accompanying Map of Landslides and Other Surficial Deposits of the City of Orinda, CA: Consultant's Report prepared by Rogers/Pacific, Inc. for the City of Orinda Public Works Department, January, 141 p, 17 pl.

Rogers, J. D., 1998, Engineering Geologic Characterization of Landslides": California Division of Mines & Geology and Southern California Earthquake Center Seismic Hazards Short Course, Los Angeles, Jan 22-24, 1998, 31 p.

Rogers, J.D., Bray, J.D., and Rathje, E.M., in press, Simplified Method for Evaluation of Permanent Deformation of Seismically-Induced Landslippage; paper submitted to Engineering and Environmental Geosciences, 26 p.

Rogers, J.D., and Doyle, B.C., in press, Mapping Earth Flows and Earthflow Complexes Using Topographic Indicators; paper submitted to Engineering and Environmental Geosciences, 35 p.

Santi, P.M. and Neuner, E.J., 2002, Preliminary Evaluation of Seismic Hazards for Emergency Rescue Route U.S. 60, Missouri, Environmental and Engineering Geoscience, Vol. 8, No. 4, pp. 261-277.

Saucier, R., 1994a, Geomorphology and Quaternary Geologic History of the Lower Mississippi Valley, Volume I; U.S. Army Engineer Waterways Experiment Station, 334 p.

Saucier, R., 1994a, Geomorphology and Quaternary Geologic History of the Lower Mississippi Valley, Volume II; U.S. Army Engineer Waterways Experiment Station, 28 pl.

Schweig, E., 2003, Paleoseismology and Its Impact on Seismic Hazard in the New Madrid Seismic Zone; presentation to the University of Missouri-Rolla Student Chapter of the Earthquake Engineering Research Institute, January, 2003.

Schweig, E., Gomberg, J., and Hendley, J.W., 1995, The Mississippi Valley-"Whole Lotta Shakin' Goin' On", USGS. Fact Sheet-168-95

Seed, H.B. and Wilson, S.D., 1967, The Turnagain Heights Landslide, Anchorage, Alaska; Journal of the Soil Mechanics and Foundations Division, American Society of Civil Engineers, v. 93, n. SM4, p. 325-353.

Selby, M.J., 1993, Hillslope Materials and Processes, Second Edition: Oxford University Press, Oxford, 451 p.

Sharpe, C.F.S., 1968, Landslides and Related Phenomena: A study of Mass-Movements of Soil and Rock, Cooper Square Publishers, New York, 137 p.

Shedlock, K.M., Johnston, A.C., 1994, Introduction – Investigations of the New Madrid Seismic Zone; USGS Professional Paper 1538AC, Shedlock, K.M., and Johnston, A.C., eds., p. A1-A6.

Soeters, R., and van Westen, C.J., 1996 Slope Instability Recognition, Analysis, and Zonation, *in* Landslides: Investigation and Mitigation, Turner, A.K., and Schuster, R.L., eds., Transportation Research Board Special Publication 247, pp. 129-173.

Steckel, Phyllis J., 1992, Relationship of Some Atypical Topographic and Drainage Features to Tectonics in Southeast Missouri: A Methodology Test; unpublished Masters thesis, Southeast Missouri State University, Cape Girardeau, MO.

Stover, C.W. and Coffman, J.L., 1993, Seismicity of the United States, 1568-1989 (Revised); USGS Professional Paper 1527.

Strahler, A.N., 1942, Landslides of the Vermillion and Echo Cliffs, Northern Arizona, Journal of Geomorphology, Vol. 5, p. 285-301

Terzaghi, K., 1950, Mechanism of Landslides: *in* Applications of Geology to Engineering Practice (Berkey Volume), Berkey, C., ed., Geological Society of America, pp. 83-123.

Tuttle, M.P., Schweig, E.S., 1995, Archeological and pedological evidence for large prehistoric earthquakes in the New Madrid seismic zone, central United States; Geology, 23 (3), p. 253-256.

Twidale, C.R., 1971, Structural Landforms: MIT Press, Cambridge, 247 p.

Van Arsdale, R.B., Schweig, E.S., Kanter, L.R., Williams, R.A., Shedllock, K.M., and King, K.W., 1992, Preliminary shallow seismic reflection survey of Crowley's Ridge, northeast Arkansas: Seismological Research Letters, v. 63, n.3, p. 309-320.

Van Arsdale, R.B., Williams, R.A., Schweig, E.S., Shedlock, K.M., Kanter, L.R., King, K.W., 1994, Preliminary Seismic Reflection Study of Crowley's Ridge, Northeast Arkansas; USGS Professional Paper 1538AC, Shedlock, K.M., and Johnston, A.C., eds., p. C1-C16.

Van Arsdale, R., 1997, Hazard in the Heartland: The New Madrid Seismic Zone; Geotimes, 42 (5), p. 16-19.

Varnes, D.J., 1958, Landslide types and processes: *in* Landslides and Engineering Practice, Eckel, E.B., ed., Highway Research Board Special Report 29, pp. 20-47.

Varnes, D.L., 1978, Slope Movement Types and Processes: *in* Landslides: Analysis and Control, Schuster, R.L., and Krizek, R.J., eds., Transportation Research Board Special Report 176, pp. 11-33.

Voight, B, and Pariseau, W.G., 1978, Rockslides and Avalanches: An Introduction; *in* Rockslides and Avalanches, 1: Natural Phenomena, Voight, B., ed., Elsevier Scientific Publishing Company, Amsterdam, p. 1-63.

von Hake, C.A., 1974, Earthquake History of Missouri; *in* Earthquake Information Bulletin, Vol. 6, No. 3.

Wheeler, R.L., Rhea, S., and Tarr, A.C., 1994, Elements of Infrastructure and Seismic Hazard in the Central United States: U.S. Geological Survey Professional Paper 1538-M, 18 p, 3 pl.

Zaruba, Q., and Mencl, V., 1982, Landslides and Their Control, 2nd ed., Elsevier Scientific Publishing Company, Amsterdam, 324 p.